UNIVERSITÀ
DEGLI STUDI
DI BRESCIA

DIPARTIMENTO DI INGENGERIA MECCANICA E INDUSTRIALE

DOTTORATO DI RICERCA IN INGEGNERIA MECCANICA E INDUSTRIALE

ING-IND/16 TECNOLOGIE E SISTEMI DI LAVORAZIONE

XXXVII CICLO

Industrial Case Study of Sustainability and Circularity in the Leather Automotive Sector: Reduction of Liquid Wastes and Recycling of Solid Residues into New Materials for FFF Additive Manufacturing

---

Ph.D. Candidate:

Rosario Mascolo

Ph.D. Supervisor:

Chiar.mo Prof. Luca Giorleo

Ph.D. Co-Supervisor:

Dr. Gianluigi Calvanese

(Stazione Sperimentale per l'Industria delle Pelli e delle Materie Concianti srl)

Anno Accademico 2025/2026

A Giusi, il mio esempio, che mi protegge e conforta sempre

A Francesco per il suo amore incondizionato

Ai miei genitori che mi hanno reso quel che sono

Al mio papà che mi guarda da lassù

All'amicizia

Candidate's declaration

I hereby declare that this thesis submitted to obtain the academic degree of Philosophiæ Doctor (Ph.D.) in Ingegneria Meccanica e Industriale is my own unaided work, that have not used other than the sources indicated, and that all direct and indirect sources are acknowledged as references. Parts of this dissertation have been published in international journals and/or conference proceedings (see list of the author's publications at the end of the thesis).

Napoli, 7 Ottobre 2025

ABSTRACT

The new industrial revolution towards sustainability and circularity, driven by major Automotive and Fashion brands, finds its motivation in the ecological transition, where production can no longer be disconnected from ethical, social, and environmental aspects. In leather production, the process involves high energy consumption, use of natural resources, and a series of complex chemical and mechanical treatments that generate significant amounts of liquid, gaseous, and solid waste, with corresponding environmental implications. Among these, liquid waste accounts for 15.2 % of the total, while solid waste comprises 26.1 %. The former primarily originates from wastewater in wet processing stages (tanning liquors), while the latter mainly results from mechanical operations such as splitting, shaving, buffing, and trimming. Specifically, every square meter of leather produced generates approximately 1.38 kg of total waste, of which about 0.36 kg is solid, and 0.21 kg is tanning liquor.

Focusing on the automotive sector and the production of metal-free leather, this study aims to address a significant industrial challenge: on one hand, reducing the environmental impacts associated with production; on the other, integrating circularity principles through the reuse and valorization of processing residues. Specifically, the study seeks to develop a more sustainable approach to glutaraldehyde tanning, reducing its environmental impact and improving process efficiency, with particular attention to the volume of liquid effluents from drum processing. Additionally, the study explores the potential of upcycling solid waste from wet-white leather shaving operations to produce fillers for thermoplastic polyurethane (TPU) composites for Additive Manufacturing using Fused Filament Fabrication (FFF) techniques.

This dual strategy supports a circular economy model within the leather industry, contributing both to waste reduction and the development of advanced materials for industrial applications.

SOMMARIO

La nuova rivoluzione industriale nella direzione della sostenibilità e circolarità, spinta dai grandi marchi dell'Automotive e del Fashion, trova le sue motivazioni nella transizione ecologica, in cui la produzione non può più essere disconnessa da valutazioni di tipo etico, sociale ed ambientale.

Per quanto riguarda la produzione di pelli, il processo prevede un elevato utilizzo di energia, di risorse naturali ed una sequenza di complessi processi chimici e meccanici che generano grandi quantità di rifiuti liquidi, gassosi e solidi, con le relative implicazioni ambientali. Di tutti i rifiuti, scarti e sottoprodotti derivanti, i rifiuti liquidi rappresentano il 15.2 % del totale, mentre quelli solidi si attestano al 26.1 % del totale. I primi sono prevalentemente derivanti dalle acque reflue dalle fasi di lavorazione ad umido (liquidi di concia), mentre quelli solidi provengono principalmente dalle lavorazioni meccaniche di spaccatura, rasatura, smerigliatura e rifilatura. In relativi, ogni metro quadrato di pelle prodotta genera 1,38 kg di rifiuti totali dei quali circa 0.36 kg sono di tipo solido e 0.21 kg di liquidi di concia.

Con particolare riferimento al settore automotive ed alla produzione di pelli metal-free, e con l'obiettivo di affrontare le sfide ambientali correlate, questo studio si propone di affrontare una sfida industriale significativa: da un lato, la riduzione degli impatti ambientali legati alla produzione; dall'altro, l'integrazione concreta dei principi di circolarità attraverso il riutilizzo e la valorizzazione dei residui di lavorazione. Da un lato, si mira a sviluppare un approccio più sostenibile al processo di concia alla glutaraldeide, riducendo il suo impatto ambientale e migliorando l'efficienza del processo, con particolare attenzione alla quantità di reflui liquidi delle lavorazioni in botte. Dall'altro lato, lo studio esplora il potenziale dell'upcycling dei rifiuti da pelli wet-white dalle fasi meccaniche di rasatura, da utilizzare come filler per compositi a base di poliuretano termoplastico (TPU) per Additive Manufacturing mediante tecniche Fused Filament Fabrication (FFF). Questa doppia strategia supporta un modello di economia circolare all'interno dell'industria conciaria, contribuendo sia alla riduzione dei rifiuti che allo sviluppo di materiali avanzati per applicazioni industriali.

AKNOWLEDGEMENTS

Part of this work arises from activities carried out:

- in the framework of LEONARDO – Solutions for driving comfort and vehicle performance efficiency, project ID B32C18000340007. LEONARDO is part of BORGO 4.0, a project financed by the Campania Region POR FESR 2014/2020 action lines.

- In the MICS (Made in Italy - Circular and Sustainable) Extended Partnership receiving funds from the European Union Next-Generation EU (PIANO NAZIONALE DI RIPRESA E RESILIENZA (PNRR) - MISSIONE 4 COMPONENTE 2, INVESTIMENTO 1.3 - D.D. 1551.11-10-2022, PE00000004). This manuscript reflects only the authors' views and opinions, neither the European Union nor the European Commission can be considered responsible for them.

I would like to thank Prof. **Luca Giorleo**, from the Department of Mechanical and Industrial Engineering at the University of Brescia, for giving me the opportunity to work with him. His support and trust have been fundamental in the development of this research work.

I am grateful to Prof. **Emiliano Bilotti**, from the Department of Aeronautics at Imperial College London, for his scientific contribution and the expertise he made available.

I also wish to thank Dr. **Gianluigi Calvanese** for the support in the characterization activities and for his contribution to the different phases of the research.

A special thanks goes to Eng. **Claudio Azzaretto** of Pasubio S.p.A. (Arzignano) for his role in the processes and in the supply of materials, and to Eng. **Fabio Piccirillo** of 3D MadeUp (Castellammare di Stabia) for his assistance in the use of FDM technologies.

List of Abbreviations

PEF-CR: Product Environmental Footprint – Category Rules

TPU: Thermoplastic Polyurethane,

AM: Additive Manufacturing,

FDM: Fused Deposition, Modeling,

FFF: Fused Filament Fabrication,

DSC: Differential Scanning Calorimetry,

TGA: Thermogravimetric Analysis,

PSD: Particle size distribution,

CF: Carbon fiber,

ISO: International Organization for Standardization,

EU: European Union,

EC: European Commission,

JAMA: Japan Automobile Manufacturers Association,

POP: Persistent Organic Pollutants,

REACh: Registration, Evaluation, Authorization, and Restriction of Chemicals,

DIP: Digital Image Processing,

FT-IR: Infrared Fourier Transform,

VOC: Volatile Organic Compounds,

SVOC: Semivolatile Organic Compounds,

VVOC: Very Volatile Organic Compounds,

DMF: Dimethylformamide,

MCP: Monochlorophenol,

DCP: Dichlorophenol,

TeCP: Tetrachlorophenol,

TrCP: Trichlorophenol,

PCP: Pentachlorophenol,

DMFu: Dimethylformamide,

SCCP: Short-Chain Chlorinated Paraffins,

PFOA: Perfluorooctanoic Acid,

PFOS: Perfluorooctane Sulfonate,

DEHP: Di(2-ethylhexyl) phthalate,

DBP: Dibutyl Phthalate,

BBP: Butyl Benzyl Phthalate,

DIBP: Diisobutyl Phthalate,

DINP: Diisononyl Phthalate,

DIDP: Diisodecyl Phthalate,

DNOP: Dinonyl Phthalate,

HD: High-Definition,

HDMI: High-Definition Multimedia Interface,

WW: Wet-White leather,

CFC: Chlorofluorocarbon,

CTUh: Comparative Toxic Unit for humans,

DALY: Disability-Adjusted Life Years,

PM: Particulate Matter,

LCA: Life Cycle Assessement,

GHG: Greenhouse Gas,

ECHA: European Chemicals Agency.

INDEX OF FIGURES

INDEX OF TABLES

Index

INTRODUCTION

Leather production is a process that transforms waste from the food industry — otherwise destined for disposal — into a durable and high value-added material (EN 15987, 2015) (ISO 15115, 2019). The tanning process involves a sequence of specific chemical and physical treatments aimed at modifying the macromolecular structure of collagen of natural skins (Hassan et al., 2023). Leather is widely used in various sectors such as fashion, personal protective equipment or in the automotive industry for seats and interior coverings. In the last decades, major fashion brands and automotive manufacturers are pushing leather producers to transform their production processes, adopt more sustainable business models, and implement circular economy principles to reduce environmental impacts (Morelli C., 2022), in line with the commitments established in the United Nations 2030 Agenda for Sustainable Development (UN, 2015). As a result, tanneries are both optimizing processes to reduce environmental impacts and implementing circular economy principles, focusing not only on leather production but also on the by-products of its processing.

According to the Sustainability Report 2023 of the Italian National Tanning Industry Association (UNIC), Italy produces 99.4 million of square meters of leather, corresponding to about USD 4.3 billion. In the Italian leather production cycle, liquid wastes from tanning represents 37.5 % of total waste, while solid waste accounts for 23.6 %. The liquid waste mainly derives from wastewater during the wet drum processing stages, while solid waste from skins derives from splitting, shaving, buffing, and trimming stages. In relative terms, every square meter of leather produced generates 1.83 kg of total waste, including about 0.43 kg of processing scraps and 0.69 kg of tanning liquids (UNIC, 2023).

Data is confirmed on a global scale. As of 2020, the annual global leather production is estimated at approximately 2 billion square meters corresponding to an estimated value of USD 394.12 billion. It is projected to grow at a compound annual growth rate (CAGR) of 5.9 % between 2021 and 2028, reaching an estimated market value of USD 624.08 billion by 2028 (Muralidharan et al., 2022). The leather footwear sector dominates the market, accounting for about 65 % of total leather consumption, while the remaining 35 % is utilized in the production of other leather goods such as garments, upholstery, and accessories (China et al., 2020). This production generates a great amount of waste; in particular, it has been estimated that the annual production of leather generates more than 600,000 tons of solid waste, 150,000 tons of

which consists of tanned shavings and trimmings (Verheijen et al., 1996) (Yorgancioglu et al., 2020).

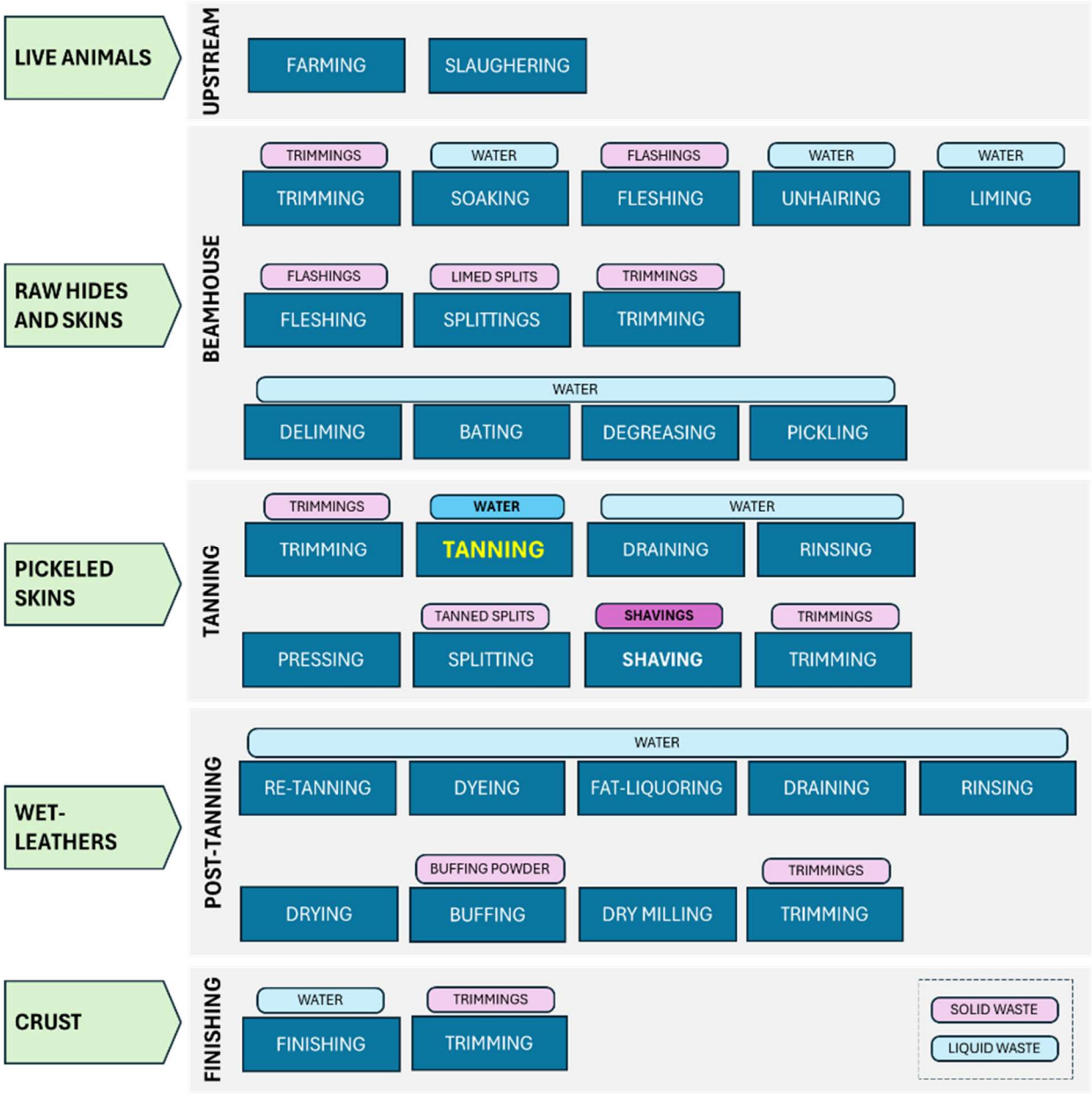

Figure 1 - Tanning process scheme, solid and liquid wastes generated

In Figure 1 a scheme of the tanning process with the liquid or solid waste generated in is represented for the specific phase. In Figure 2 a typical wet-end area of a tannery, equipped with drums for processing hides through tanning and other wet treatments, is reported.

Figure 2 - Wet-end processing department of a tannery

Furthermore, in Table 1 a quantification of the solid waste of tanning process in kilograms per 1,000 kilograms of raw hide processed is provided (Yorgancioglu et al., 2020).

SOLID WASTES FROM TANNING	**QUANTITY (kg / 1,000 kg)**
Preservation salts	80
Hair	100
Raw trimmings	40
Lime sludges	60
Fleshings	120
Wet trimmings	30
Splittings	65
Shavings	95
Buffing dusts	65
Crust trimmings	35
Dry sludges from effluent treatments plants	125

Table 1 - Solid wastes produced from tanning process

About liquid waste, in tanneries the water cycle begins with sourcing from either groundwater or from public and industrial water supply systems. Before being used in the production process, the water undergoes a pretreatment phase aimed at removing potentially harmful substances such as metals that could negatively impact processing efficiency or the quality of the final leather product. Once treated, the water is used throughout several stages

of the tannery's operations. It plays a key role in wet processing stages, steam generation, cleaning procedures, and in air treatment or cooling systems. As it flows through the tannery, water quality deteriorates considerably. It accumulates chemical compounds — either unabsorbed by the hides or resulting from process reactions. Because of this, the wastewater must undergo rigorous treatment to ensure that it meets environmental discharge standards. To minimize ecological harm, tanning industry hubs are equipped with treatment plants specifically engineered to handle the unique chemical profile of tannery effluents (UNIC, 2023).

This study addresses a specific industrial issue within the automotive leather supply chain, concentrating on the tanning phase and the subsequent shaving mechanical operations. A targeted section of the tanning workflow has been intentionally isolated and analyzed in detail to demonstrate that a circular and sustainable approach can be effectively applied to each individual stage of the leather manufacturing process. In particular, the study focuses on thorium hides tanned using glutaraldehyde intended for automotive interior upholstery. This kind of tanning is widely spread in the automotive sector due to its superior resistance to dimensional changes caused by external environmental stresses — both at high temperatures and under hot/dry and cold/humid cycles (Schröpfer M. and Meyer M., 2011) — to which the occurrence of certain surface defects of the leather it is linked (e.g. wrinkling, detachment from the underlying substrate). Glutaraldehyde tanning is also used for issues related to disposal. The absence of inorganic tanning agents prevents the production of metals after the incineration of materials. Nevertheless, its presence in wastewater introduces some environmental concerns. As a strong biocidal agent, even low concentrations of glutaraldehyde in effluents can disrupt microbial populations that are essential for water biological treatment processes like nitrification and denitrification. This disruption may result in higher chemical oxygen demand (COD) levels and lower biodegradability, thereby complicating wastewater treatment and increasing the risk of violating environmental discharge regulations (*Toxicological Profile for Glutaraldehyde*, 2017). Consequently, finding effective solutions to manage and mitigate the impact of glutaraldehyde in wastewater is essential for promoting more sustainable practices in leather production. In this work, the circular and more sustainable approaches in tanning phase have been studied into two different studies:

- The first involves the optimization of the tanning agent, aiming to make the process more sustainable by reducing the volume and pollutant load of wastewater sent to the treatment plant. Process parameters and formulations were adjusted to reduce environmental impact without compromising leather functionality.
- The second part addresses the circularity aspect by developing a strategy for recycling glutaraldehyde-tanned leather shavings. These residues were repurposed as raw material for the production of TPU-based composites, suitable for additive manufacturing Material Extrusion techniques via Fused Filament Fabrication (FFF). This approach explores the potential for reintegrating waste into the production cycle through material recovery.

Through this dual approach — process optimization and material upcycle — this study provides an example of how sustainability and circularity can be implemented even at specific stages of a traditionally resource-intensive industry, responding to specific goals of the United Nations 2030 Agenda (UN, 2015):

- (3.9) By 2030, substantially reduce the number of deaths and illnesses from hazardous chemicals and air, water and soil pollution and contamination.
- (6.3) By 2030, improve water quality by reducing pollution, eliminating dumping and minimizing release of hazardous chemicals and materials, halving the proportion of untreated wastewater and substantially increasing recycling and safe reuse globally.
- (9.2) Promote inclusive and sustainable industrialization and, by 2030, significantly raise industry's share of employment and gross domestic product, in line with national circumstances, and double its share in least developed countries.
- (12.2) By 2030, achieve the sustainable management and efficient use of natural resources.
- (12.4) By 2020, achieve the environmentally sound management of chemicals and all wastes throughout their life cycle, in accordance with agreed international frameworks,

and significantly reduce their release to air, water and soil in order to minimize their adverse impacts on human health and the environment.

- (12.5) By 2030, substantially reduce waste generation through prevention, reduction, recycling and reuse.
- (17.8) Fully operationalize the technology bank and science, technology and innovation capacity-building mechanism for least developed countries by 2017 and enhance the use o enabling technology, in particular information and communications technology.

Figure 3 - UN Sustainable Development Goals for the study

About the reuse of solid wastes, he recovery of waste from pre-tanning phases (animal-origin by-products – AOBPs) is well established as a raw material source for various sectors (UNIC, 2023), such as pharmaceuticals (Irwanto, 2021), biomedical (Maistrenko et al., 2022), fertilizers (Stefan et al., 2022), fuel production (Alptekin et al., 2012), and adhesives (Akter et al., 2024). Waste from already processed tanned hides, residues from splitting of tanned leather (EN 15987, 2015) (ISO 15115, 2019) are reused by tanneries as by-products to produce pigmented split leather or suede (EN 15987, 2015) (ISO 15115, 2019), which are intended for the same industries as full-grain leather, such as automotive, fashion, and furniture.
Shavings, that are mechanical waste from thickness equalization of wet-state hides, constitute approximately 33 % of total waste produced after tannage (Yorgancioglu et al., 2020) and 75

% of the solid waste produced by tanneries (UNIC, 2023).They have been already used in the production of chemicals for the tanning process (Dettmer et al., 2010) or as reinforcements in different polymer matrices to create composite materials like leather fiber board (Ding C et al., 2017). Other by-products such as trimmings, which may contain chemicals from the finishing, dyeing, fatliquoring, and top-coating phases (less than 7%), have also been reused in the small leather goods, clothing, and footwear industries after being assembled into patchwork designs for secondary markets. Numerous studies have been conducted on the use of leather waste as fillers in both thermoplastic and thermosetting polymer matrices (Pati et al., 2014). Leather waste has been used as a filler in matrices such as epoxy resins (Kale and Jadhav, 2019), high-density polyethylene (Kiliç et al., 2020), natural rubber (Cavalcante et al., 2018), polyvinyl alcohol (Liu et al., 2016), polylactic acid (Ambone et al., 2017), and thermoplastic polyurethane (TPU) (Li et al., 2021) (Nazir et al., 2025). Regarding TPU matrices, Nazir et al. defined the mechanical properties of TPU composites filled with different types of leather waste powders, including wet-blue shavings, glutaraldehyde shavings, chromium-finished leather, and vegetable-tanned leather trimmings, using various waste contents (5% to 30% by weight) and different particle size distributions. The study demonstrated that improved mechanical properties (Young's modulus of 305 MPa) and abrasion resistance are significantly influenced by the average particle size of leather waste, with wet-blue leather offering the best performance due to its optimal aspect ratio.

Thermoplastic polyurethanes (TPUs) are a class of versatile polymers widely used in additive manufacturing (AM) due to their unique combination of flexibility, processability, and durability. These materials consist of two distinct segments: a hard segment and a soft segment. The hard segment is formed by the reaction of an isocyanate functional group with a chain extender, such as 1,3-butadiene-1,4-diol. This reaction creates a rigid structure that provides strength to the material. The soft segment consists of flexible polyurethane or polyester chains connecting the hard segments. The soft segment gives TPUs their elastic behavior, allowing them to stretch and return to their original shape, making them ideal for applications requiring flexibility and elasticity (*Handbook of Thermoplastic Elastomers*, 2014).

In this part of the work, the possibility of using TPU-leather waste compounds as material for Fused Filament Fabrication (FFF) has been studied. Fused Filament Fabrication (FFF), also due to the low cost of the devices, is one of the most widely used additive manufacturing

techniques. This technique, also known as Fused Deposition Modeling (FDM), is a type of additive manufacturing (AM) that falls under the material extrusion category. In this process, a thermoplastic polymer filament is deposited layer by layer to build up a three-dimensional object. The filament is fed through a heated nozzle which melts the material for extrusion. The heated nozzle, controlled by motors, moves across the build area in the x-y plane to form each layer of the object. After completing one layer, the system moves vertically along the z-axis to begin the next layer, repeating this process until the object is fully formed. Additionally, the use of multiple print heads enables the simultaneous extrusion of different materials, allowing for the creation of multi-material objects or designs with complex geometries, including those that require support materials which can later be removed (Ligon et al., 2017).

With reference to natural fibers or reinforcements, some studies have been found in literature about the use of TPU for Additive Manufacturing applications. Composites of thermoplastic polyurethane (TPU) and cork particles obtained from industrial waste at different concentrations have been studied as material for Material Extrusion Technologies (Alvarez Gómez et al., 2023), focusing on the effects of deposition strategy. In another study, the combination of poplar wood particles with TPUs for FFF was reported, analyzing the behavior of different additives (Bi et al., 2018). Others studied thermoplastic polyurethane/lignin composites, with and without carbon fiber (CF) reinforcement, to improve the mechanical properties of the material printed using FFF techniques (Zhou et al., 2022).

No studies have been found on the production of printable material for FFF using TPU and leather fibers from tanning wastes, particularly wet-white, without the use of modifiers or compatibilizers. In this work ground wet-white leather shavings powder has been used to produce TPU compounds at different leather waste concentrations to be used in FFF devices. The compounds have been previously tested for morphological, mechanical, thermal and rheological characterization. Subsequently, printability tests have been carried out by setting different nozzle temperatures and printing speed to identify the range of composite printing process parameters. As a result, this study introduces new opportunities and design strategies for the valuable use of leather waste, promoting circularity in manufacturing processes. By incorporating waste materials, it not only enhances resource efficiency but also contributes to the reduction of environmental impacts, expanding the availability of cost-effective and eco-friendly filament options for Fused Filament Fabrication printing.

Chapter 1:
Reduction of Liquid Wastes

1. Introduction

The concept of environmental sustainability has become increasingly central to the tanning industry, driven by stricter regulatory frameworks and growing consumer demand for environmentally responsible products. The evaluation of environmental impacts associated with tanning processes is critical in supporting sustainable innovations and optimizing industrial performance. Among the methodologies available, the Product Environmental Footprint Category Rules (PEF-CR) for leather, introduced by the European Commission (European Commission, 2018), provide a harmonized approach for the environmental assessment of leather products, ensuring comparability and transparency across different production scenarios.

This section of the work focuses on the characterization and quantification of the environmental impact indicators associated with glutaraldehyde tanning, using the "Faibenelapelle" tool developed by the Stazione Sperimentale per l'Industria delle Pelli e delle Materie Concianti (SSIP) within the GaBi platform by Sphera. This digital tool incorporates the methodological principles of the Product Environmental Footprint (PEF) and supports tanneries in identifying resource consumption, emissions and waste generation throughout the entire production cycle. The SSIP tool enables the evaluation of the environmental impact of each individual phase of the tanning process, allowing for a comprehensive footprint assessment through the quantification of relative contributions and the identification of environmental improvements achieved by implementing optimized process conditions.

Once the environmental footprint of the glutaraldehyde tanning process was established, an optimization study was conducted with the aim of reducing chemical consumption while maintaining performance. The study focused on evaluating the cross-linking efficiency of glutaraldehyde tanning at various concentrations. Two key parameters were used to determine the optimal concentration: the degree of cross-linking achieved and the level of glutaraldehyde exhaustion from the tanning bath. Residual aldehyde content in the wastewater was measured using High-Performance Liquid Chromatography (HPLC). To assess the hydrothermal stability of the tanned leather, expressed by the shrinkage temperature (T_s), an instrumental method based on Dynamic Mechanical Analysis (DMA) was developed as an alternative to the ISO 3380 standard. While replicating the test conditions of ISO 3380, the DMA-based method offers improved control over the heating rate and enables more accurate detection of the transition temperature. This approach reduces result variability and enhances sensitivity to small temperature variations associated with different concentrations of the tanning agent.

Finally, the suitability of the optimized tanning process was validated by producing finished leather and verifying its compliance with Maserati's interior leather specifications, in accordance with standard I.DSPM 020:2018.

In Figure 4 the chart of the arguments involved in this part of the work is reported.

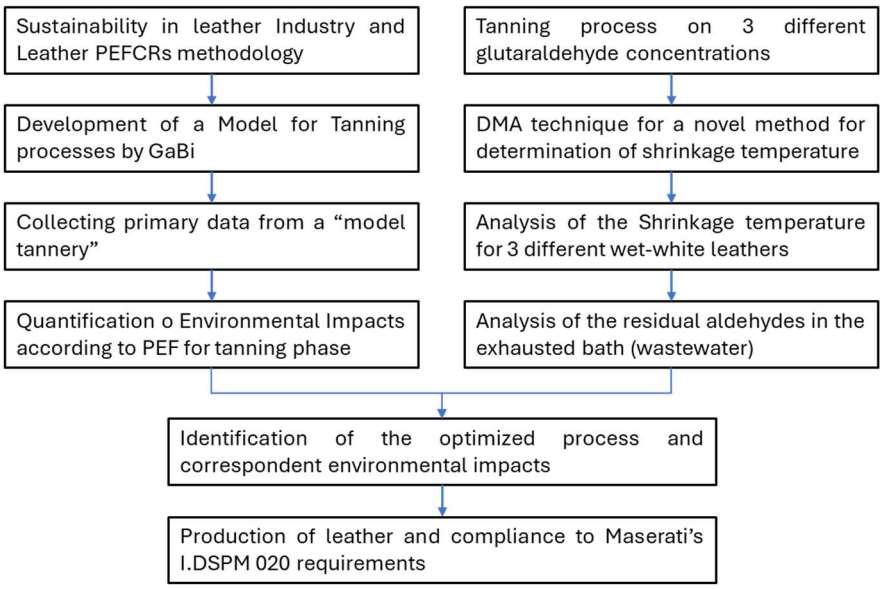

Figure 4 - Chart of the argument in part 1 of the study

2. Environmental Impact, Sustainability and Evaluation Tools

Over the years, the leather industry has seen growing attention to environmental issues, resulting in additional restrictions for all stakeholders in the value chain that go beyond legal requirements. Initially, these restrictions focused mainly on verifying the presence or use of chemical substances with specific ecotoxicological profiles that could pose risks to human health. Over time, system-wide requirements aimed at achieving sustainability goals and raw material traceability have also been introduced, with certification becoming a key tool to meet these objectives.

Public authorities have also aligned with this approach. In the context of public procurement of goods and services, the Ministry of the Environment has implemented an action plan to enhance the environmental sustainability of public administration consumption. This plan is designed to promote and expand Green Public Procurement (GPP), which directs the purchase of goods and services through the application of Minimum Environmental Criteria (CAM, 2018). These criteria are legal requirements aimed at guiding purchasing processes toward the most environmentally beneficial solutions over the lifecycle of a product or service, including monitoring market availability and offerings (e.g., footwear).

Certification processes in the leather industry define environmental sustainability criteria based on three key principles: control of processed raw materials, process efficiency, and pollution prevention and control. Examples of these efforts include:

- *Adherence to specific programs such as the ZDHC MRSL Program*, which manages chemical products to avoid the use and registration of banned substances in leather production, in compliance with brand-specific requirements.
- *LWG (Leather Working Group) certification*, issued by a leading global non-profit responsible for environmental certification in the leather manufacturing industry. LWG certification is the most widely recognized in the sector, with over 1,300 members across the leather value chain, including brands, tanneries, leather traders, manufacturers of leather goods (such as clothing, footwear, and furniture), as well as suppliers of chemicals, machinery, and testing services. LWG sets best environmental practices and provides continuous improvement guidelines.

- *Certification under UNI EN 11427:2015*, "Leather – Criteria for defining the performance characteristics of leather with reduced environmental impact." This standard defines process indicators and their maximum reference values for each stage of production. Environmental indicators are set for resource consumption (water, electricity, including renewable sources, thermal energy, and chemical use) and processing outputs (waste, air emissions, emissions from thermal power plants). Requirements are differentiated between vegetable tanning and other tanning processes.
- *Certifications for supply chain traceability*, which ensure transparency regarding the origin of materials used in production.
- *UNI EN ISO 14001:2015*, the general environmental management systems certification, setting requirements and guidance for implementing effective environmental management systems.
- *EMAS Regulation No. 1221/2009*, the EU's Eco-Management and Audit Scheme, a voluntary tool available to companies and organizations (both public and private, within or outside the EU) to evaluate, report and improve their environmental performance.

The approaches based on these methodologies described above allow the definition of organizations focused on environmental performances, but do not allow a general view of production processes or an effective intrasectoral comparison. For this reason, in the last decade, the *Life Cycle Assessment* (LCA) according to ISO 14040 / ISO 14044 standards approach has been preferred. LCA is a holistic methodology that define a method to analyze the environmental impacts of a product or process from "cradle to grave", that is from raw material extraction to end-of-life disposal or reuse/recycle. LCA approach provides four phases that are: the identification of the scope, the definition of the Life Cycle Inventory, the Life Cycle Impacts Assessments, the interpretation of the results.

Once identified the scope, such as product impact comparison or the definition of an EPD, the process mapping and the production layout are defined to carry out the Life Cycle Inventory (LCI). This activity includes the collection of data on all the inputs involved into production (e.g., raw materials, energy, water) and into the produced outputs (e.g., emissions during transportation or incineration at end of life, solid wastes) for each process in the product's life cycle. Subsequently, the Life Cycle Impact Assessment (LCIA) is carried out

transforming the input/output data previously collected into environmental impact categories, such as:

- *Climate Change*, that measures the emissions of greenhouse gases (e.g. CO_2, CH_4, N_2O) expressed in kg CO_2-equivalent, that is the potential contribution to global warming.
- *Ozone Depletion*, expressed in kg CFC-11-equivalent, that accounts for substances that deplete the stratospheric ozone layer.
- *Human Toxicity*, Cancer Effects that, expressed in comparative toxic units for humans (CTUh), provides an estimation of long-term exposure to carcinogenic substances.
- Human Toxicity, Non-Cancer Effects that, expressed in comparative toxic units for humans (CTUh), provides impacts from non-carcinogenic substances (e.g. heavy metals, solvents).
- *Particulate Matter / Respiratory Inorganics*, expressed as disease incidence or DALYs, that measures health effects from fine dust particles (e.g. $PM_{2.5}$, PM_{10}).
- *Ionizing Radiation – Human Health*, expressed in kBq U235 eq. or DALY assesses exposure to ionizing radiation from sources such as nuclear power.
- *Photochemical Ozone Formation* (Smog), expressed in kg NMVOC-equivalent (non-methane volatile organic compounds) refers to the formation of harmful ground-level ozone due to VOC and NOx emissions.
- *Acidification* (Terrestrial and Freshwater), expressed in mol H^+ equivalent, provides an evaluation of acid rain effects on soil, vegetation, and infrastructure.
- *Eutrophication – Freshwater*, expressed in kg P-equivalent, that measures nutrient enrichment (mostly phosphorus) in freshwater bodies.
- *Eutrophication – Marine*, expressed in kg N-equivalent, that determines nitrogen-driven eutrophication in marine environments.
- *Eutrophication – Terrestrial*, expressed in mol N-equivalent, that considers nutrient overload (nitrogen) in soil ecosystems.

- *Ecotoxicity – Freshwater*, expressed in comparative toxic units for ecosystems (CTUe), that quantifies the potential toxic effects of pollutants on freshwater ecosystems.
- *Land Use*, expressed, for example, in $m^2 \cdot$per year, that provide an estimation of land occupation, transformation or degradation.
- *Water Use*, expressed in m^3, that assesses the direct and indirect consumption of freshwater.
- *Resource Use* – Energy Carriers, expressed in MJ or kg oil-equivalent, that measures the depletion of fossil fuels and other energy resources.
- *Resource Use* – Minerals and Metals, expressed in kg Sb-equivalent (antimony equivalents), that estimates the use of non-renewable mineral and metal resources.

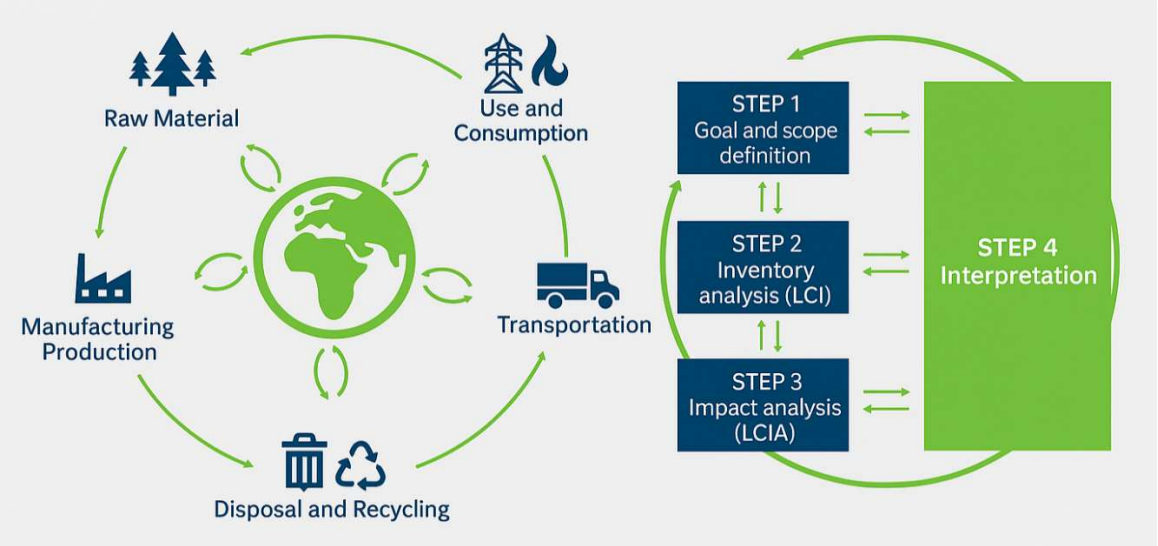

Figure 5 - LCA Assessement Scheme

The final phase of a Life Cycle Assessment (LCA) is the *interpretation* of the results (Figure 5). During this phase, the findings from the LCIA are analyzed and evaluated to draw meaningful conclusions and support decision-making. The goal is to identify the most significant environmental impacts, check the robustness of the data and assumptions and highlight areas where improvements can be made.

Two of the most widely used among these are the Carbon Footprint and the Water Footprint. While LCA evaluates multiple environmental indicators simultaneously, these tools

allow for a deeper understanding of particular impact categories, making them especially useful for targeted environmental strategies and communication. The *Carbon Footprint* focuses solely on greenhouse gas emissions and their contribution to climate change. It measures the total amount of emissions (expressed in carbon dioxide equivalents - CO_2e) that are associated with a product, service, or organization over its entire life cycle. This includes not only direct emissions, such as those from fuel combustion, but also indirect emissions from electricity use and upstream processes, like raw material extraction and transport. The methodology is based on international standards such as ISO 14067 for products and the GHG Protocol for organizational assessments. By quantifying climate impact in a clear and standardized way, the carbon footprint is a powerful tool for identifying emission hotspots and developing effective reduction strategies. Similarly, the *Water Footprint* addresses the use and impact of freshwater resources throughout a product's life cycle. Governed by ISO 14046, this methodology accounts for different types of water use: blue water (surface and groundwater), green water (rainwater stored in soil), and grey water (the volume needed to dilute pollutants). In addition to measuring total consumption, the water footprint considers the geographical context, which is crucial for assessing the true environmental significance of water use, especially in regions where water scarcity is an issue.

3. Product Environmental Footprint (PEF)

The Product Environmental Footprint (PEF) is a standardized methodology developed by the European Commission to assess the environmental impacts of products throughout their life cycle. It is based on Life Cycle Assessment (LCA) principles and aims to provide consistent, transparent and comparable environmental performance data for products in the EU market and align with EU policies like the Green Deal. It includes 16 mandatory harmonized environmental impact categories and uses Product Environmental Footprint Category Rules (PEFCRs) to enable fair comparison between products (EU, 2018).

PEFCRs ensure that all relevant life cycle stages are covered and that calculations are based on high-quality, relevant data. One of the key principles of the PEF methodology, in fact, is ensuring high data quality, with a strong preference for primary data, that is, data directly collected from the company or its contractors. The PEFCRs specify that such data should be applied to all activities that fall under the company's operational control, particularly those that account for a significant share of the product's total environmental impact. To have

a suitable effective representation of product environmental impact, data based on preliminary evaluations should be typically at least the 70 %, so to cover "core activities" like manufacturing, on-site energy consumption, internal logistics, and waste treatment managed directly by the company.

However, in practice, obtaining detailed and reliable company-specific data for all relevant processes is not always feasible, especially when the supply chain is complex or certain processes are outsourced or take place upstream. In these cases, the methodology allows for the use of secondary data, but under defined conditions.

When primary data is not available, the *secondary data* can be collected from published databases, literature, or PEFCR-recommended datasets. This data must meet the data quality requirements defined in the PEF guidelines, which include aspects such as technological representativeness, geographical representativeness, temporal representativeness and completeness and consistency. For solid secondary data collection, the PEFCRs often provides a list of approved background datasets or databases that are considered appropriate. In some cases, PEFCRs provides default datasets for commonly used processes (e.g. transport, packaging materials, electricity mix), which may be used when no primary data is available. In any case this secondary data shall be used only after justification and the reasons shall be documented.

4. PEF Meta-Model for leather production

To assess the environmental impact of the reference automotive leather tanning and to evaluate the potential benefits achievable through process optimization described in the next paragraphs, a tool (SSIP's "Faibenelapelle") has been developed that establishes a calculation model for assessing the environmental footprint of leather products in accordance with the PEFCRs - Leather (April 2018).

For the purposes of this part of the study, this tool allows the complete evaluation of an entire tanning process as sum of the single process phase, that means it allows the isolation of the contribution of the single tanning one. The *Leather PEFCRs* define the life cycle of the production of 1 m² of leather, including the *upstream* phases of "farming", "slaughterhouse" and "preservation," as well as the leather tanning process itself (*core process*), as illustrated in Table 2. In addition, the PEFCR identifies the pre-production phase of "transport," referring

to all transport activities related to the delivery of raw hides to the tannery site. In Table 2 the details of processes to be considered in the PEFCRs are reported.

STAGE	PROCESSES
Farming	Breeding of animals, including: – Feed cultivation. – Feed products preparation. – Animal breeding. – Energy and water consumption for animal raising. – Manure management.
Slaughtering	Animals are professionally slaughtered and flayed (separating the hides or skins from the carcases).
Preservation	Immediately after the animal has been slaughtered, the flayed skin can be subjected to preservation processes to avoid putrefaction. Preservation, i.e. salting, is carried out by specialized companies.
Tanning	Transformation of hides/skins in finished leathers through production processes that can take place at different locations depending on the mix of in-house production and third parties commissioned work. Within the core processes, all tanning activities are considered. From the input side: – Raw hides and skins supply and consumption. – Energy production and consumption. – Water consumption. – Chemical production, supply and consumptions. – Packaging materials production, supply and consumption. From the output side: – Wastewater generation – Wastewater treatment, either performed inside or outside the organization. – Waste generation and treatment. – Air Emissions. – Splits when applicable (flesh and middle splits, when destined to tanning).

Table 2 - PEFCR – Leather processes

4.1. Methodological approach and assumptions for the meta-model

For the definition of the calculation tool, the *tanning* process was defined and developed at a more detailed level than that required by the PEFCR itself, thanks to the direct involvement of a "model tannery" that enabled the detailed classification of individual processes and provided the primary data essential for the quantification of environmental

impacts. The tanning process was therefore broken down into several macro-groups, each containing multiple leather processing steps, so that the final structure of the calculation model related to the *core* tanning stage was defined by the following steps:

- *Analysis of the tanning process* carried out at a model tannery referring to the production of three different leather items, covering all stages of the process that are not outsourced to subcontractors. This allowed for direct access to all primary data related to the process. The three selected references were chosen because they represent three different processing types for bovine hides. The three production processes were integrated to develop a meta-model capable of representing one or the other type of processing.
- The *production process* based on the model tannery was schematized in the form of a flow diagram to identify, among all the variable elements, the key ones to be implemented in the meta-model to ensure the required flexibility to characterize a specific production (eg. wet-white tanning).
- Finally, the meta-model was internally *validated* by assessing the environmental performance of the three reference leather articles produced by the "model tannery".
- Subsequently, for the purpose of the project, given the initial operational impossibility of involving an Automotive tannery, the meta-model was designed based on chrome-tanned bovine hides and was later integrated with information related to the production of glutaraldehyde-tanned hides.

In the model, the life cycle stages included were the following:

- **Livestock farming and slaughtering**, consisting of a single dataset in which the allocation factors defined by the PEFCR are already set, so that no primary data needs to be provided for the relative evaluations.
- **Hide Preservation**, included only for hides transported in salted form. In this case, too, no primary data is required from the client.
- **Transport**: Since the hide supply is company-specific, it is necessary to collect all related data, as detailed in the parameter list (Section 5.4).
- **Tanning process**, subdivided into the following blocks:

1. *Beamhouse:* the listed processes are modelled as a single aggregated process with input data including the kg of hide to be processed (to obtain 1 m² of finished leather from block 12), all chemicals, energy, and water, and with outputs including emissions and, for block 1b, salt that may be classified as waste or co-product:

    1a – Beamhouse operations for fresh raw hides, including trimming, soaking, green fleshing, and unhairing and liming.
    1b – Beamhouse operations for salted raw hides, including trimming, soaking, green fleshing, liming and unhairing.

2 – Mechanical operations post-liming, including fleshing, splitting, and trimming. These are modelled in a series, with the output of one process serving as input for the next. Each process has associated to energy consumption, emissions, yield, and a specific source of electricity, as each can be subcontracted. The model includes the transport for hides sent to subcontractors.

3 – Tanning preparation includes deliming, bating, degreasing, and pickling. All these operations take place in drums and are modelled as a single aggregated process with input data (kg of hides, chemicals, energy, water) and emissions as output. Electricity source selection is also included.

*4 – Trimming of h*ides purchased in pickel: this process is considered only when hides are bought pickled. It may be subcontracted and does not require specifying electricity source.

5 – Tanning operations, includes tanning, draining, and rinsing. This is modelled as a single aggregated process requiring input data (chemicals, water, energy) and output (process yield). The electricity mix may be specified.

6 – Mechanical operations post-tanning includes pressing, wet splitting, wet shaving, and trimming. This block is mutually exclusive with block 2 (splitting is done either post-liming or post-tanning). The four processes are modelled in series, with consumption, emissions, yield, and electricity source assigned to each. Transport to subcontractors is included.

7 – First selection: involves initial quality sorting of hides. This phase does not involve energy consumption as it is performed manually.

8 – Retanning and dyeing operations, includes neutralization, retanning, dyeing, fatliquoring, draining and rinsing. This is modelled as a single aggregated process with input data (chemicals, water, energy) and output (yield). The electricity mix can be selected.

9 – *Drying*: this macro-block may include several drying processes. Given the variability of processes, the model includes four generic drying processes where primary data (including electricity source and consumption) can be entered. Although multiple drying methods can be modelled, they refer to the same input quantity of hide; these are not serial processes with individual yields. The yield is calculated as the total kg of hide output from "block 9" divided by the total kg of hide input into the block. Water consumption is also reported as an aggregated value for the block. The processes have been classified as:

- Hanging dry (drying and stretching using roller systems).
- Overhead chain (hides suspended on a moving system in a ventilated space).
- Vacuum drying (drying under vacuum on heated plates).
- Heated tunnel (drying in controlled hot air tunnels).
- Centrifuge (water removed by centrifugal force).
- Controlled drying (in closed, temperature-controlled chambers).

10 – Dry mechanical operations: This macro-block includes various processes such as toggling, staking, buffing, polishing, flattening, embossing (raised patterning) and others. Due to the wide variety of possible operations, the model includes five generic processes, each associated with its own specific electricity source, energy consumption and potential air emissions, since these operations can be performed by subcontractors. Water consumption data, however, is aggregated. The model also allows for the inclusion of transport data related to subcontractor operations. Starting from process 10 and continuing into 11, the reference flow shifts from kilograms of processed leather to square meters of leather.

11 – Finishing: As with macro-blocks 9 and 10, this block may include several operations. The model defines five generic processes arranged in series. Three of these are modeled as chemical coating processes with quantified consumption of chemicals, energy, and water, as well as emissions of particulate matter and VOCs. The remaining two are physical processes that require only electricity and water as inputs and may produce particulate emissions as outputs. These finishing processes are not associated with a yield value.

12 – Trimming and measuring: Trimming involves removing peripheral imperfections from the leather, such as scraps or irregularities. In this macro-block, total energy consumption for these operations is defined, as well as transport data if performed by subcontractors. The user must also select the electricity mix used. A global yield value is included in the performed processes.

13 – Other parameters: This macro-block includes facility-level aggregated parameters such as: natural gas consumption for thermal energy production, diesel use for internal leather transport, general electricity consumption (warehouses, offices, services, etc.), wastewater production and treatment from the entire tanning process, and different categories of packaging waste (paper, plastic, and hazardous waste).

In Figure 6, the flow chart of the entire tanning process used in the modeling is reported. Furthermore, Table 3 presents the main characteristics of the study for which the meta-model was configured (in line with the specifications of the Leather PEFCR), along with the key assumptions and methodological choices underlying the calculation model.

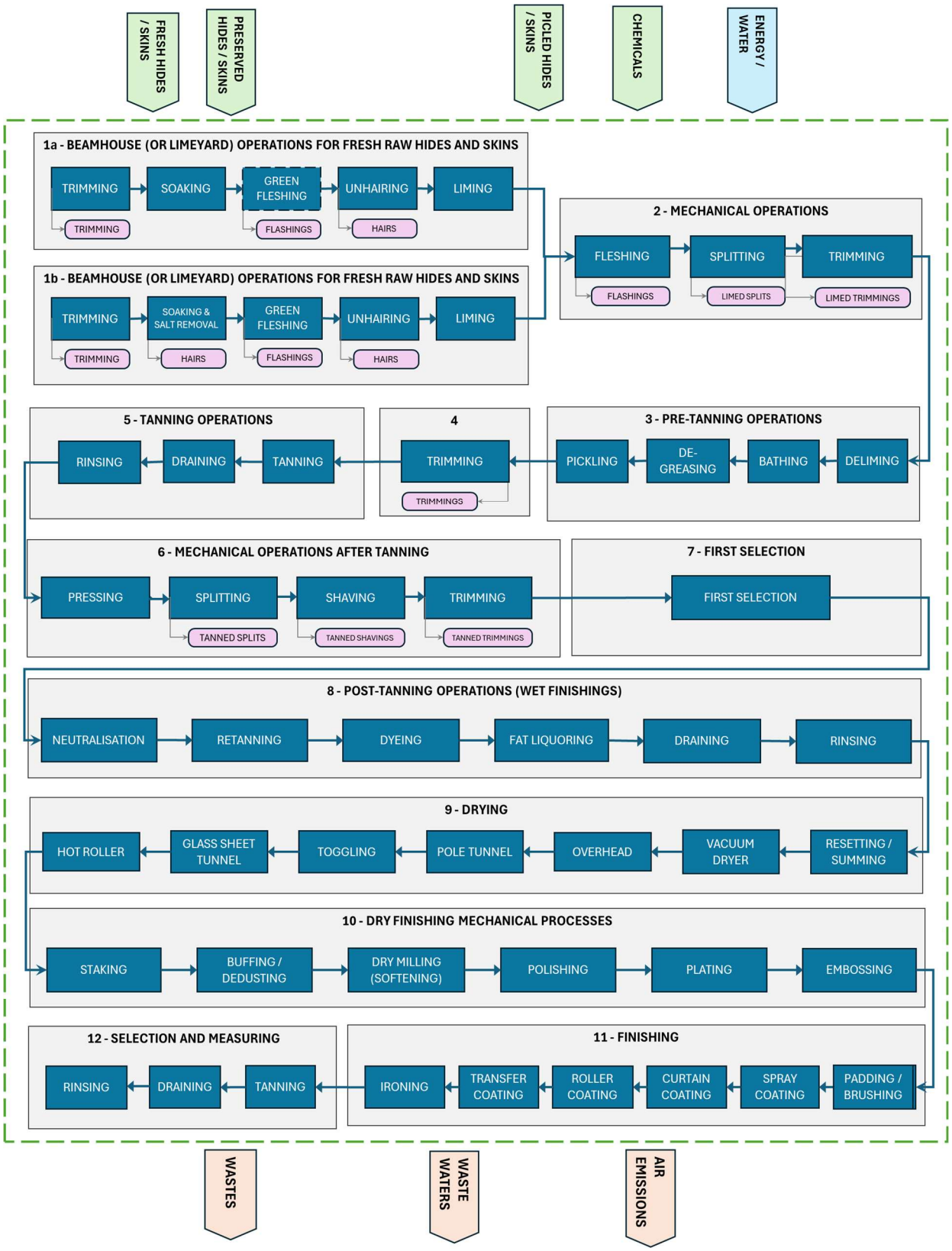

Figure 6 - Flow diagram of the tanning process stages

ELEMENT	DESCRIPTION
Software used	GaBi – Version 10.0.0.71
Compliance	Product Environmental Footprint Category Rules (PEFCR) Leather. Final version 25 April 2018 Product Environmental Footprint Category Rules Guidance. Version 6.3, May 2018
Declared unit	1 m² of finished leather (ready for distribution)
System boundaries	Cradle to gate (i.e., including all upstream processes leading to the production of 1 m² of finished leather, excluding all downstream stages such as distribution, use, and end-of-life)
Reference flow	Defined at the entrance of the tanning process as the amount of material needed for 1 m² of finished leather as output. This value is calculated from primary tannery data (total amount of raw hides purchased during the reference year divided by the total m² of finished leather produced in the same year). If such primary data is not available, the PEFCR provides default values to be used in the model. Throughout the tanning process, this quantity changes due to yield losses in various processes and always represents the quantity to which all consumption and emissions are related in the different processing steps. Between macro-block 10 (mechanical dry processing) and block 11 (final finishing), the reference flow is converted from kg of processed leather to square meters. For block 11, all consumption and emissions are therefore reported per m² of processed leather.
Multifunctionality	Circular Footprint Formula (CFF); CFF parameters: Annex C of PEFCR Guidance v6.3
Methodological approach for co-products	Outputs such as hair and grain or split layers are classified by the PEFCR as co-products. The approach adopted follows the PEFCR, which provides allocation factors based on protein content (9 % for hair; 31 % for split; 60 % for grain). Other outputs that the model tannery classifies as co-products but for which no PEFCR approach is suggested have not been modelled.
Methodological approach for leather waste	Waste generated from processing tanned leather, particularly from mechanical operations (trimming, shaving, buffing, and possibly splitting), has been classified by the model tannery as waste. The most conservative methodological choice was adopted for these: disposal via incineration as hazardous waste, due to the lack of data on recovery processes.
Handling of site-level aggregated data	If data is only available aggregated at the site level and cannot be attributed specifically to the processing of the assessed product, allocation is done based on the square meters of leather produced. For example: annual methane gas consumption of X m³/year and total production of Y m²/year would result in a specific consumption of X/Y m³/m².
Modelling of wastewater pre-treatment	This is a process present in the reference tannery but may not be present elsewhere. It is considered a site-level aggregated data point, with its consumption and emissions reported per m² of leather, calculated by dividing annual totals by the total m² of finished leather produced in the reference year. The model allows energy consumption input for this stage (representative of the forced aeration phases) and oxygen consumption. The two outputs from pre-treatment were modelled based on the following assumptions: • Screenings (solids separated during screening) are disposed of in landfills for biodegradable materials (as they are mostly composed of leather and meat residues). • Sludge from forced aeration is not assigned a specific end-of-life treatment, as the volume of sludge is not subtracted from the total wastewater volume (in m³). The entire wastewater flow is assumed to be treated in a municipal water treatment plant, as suggested by the PEFCR. The dataset used already includes sludge treatment from water sedimentation.
Leather transport	For transport processes, the PEFCR requires primary data collection for the raw hide supply distance. In the meta-model, the purchase of fresh and salted raw hides is kept separate. For each of the two types of hides, it is necessary to identify: • All supply distances (in the case of multiple suppliers); • For each supplier, the transported quantity: i) by truck; ii) by refrigerated truck; iii) by ship. The life cycle stage of transport includes these supplies as well as the transport from slaughterhouses to preservation sites. Due to a lack of information, the following assumptions were made in the model: • Fresh hides are assumed to be transported directly from the slaughterhouse to the tannery. • Salted hides are assumed to be first transported from the slaughterhouse to the preservation site (using PEFCR default distance), then from the preservation site to the tannery (using primary data collected at the tannery).
Capital goods	Not included in the study.
Cut-off	Although PEFCR doesn't allow any cut-offs, consumption of cleaning detergents and machine lubricants were not considered for their negligible impact compared to chemical consumption.
Packaging for chemical supply	The PEFCR considers the supply of chemicals as primary data to be collected from the tannery. Due to the wide range of chemicals used and the need to limit model parameters, packaging data for the model tannery's products was kept fixed. Thus, no primary data collection is required.
Other packaging	Not included.

Table 3 - Characteristics of the calculation model and assumptions

4.2. Modeling of Chemical Substances

Chemical products represent one of the most variables characteristics in the entire tanning process. With reference to the flow diagram of Figure 6, chemicals are used as inputs in the following macro-blocks:

- *1a* and *1b* - for beamhouse operations for fresh and salted raw hides,
- *3* - in pre-tanning operations,
- *5* - in tanning operations,
- *8* - in re-tanning and dyeing operations
- *11* - in finishing operations.

To model each chemical substance, for each process, the following steps were taken involving the collection of primary data:

- The tannery compiled a list of chemical substances divided by macro-block, identifying each one by its commercial name.
- For each substance, the technical data sheet has been analyzed to identify the main component of the chemical product in terms of composition.
- Then, to model the product, this information was cross-referenced with Table 36 in Annex 7 "Default values of the PEFCR": for each product, the compound category was defined based on its function (e.g., acids, degreasing agents, dyes, etc.) and subsequently it was assigned to one of the compound families specified by the PEFCR. Finally, the most appropriate representative substance proposed by the PEFCR was identified. Once the representative substance was selected, Table 36 also indicates the EF (Environmental Footprint) background dataset to be used for modeling.

The primary data collected at the tannery for modeling each chemical substance includes:

- The specific consumption of each chemical, defined for all processes (except macro-block 11) as the amount of chemical needed to process 1 kg of input hide (expressed as kg $_{CHEMICAL}$ / kg $_{HIDE}$). For macro-block 11, the specific consumption is referred to

the square meter of processed leather (kg $_{CHEMICAL}$ / m² $_{LEATHER}$). These specific consumption values can be directly provided by the tanning process recipe.

- Based on the analysis of the technical data sheet of the specific chemical substance, the tannery should also provide the percentage concentration of the main component of the product to which the PEFCR representative substance can be associated. If this information is not available, as a second option the default concentrations reported in Table 4 may be used. It is important to note that, according to the PEFCR, the remainder of the chemical product (i.e., the percentage not represented by the representative substance) is modeled as water.
- The distance of the supplier for the chemical product.

To simplify the model and limit the number of parameters, compared to the primary data required by the PEFCR, the types and quantities of packaging associated with the supply of chemicals and the transportation mode have been kept fixed. Therefore, when a chemical is selected from the list, the type of primary packaging and its specific quantity (expressed as kg $_{PRIMARY\_PACKAGING}$ / kg$_{CHEMICAL}$) defined by the model tannery is directly aggregated with it. This simplification is also supported by the negligible life cycle impact of the packaging of the chemicals used.

FAMILY	REPRESENTATIVE SUBSTANCE	PROCESS	COMPOSITION	MODELLING ACCURACY
Hydroxy-carboxylic acids (Deliming agents)	Adipic	Adipic acid	100.0%	1
	Citric	Citric acid Water, tap	50.0% 50.0%	1
	Lactic	Lactic acid Water, tap	80.0% 20.0%	1
Strong mineral acids	Hydrochloric acid	Hydrochloric acid Water, tap	30.0% 70.0%	1
	Phosphonic acid	Phosphoric acid Water, tap	17.0% 83.0%	3
	Phosphoric acid	Phosphoric acid	100.0%	1
	Sulfuric acid	Sulphuric acid	100.0%	1
Strong organic acids (fixing agent)	Acetic acid	Acetic acid Water, tap	98.0% 2.0%	1
Strong organic acids (clearing agent)	Oxalic acid dehydrate	Adipic acid	100.0%	4
Strong organic acids (pickling and fixing agent)	Formic acid	Formic acid Water, tap	85.0% 15.0%	1

Table 4 - Example of chemicals (acids) from Table 36 Default values of the PEFCR, guideline table for the modelling of chemicals

4.3. Modelling of the electricity mix

The choice of the electricity mix is the same across all macro-blocks, but within some of them, the mix can also be selected at the individual process level. Its definition involves the introduction of parameters, as shown in Table 5. With reference to the block *1a* and based on the availability of supply information, the following options are possible:

1. If the percentage breakdown of the energy mix is available as primary data, along with the necessary supporting documentation, the required mix percentages will be defined as follows: _1a_Ecarbon, _1a_Enat_gas, _1a_Eother, _1a_Epetrol, _1a_ERES. If this information is not available, a value of 0 must be entered.
2. Specify the source of renewable energy between the two main types, by entering the appropriate value for parameter _1a_Eselec_GO: indicate whether it is wind energy and/or hydroelectric energy.
3. Use the residual electricity mix (i.e., the total annual national electricity mix [Italy] minus the share represented by cancelled guarantees of origin).

Select the national electricity mix only as a last option, as established by the PEFCR hierarchy. This applies if a Guarantee of Origin (an electronic document certifying that a specific share of energy comes from renewable sources) is available. In the absence of certified sources (e.g., when not indicated on the electricity bill), the residual electricity mix is used by default. This represents the national annual electricity mix for Italy, excluding the share covered by cancelled guarantees of origin. All tanneries consulted during model development either lack detailed information on their electricity sources or provide data without sufficient geographic detail. Therefore, the residual mix is used as the standard approach.

To these four options, the possibility of integrating self-produced photovoltaic electricity has been added (as in the case of the model tannery). If there is no on-site photovoltaic production, a value of 0 is entered for the parameter _1a_E_PV, and the total specific electricity consumption for the operation (always expressed in kWh/kg, except for macro-block 11) is entered under the parameter _1a_E. Otherwise, if photovoltaic self-production is present in addition to one of the four previously described sources, the total specific electricity consumption of the operation should be split in two contributions:

- In *_1a_E*, the specific consumption from purchased electricity should be entered, calculated as: total specific consumption of the operation × % of purchased energy over the total consumption.
- In *_1a_E_PV*, the specific consumption covered by photovoltaic self-production should be entered, calculated as: total specific consumption of the operation × % of self-produced energy over the total consumed.

PARAMETER	ID	PARAMETER DESCRIPTION
Modelling selection	_1a_Eselec	n. code for electricity switch [1] specific mix, [2] national mix IT, [3] residual mix, [4] GO
Guarantee origin (GO): source selection	_1a_Eselec_GO	n. code for source switch [1] wind, [2] hydro
Amount	_1a_E	[kWh/kg] Electricity consumption per kilogram of input skin
Amount (on site electricity generation from PV)	_1a_E_PV	[kWh/kg] electricity consumption from photovoltaic (on site electricity generation from PV)
Specific mix: power from carbon	_1a_Ecarbon	[%] percentage power from carbon
Specific mix: power from natural gas	_1a_Enat_gas	[%] percentage power from natural gas
Specific mix: power from nuclear	_1a_Enuclear	[%] percentage power from nuclear
Specific mix: power from other sources (waste)	_1a_Eother	[%] percentage power from other sources (waste)
Specific mix: power from petrol	_1a_Epetrol	[%] percentage power from petrol
Specific mix: power from renewable resources	_1a_ERES	[%] percentage power from Renewable Energy Sources

Table 5 - Parameters for the electrical mix. Example for block 1a

With reference to the process of the block *1a,* in Table 5 the parameters of the electrical mix that shall be considered are reported.

5. Free-metal glutaraldehyde tanning for automotive

Glutaraldehyde ($C_5H_8O_2$, see Figure 7) tanning was developed in the early 1959 in the United States at the Eastern Regional Research Center (ARS, ERRC) and in the 1960 was patented (U.S. Patent No. 2,941,859, 1960). It quickly became the most widely adopted metal-free alternative to chrome tanning, primarily due to the substance high-water solubility, an essential property for wet processing stages carried out in drums, its commercial availability and relatively low cost. Glutaraldehyde tanned leathers are classified as “metal-free”, as defined by European Standard EN 15987:2015, according which “metal-free” leathers are

those in which the total content of tanning metals (chromium Cr, aluminum Al, titanium Ti, zirconium Zr and iron Fe), as determined in accordance with EN ISO 17072-2:2019, does not exceed 0.1 % by mass relative to the dry weight of the sample.

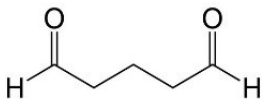

Figure 7 - Molecular structure of glutaraldehyde

For over 30 years, glutaraldehyde tanning has been one of the most widely used technologies in automotive leather production. The choice is motivated both by environmental concerns related to end-of-life and by performance-related aspects of the material. From the sustainability point of view, the use of glutaraldehyde as tanning agent reduces the potential risk of chromium VI formation, which has been always considered a significant concern in automotive applications, minimizing the presence of undesirable metallic residues at the end of the product's life cycle. This applies both from the point of view of the disposal of the finished product (e.g. seats or dashboard covered in leather) and to tannery solid waste such as shavings. However, glutaraldehyde itself has been recently included in the European Chemicals Agency (ECHA) Candidate List of substances of very high concern for authorization. Despite its inclusion in the Candidate List, it could be safely handled in industrial processes, implementing appropriate risk management measures to protect workers, consumers and the environment. For this reason, it remains widely used in many sectors, including the automotive industry.

From the material performances point of view, one of the key reasons for its use is related to its resistance to environmental stresses. Glutaraldehyde-tanned leather demonstrates the best performance in terms of surface dimensional variation resistance under alternating conditions, in comparison with chrome tanned leathers. These characteristics are critical for automotive interiors, where materials must endure extreme thermal (cold and heat) and humid conditions. Regarding these properties, automotive manufacturers, such as Maserati or Porsche, enforce very strict technical specifications, as many interior defects including leather wrinkling and detachment from the underlying substrates are attributed directly to insufficient thermal and dimensional stability of the leather. For leather for interiors (seats, dashboards or trims) one of the most common tests consists in subjecting the material to several alternate

cycles of high and low temperatures combined with high humidity, after which the maximum dimensional change of the sample shall be less than 10%. Figure 8 shows the ageing cycle diagram of the test described in the Maserati specification I.DSPM 020:2018 that, for the qualification of a leather batch, provides a requirement of 11 % of surface variation after 30 cycles at the following conditions: (4 ± 0.2) hours at (10 ± 2)°C and (90 ± 5)% relative humidity, (2 ± 0.2) hours at (120 ± 2)°C with a maximum of 20% relative humidity (1 cycle).

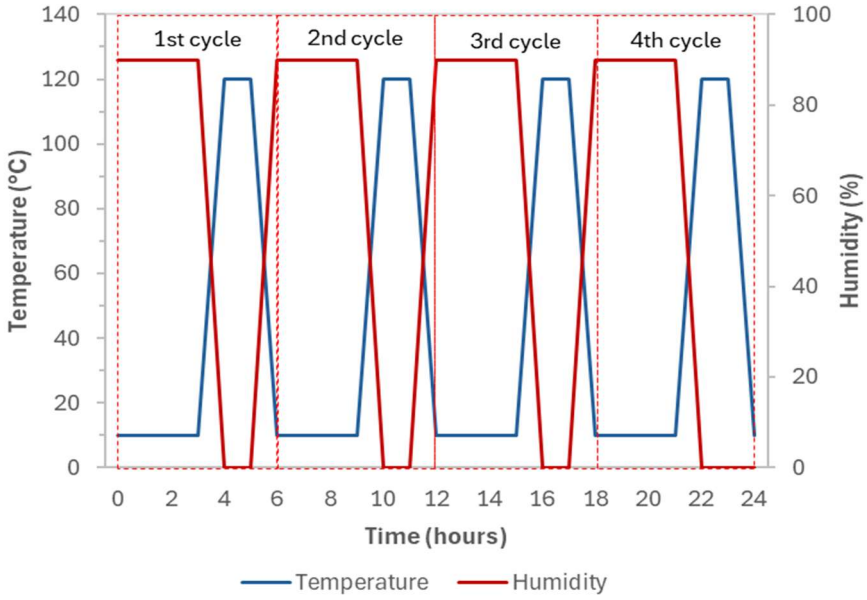

Figure 8 - Alternate ageing test for dimensional stability according to Maserati I.DSPM 020:2018

About the reaction mechanism between glutaraldehyde and skin collagen, it is not yet fully understood. However, as for all aldehyde-based tanning agents, it has been established that crosslinking reactions are involved. These occur between the aldehyde functional groups and the amino groups of lysine or hydroxylysine residues, which are located on the lateral chains of collagen fibers (Figure 9).

(a) *(b)*

Figure 9 - (a) Lysine; (b) Hydroxylysine

Glutaraldehyde contains two aldehyde groups and is therefore capable of reacting with two amino groups. When these groups belong to different polypeptide chains, inter-chain crosslinking occurs, resulting in a tanning effect. The chemical reactivity increases by rising pH above the isoelectric point of collagen and optimal tanning is typically achieved by raising the pH of the tanning bath to values above 8. Furthermore, efficient crosslink formation requires close proximity between polypeptide chains and direct interaction between the amino and aldehyde groups (Figure 10). Due to the relatively low abundance of lysine in collagen (approximately 1 in every 21 amino acids), the probability of effective crosslinking is limited. As a result, glutaraldehyde tanning yields lower hydrothermal stability than chrome one. Indeed, glutaraldehyde-tanned leathers typically have a shrinkage temperature (T_s) slightly above 80 °C, while chrome-tanned one exceed 100 °C (EN ISO 3380) (Sammarco U., 2011).

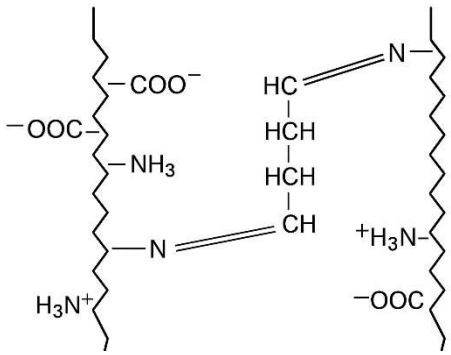

Figure 10 - Glutaraldehyde crosslink between adjacent polypeptide chains

In tanning processes, glutaraldehyde is typically used at concentrations of 2 – 3 % of a 25 % or 50 % solution. Compared to other dialdehydes, it demonstrates superior reactivity and achieves a higher bath exhaustion rate, meaning that the residual aldehyde concentration in the bath is usually only a few percent. In solution, in fact, glutaraldehyde reacts not only with collagen but also with other proteins present in the bath. It is only partially degradable and exhibits high toxicity when unbound. In wastewater streams, if glutaraldehyde remains unreacted with proteins, it can interfere with biological treatment processes due to its biocidal properties (Sammarco U., 2011).

A typical formulation to produce automotive bovine leather is reported in Table 6. This formulation has been considered for the quantification of the environmental impact of

glutaraldehyde tanning according to PEFCR methodology. In Figure 11 an image of bovine leathers in wet state after glutaraldehyde tanning is reported.

%	PRODUCT	T(°C)	TIME (MIN)	OPERATIONS / CHECKS
Pickling				
50	Water	20		
—	Salt	—	10	d = 6.5° Bé
0.5	HCOOH 85%	—	20	
1.2	H_2SO_4 96%	—	120	pH 2.8–2.9 (section passed)
Tanning				
3.0	Glutaraldehyde 25%	—	30	
0.5	Synthetic fatliquor 70%	—	90	
2.5	Solid synthetic tannin	—	60	
2.0	Sodium acetate (powder)	—	30	
0.5	Sodium bicarbonate	—	60	pH 4.0–4.2
0.1	TCMTB	—	—	Automatically rotate 3 min every hour overnight. In the morning: rotate 10 min, check pH 4.0–4.2
150	Water	25	—	Drain
0.5	Sodium bisulfite	—	30	Drain

Table 6 - Recipe of a glutaraldehyde tanning for bovine leathers

Figure 11 - Wet-White Glutaraldehyde tanned leather

6. PEF Quantification for Automotive Glutaraldehyde Tanning

The developed metamodel, as described in paragraph 5, enabled the calculation of environmental impacts for the entire leather tanning process, with the possibility of extrapolating the contributions of individual processes or subprocesses. This makes it possible to intervene at each stage to identify potential alternatives or more rational solutions from a sustainability perspective. By quantifying the environmental impacts, companies can improve their awareness and understanding of their specific environmental footprint, allowing them to adjust process inputs to optimize production and selectively reduce their contributions.

As described above, the glutaraldehyde tanning was not conducted in the "model tannery" and the quantification of the impacts has been carried out by substitution of the tanning agents of the recipe reported in Table 6 in the modeling of the chemical substances. With reference to tanning process described in block 5 of the developed meta-model, the environmental impacts defined in the PEFCRs is reported in the following Table 7.

ENVIRONMENTAL IMPACT	UNIT	VALUE
Acidification terrestrial and freshwater	Mole of H+ eq.	6,76E-03
Climate Change (biogenic)	kg CO_2 eq.	8,88E-04
Climate Change (fossil)	kg CO_2 eq.	1,08E+00
Climate Change (land use change)	kg CO_2 eq.	2,67E-04
Ecotoxicity freshwater	CTUe	1,17E+00
Eutrophication freshwater	kg P eq.	5,70E-05
Eutrophication marine	kg N eq.	8,37E-04
Eutrophication terrestrial	Mole of N eq.	7,94E-03
Cancer human health effects	CTUh	1,08E-08
Non-cancer human health effects	CTUh	6,43E-08
Ionising radiation - human health	kBq U235 eq.	6,40E-02
Land Use	Pt	3,46E+01
Ozone depletion	kg CFC-11 eq.	3,51E-07
Respiratory inorganics	Disease incidences	6,40E-08
Photochemical ozone formation - human health	kg NMVOC eq.	3,15E-03
Resource use, energy carriers	MJ	2,15E+01
Resource use, mineral and metals	kg Sb eq.	3,59E-06
Water scarcity	m^3 world eq.	1,30E+00

Table 7 - PEFCR Environmental Impacts for the Glutaraldehyde tannage

7. Hydrothermal stability of leathers using DMA techniques

As above, to verify the efficiency of the crosslinking by tanning agents is quantified by means of the shrinkage temperature (*Ts*) that represents the hydrothermal stability of leather. The official EN ISO test method to assess this parameter is the ISO 3380:2015 (IULTCS/IUP 16) that provides the immersion of a rectangular leather test piece in a vessel under iso-strain conditions using a special specimen holder. The test is conducted with a controlled temperature ramp of 2 °C ± 0.2 °C per minute starting from ambient temperature up to boiling. One of the clamps on the specimen holder is moveable and connected to a precise displacement measuring device (e.g., a millesimal dial comparator) capable of detecting movements with an accuracy of 0.15 mm. When shrinkage occurs, the indicator moves. The temperature *Ts* corresponding to a contraction of 0.3 % is recorded as the hydrothermal stability of the sample.

This test method, however, has some critical aspects that can affect the results in terms accuracy that, for this part of the study, is considered a very important issue in order to accurately detect small variations in the shrinkage temperature as a function of the glutaraldehyde concentration during the tanning process. The ISO 3380 does not require a device equipped with an automatic detection system; for this reason, on one side, if there is not an automatic means to assess the temperature when contraction occurs, the measurement is directly related to the visual assessment of the analyst. On the other hand, many commercial devices have problems in compliance with ISO 3380 in maintaining constant the rate of heating in the tolerances indicated in the standard (2 ± 0.2 °C/min) that is one of the key parameters of the test. For this reason, for a more accurate assessment of shrinkage temperature a novel and alternative instrumental test method using DMA has been validated. The DMA technique was chosen for its high sensitivity in detecting deformations and applied loads and its precise control over the temperature ramp. In particular, the TA Instruments DMA (e.g., model 850 used in the present study) offers a displacement resolution as low as 1 nm and a force sensitivity of up to 10 µN, with an operating range up to 18 N. These specifications enable highly accurate detection of mechanical transitions, even in materials with minimal deformation responses. Moreover, the integrated data acquisition and analysis software minimizes user-dependent variability, ensuring repeatable and objective results. In literature, alternative methods to ISO 3380 have been already studied, but they do not follow perfectly the key parameters of the standard. For example, a method has been proposed based

on a modification of a Dynamic Mechanical Analyzer (DMA) applied to test specimens immersed in water, which is heated in increments of 5 °C every 10 minutes and the hydrothermal stability is determined by recording the temperature at which a displacement of the specimens due to shrinkage is observed (Cohen et al., 2000). Another study investigated a test method in which the shrinkage temperature is determined using isometric tension measurements by integrating a load cell into a device compliant with ISO 3380. During the heating process, the strain versus temperature relationship is recorded, and the shrinkage temperature is identified by analyzing the peak in the derivative of the stress curve with respect to temperature (Esteban et al., 2021).

Figure 12 - Giuliani Tecnologie Automatic Shrinkage Device mod. TG/GT to ISO 3380

Figure 13 - DMA 850 of TA instrument that is equipped with a submersion film clamp

In the development of the test method the key technical elements of the ISO 3380 have been identified and reproduced with a specific setting of the DMA to guarantee comparability of the results with the traditional device. These key elements are:

- *Iso-strain condition*: to ensure suitable flat condition and a uniform mechanical condition on the sample during heating,
- *Controlled heating rate*: of 2 °C/min for the accurate determination of the shrinkage point,
- *Sensitive displacement measurement*: enabling an early detection of dimensional change,
- *Shrinkage threshold* of 0.3 %, used as the reference for the shrinkage temperature.

In Figure 12 and Figure 13 a device compliant to ISO 3380 produced by Giuliani Tecnologie and the DMA model 850 of TA instrument used are reported.

DMA testing has been carried out using a submersible tensile clamp for polymeric films with an integrated temperature sensor, so that clamped test pieces are totally immersed in water for the entire duration of the test. DMA has been set in iso-strain conditions after the application of a 0.05 newtons preload so that the test piece results properly distended during the test; this condition is necessary to detect the first contraction due to shrinkage. The shrinkage temperature was instrumentally determined from the load/temperature curve by identifying the onset point. The onset point refers to the temperature at which the first measurable change in the material's mechanical response occurs, indicating the beginning of shrinkage. It is defined as the intersection between the baseline and the tangent to the curve at the initial slope deviation. This method allows for an objective and reproducible identification of the start of the shrinkage process, minimizing operator influence.

To verify the performance of the DMA instrumental method compared to a traditional device, a test series consisting of 10 replications was conducted. Both automatic and manual temperature assessments were considered in the case of the traditional device with an accuracy of 0.1 °C. Those tests have the scope to identify eventual differences in the repeability related to the direct measurement of the analyst.

Tests series have been carried out on the glutaraldehyde wet-white leather produced using the traditional recipe of Table 6. In accordance with ISO 3380, to consider the anisotropy of leather, test pieces have been cut from whole leather in two different directions according to ISO 2418 that are with the longer edge of test pieces parallel and perpendicular to backbone.

For the comparison of the results, each dataset was statistically analyzed by verifying the normality of the distributions using the Shapiro - Wilk test and identifying potential outliers through both one-sided and two-sided Grubbs' tests. After the identification of the outliers, the repeability standard deviation (s_r) and repeability limit (r) have been assessed for each level of each method. For the verification of the performances of the tests, no precision data is available in literature or in the ISO 3380 standard; for this reason, the acceptability criteria related to tests in repeatability conditions have been based on the estimation of the expanded uncertainty (U) according to the following requirements:

- compliance with the relationship $r < 2U$.
- fixing a guard band (g) equal to $0.83 \times U$, the performance of the method must be such as guarantee that the ratio between g and the average value is less than or equal to 0.5.

For the estimation of expanded uncertainty (U), the following contributions were considered:

- *experimental uncertainty* (Eq. 1), where the correspondent variance for the combined uncertainty has been corrected with the ratio N/m, that is the samples number in repeability experiment ($N = 10$) divided by the routine number of replications indicated in ISO 3380 ($m = 4$):

$$u_r = \sqrt{\frac{\sum(x_i - x_m)^2}{v+1}} \qquad \text{(Eq. 1)}$$

- *Calibration uncertainty* of the thermometers.
- *Resolution uncertainty* ($a = 0.1$ °C), having a rectangular distribution (Eq. 2):

$$u_a = \frac{a}{\sqrt{3}} \qquad \text{(Eq. 2)}$$

– *Sampling uncertainty*, related to anisotropy of leather in sampling area, that is supposed to have a rectangular distribution (Eq. 3):

$$u_s = \frac{x_{max} - x_{min}}{\sqrt{3}} \qquad \text{(Eq. 3)}$$

The *expanded* uncertainty *U* has been determined using a coverage factor (*k*) that corresponds to a 95 % level of probability at the specific degree of freedom.

STATISTIC		DMA	AUTO	MANUAL
AVERAGE VALUE	**x_m**	73.6	73.9	74.6
REPEABILITY STANDARD DEVIATION	**s_r**	0.21	0.54	0.71
ROUTINE SAMPLE NUMBER	**m**	4	4	4
DEGREE OF FREEDOM	**v**	9	9	9
SHAPIRO-WILKS NORMALITY TEST	**P-value**	1.13	0.79	0.33
	W	0.88	0.96	0.91
	H0	Accepted	Accepted	Accepted
ONE-SIDED GRUBBS' TEST	**G1,n (Largest)**	0.973	1.839	1.185
	G1,1 (Smallest)	1.947	1.319	1.636
	Sk,Lk (0.05)	2.290	2.290	2.290
	Sk,Lk (0.01)	2.482	2.482	2.482
	Outliers	No	No	No
TWO-SIDED GRUBBS' TEST	**G2;n-1,n**	0.737	0.371	0.654
	G2;1,2 (Smallest)	0.355	0.636	0.318
	Sk,Lk (0.05)	0.186	0.186	0.186
	Sk,Lk (0.01)	0.115	0.115	0.115
	(Largest)	No	No	No
	(Smallest)	No	No	No
COMBINED UNCERTAINTY	**$u_{combined}$**	0.9	1.4	2.0
COVERAGE FACTOR	**k**	2.26	2.26	2.26
EXPANDED UNCERTAINTY	**U**	2.1	3.2	4.6
REPEATABILITY LIMIT	**r**	0.7	1.7	2.3
REPEATABILITY VS UNCERTAINTY	**r < 2U**	Verified	Verified	Verified
GUARD BAND	**g**	1.7	2.7	3.8
GUARDBAND ON AVERAGE VALUE	**g/x_m**	0.02	0.04	0.05
GUARDBAND CRITERION	**$g/x_m < 0.5$**	Verified	Verified	Verified

Table 8 - Statistical analysis for test pieces parallel to the backbone

STATISTIC		DMA	AUTO	MANUAL
AVERAGE VALUE	x_m	73.2	73.8	74.3
REPEABILITY STANDARD DEVIATION	s_r	0.41	0.66	0.65
ROUTINE SAMPLE NUMBER	**m**	4	4	4
DEGREE OF FREEDOM	**v**	9	9	9
SHAPIRO-WILKS NORMALITY TEST	**P-value**	0.396	0.7665	0.6819
	W	0.92	0.95	0.95
	H0	Accepted	Accepted	Accepted
ONE-SIDED GRUBBS' TEST	**G1.n (Largest)**	0.971	1.409	1.225
	G1.1 (Smallest)	2.196	2.076	1.837
	Sk.Lk (0.05)	2.290	2.290	2.290
	Sk.Lk (0.01)	2.482	2.482	2.482
	Outliers	No	No	No
TWO-SIDED GRUBBS' TEST	**G2;n-1.n**	0.738	0.556	0.632
	G2;1.2 (Smallest)	0.221	0.357	0.328
	Sk.Lk (0.05)	0.186	0.186	0.186
	Sk.Lk (0.01)	0.115	0.115	0.115
	(Largest)	No	No	No
	(Smallest)	No	No	No
COMBINED UNCERTAINTY	$u_{combined}$	1.3	1.7	2.9
COVERAGE FACTOR	**k**	2.26	2.26	2.26
EXPANDED UNCERTAINTY	**U**	2.8	3.8	6.6
REPEATABILITY LIMIT	**r**	1.3	2.1	2.1
REPEATABILITY VS UNCERTAINTY	**r < 2U**	Verified	Verified	Verified
GUARD BAND	**g**	2.4	3.1	5.5
GUARDBAND ON AVERAGE VALUE	g/x_m	0.03	0.04	0.07
GUARDBAND CRITERION	$g/x_m < 0.5$	Verified	Verified	Verified

Table 9 - Statistical analysis for test pieces perpendicular to the backbone

In Table 8 and Table 9 the results of the statistical analysis for test pieces cut in parallel and perpendicular direction to the leather backbone are reported for each test series. In particular, the results marked as “Auto” and “Visual” (or “Manual”) correspond to the analysis carried out using the traditional device for shrinkage temperature using both the automatic and the visual assessment. In the first section, the general statistics are reported, while in the second one the results of the normality and outliers’ tests have been shown. Finaly, in the third section, the results of the acceptability criteria related to repeatability and uncertainty of measurement are reported. With reference to the results, all the distributions comply with the Shapiro-Wilk’s normality test and no outliers have been found using one sided and two-sided Grubbs’ tests. About the repeability performances, in all cases the criteria on repeability limit versus expanded uncertainty and guard band criteria have been complied.

In terms of repeability and uncertainty, Table 8 and Table 9 show that the novel DMA method provides the greater accuracy, which is crucial in this part of the study for detecting small variations in the shrinkage temperature resulting from changes in the concentration of the glutaraldehyde tanning agent. To validate the consistency of data obtained using DMA with those derived from the equipment specified in the ISO 3380 method, the average values and their respective confidence intervals calculated by applying the guard band were compared. As can be seen from the comparison (Figure 14), the data obtained with the DMA are consistent with the reference data obtained with the equipment reported in ISO 3380.

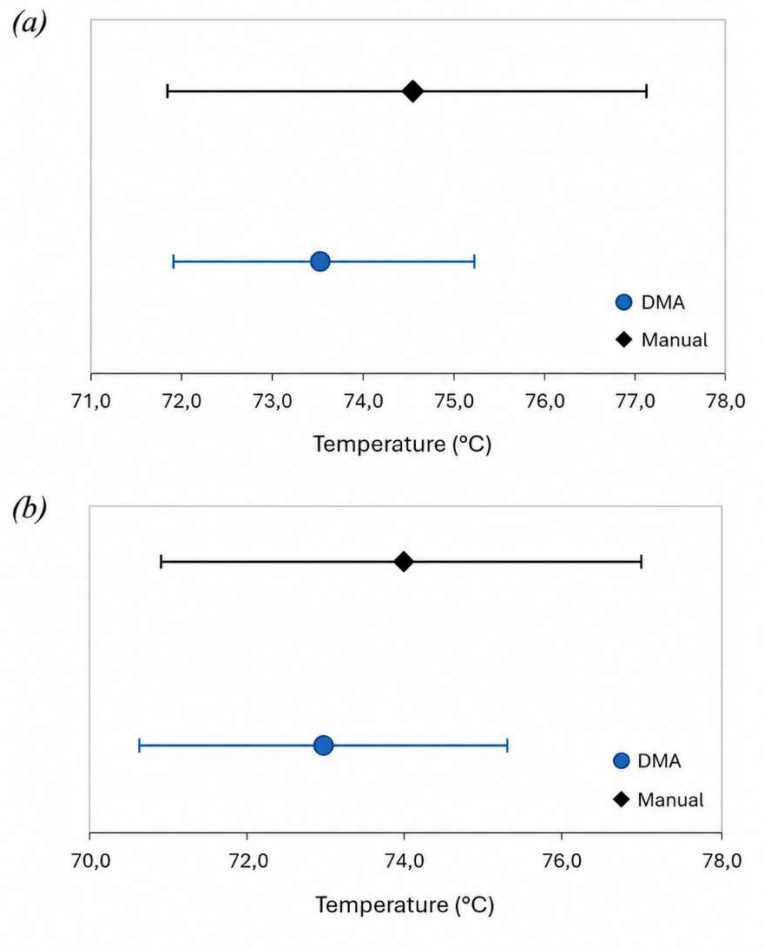

Figure 14 - Comparison of average values and confidence intervals data using the guard band for (a) parallel and (b) perpendicular test pieces

In the end, to visualize the difference in the results, a comparative box plots analysis is reported in Figure 15. Box plot analysis was performed to visualize the distribution of the

data, highlighting the median, interquartile range, and potential outliers. This method allows for a clear comparison between groups in terms of central tendency, variability, and the presence of extreme values through the following parameters:

- *Median (Q2)*: the central line inside the box, representing the 50th percentile of the data.
- *First quartile (Q1)*: the lower edge of the box, corresponding to the 25th percentile.
- *Third quartile (Q3):* the upper edge of the box, corresponding to the 75th percentile.
- *Interquartile range (IQR):* the difference between Q3 and Q1 (IQR = Q3 – Q1), representing the spread of the central 50% of the data.
- *Whiskers*: lines extending from the box to the smallest and largest values within 1.5 × IQR from the quartiles.

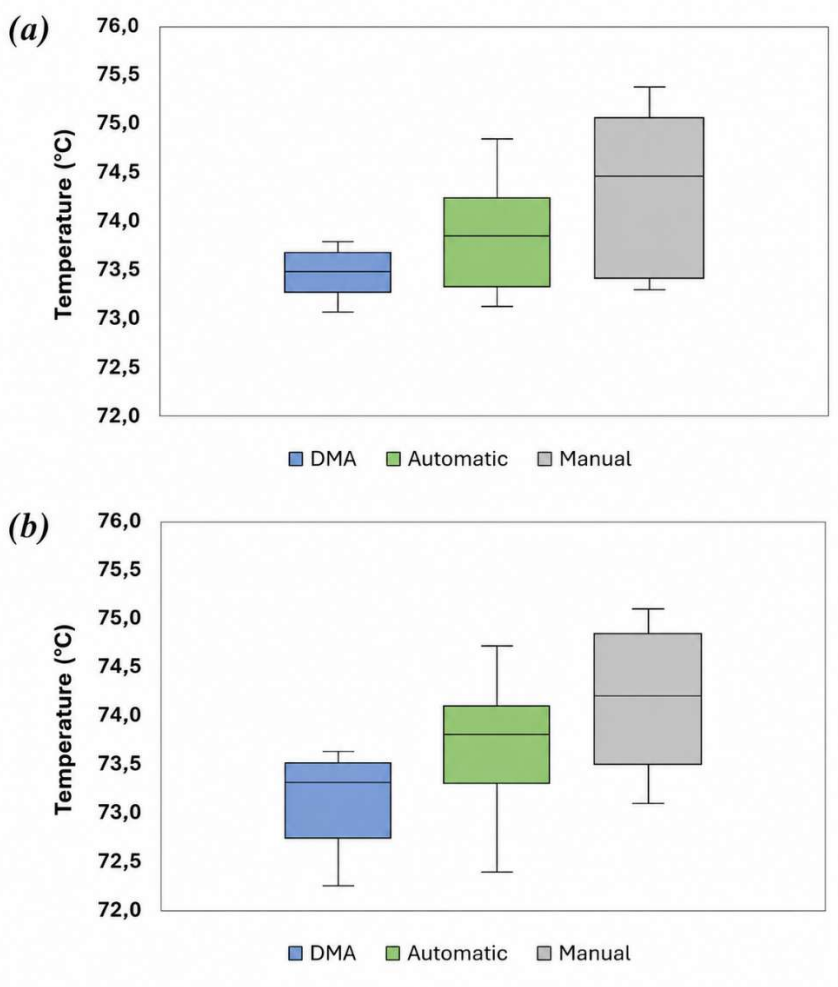

Figure 15 - Box Plot analysis for (a) parallel and (b) perpendicular test pieces

The analysis highlights the following:

- The interquartile ranges (IQR, the box) overlap in all cases, even if for the transverse specimens of DMA and Automatic assessment according to ISO 3380, it is minimal.
- In any case the median falls into the box of the other sample. However, all medians appear to be within the range of comparative sample data.
- In all cases, the data distribution was more dispersed for the visual assessment method according to the ISO 3380 standard, while it was less dispersed for the DMA test method in both sampling directions.
- In all cases, the DMA test method yielded lower shrinkage temperature values compared to the automatic assessment using the ISO 3380 device. The highest values were consistently obtained through visual/manual assessment.

From the results above it is possible to conclude that the application of the DMA method yielded shrinkage temperature results comparable to those obtained using both modes of the ISO 3380 standard (automatic equipment and manual or visual assessment). The data demonstrate that the use of DMA improves the accuracy of thermal measurements. For this reason, the DMA-based method will be adopted for testing leathers tanned with increasing concentrations of glutaraldehyde. The higher precision of the technique allows for more effective detection of subtle variations in hydrothermal stability as a function of tanning agent concentration, thereby enhancing the sensitivity and reliability of the analysis.

8. Tanning Optimization and Environmental Impact Assessment

In order to reduce the wastewater load and achieve a more sustainable process, laboratory-scale tanning trials were carried out by modifying the concentration of the glutaraldehyde tanning agent (Figure 16). The effectiveness of crosslinking was evaluated by determining the shrinkage temperature. Two whole raw hides have been cut in correspondence of the sampling area reported in ISO 2418. For each tanning condition, three to four hide strips with a total mass of approximately 600 – 700 grams were processed using the formulation of Table 6. A commercial glutaraldehyde-based tanning agent was used at a standard concentration of 25%, which served as the baseline recipe and was subsequently reduced by 25% and 50% in the following process trials.

Figure 16 - Laboratory-scale tanning drums

At the end of the processes, shrinkage temperature of leather has been assessed according to the DMA method described above and the residual glutaraldehyde in the tanning bath has been assessed using HPLC method. For the preparation of the sample, the tanning bath has been filtered through a 0.45 µm membrane to remove particulate matter. An aliquot of the filtrate was then subjected to derivatization with 2,4-dinitrophenylhydrazine (DNPH) under acidic conditions, forming stable hydrazone derivatives of the aldehyde functional groups. This derivatization step enhances detectability and selectivity during chromatographic

analysis. The HPLC analysis was carried out using a reverse-phase C18 column, with the mobile phase typically consisting of a mixture of acetonitrile and water (in isocratic or gradient mode, depending on method optimization). The flow rate was set at 1.0 mL/min, and the column temperature was maintained at 30 °C. Detection was performed using a UV-Vis detector set at 360 nm, which corresponds to the maximum absorbance of the glutaraldehyde-DNPH hydrazone complex. Quantification was achieved by comparing the peak area of the sample with those from calibration standards prepared with known concentrations of glutaraldehyde. The results were expressed in mg/L of free aldehyde in the tanning bath. This method ensures accurate monitoring of residual glutaraldehyde, providing critical data for assessing tanning efficiency and wastewater impact.

Table 10 and Figure 17 report the results of the analysis at the different concentration of tanning agents.

PRE TANNING VALUES				POST TANNING VALUES				
N.	**SKIN (g)**	**GTA 0.25 (%)**	**WATER (L)**	**GTA RESIDUAL (g/L)**	**St. Dev**	**FIXED GTA (%)**	**Tg (°C)**	**St. Dev**
SAMPLE 1	681	1.5	0.272	1.50	*0.55*	96%	70.9	*0.32*
SAMPLE 2	655	2.25	0.262	3.38	*0.41*	94%	72.0	*0.40*
SAMPLE 3	663	3.0	0.265	4.50	*0.68*	94%	73.2	*0.21*

Table 10 - Results of glutaraldehyde tanning trials

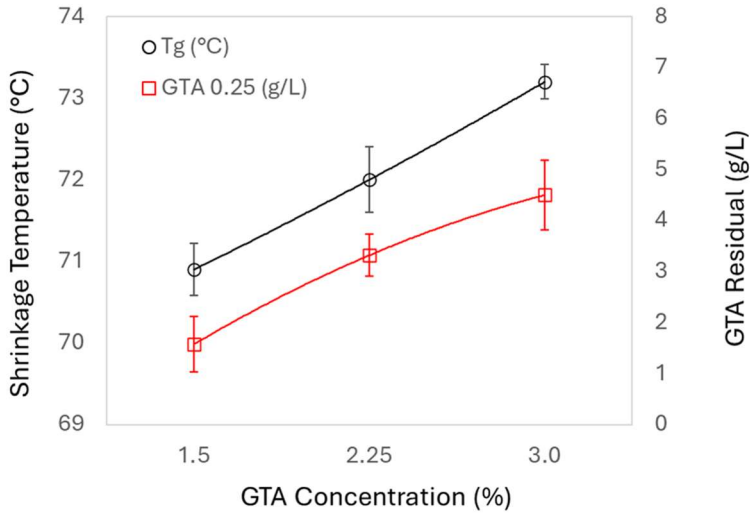

Figure 17 - Shrinkage Temperature and residual GTA in the bath at different concentrations

The reduction in tanning agent concentration leads to a decrease in shrinkage temperature (Tg). However, it provides environmental benefits by lowering the amount of glutaraldehyde used, as shown in the Table 11. Process optimization therefore enables a more efficient use of resources, resulting in improved environmental performance.

ENVIRONMENTAL IMPACT	UNIT	GLUTARALDEHYDE 0.25		
		3.00 %	2.25 %	1.50 %
Acidification terrestrial and freshwater	Mole of H+ eq.	6.76E-03	-1 %	-3 %
Climate Change (biogenic)	kg CO_2 eq.	8.88E-04	-4 %	-9 %
Climate Change (fossil)	kg CO_2 eq.	1.08E+00	-2 %	-5 %
Climate Change (land use change)	kg CO_2 eq.	2.67E-04	-2 %	-4 %
Ecotoxicity freshwater	CTUe	1.17E+00	0 %	-1 %
Eutrophication freshwater	kg P eq.	5.70E-05	-2 %	-4 %
Eutrophication marine	kg N eq.	8.37E-04	-2 %	-4 %
Eutrophication terrestrial	Mole of N eq.	7.94E-03	-2 %	-5 %
Cancer human health effects	CTUh	1.08E-08	-2 %	-4 %
Non-cancer human health effects	CTUh	6.43E-08	-2 %	-3 %
Ionising radiation - human health	kBq U235 eq.	6.40E-02	-3 %	-6 %
Land Use	Pt	3.46E+01	0 %	0 %
Ozone depletion	kg CFC-11 eq.	3.51E-07	0 %	0 %
Respiratory inorganics	Disease incidences	6.40E-08	-1 %	-3 %
Photochemical ozone formation - human health	kg NMVOC eq.	3.15E-03	-2 %	-5 %
Resource use, energy carriers	MJ	2.15E+01	-4 %	-8 %
Resource use, mineral and metals	kg Sb eq.	3.59E-06	-2 %	-3 %
Water scarcity	m^3 world equiv.	1.30E+00	0 %	0 %

Table 11 - PEFCR Environmental Impacts for the different concentrations of glutaraldehyde

It is important to note that the Product Environmental Footprint (PEF) methodology only accounts for input quantities and does not evaluate the quality of wastewater discharges. In this context, using lower glutaraldehyde concentrations also results in significantly reduced levels of residual aldehydes in the bath, which contributes to improved performance in wastewater treatment and reduced environmental impact. Considering a large industrial drum with a capacity between 6,000 and 8,000 liters capable of processing approximately 100 bovine hides, the amount of glutaraldehyde present in the wastewater (excluding contributions from other substances) can be reduced to approximately 25 % and 65 % compared to the

reference formulation. This corresponds to a reduction of about 0.5 to 1.0 kg of chemical products, resulting from process optimization for a single a drum load of 100 hides. Such a decrease leads to significant benefits during the wastewater treatment phase, due to the lower residual aldehyde load entering the depuration system.

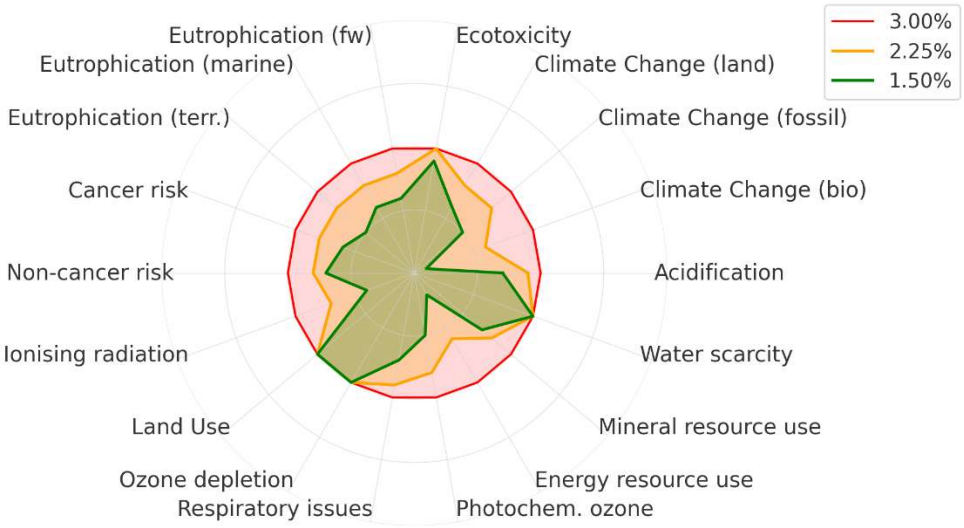

Figure 18 - PEFCR Environmental Impacts diagram for the different concentrations of glutaraldehyde

9. Leather production and Compliance to I.DSPM 020:2018

This section reports the verification of compliance with the Maserati I.DSPM 020:2018 specification for automotive interior leathers. The purpose of this assessment was to confirm that, beyond considerations related to sustainability and material circularity, the optimized tanning and finishing process results in a product fully compliant with the technical and performance requirements defined for premium automotive interiors.

Following the tanning phase, the wet-white leather was subjected to a complete leather processing cycle, including retanning, dyeing, fatliquoring, and finishing, in accordance with the standards and performance requirements established for automotive interior applications. A total of five full hides were produced under controlled laboratory conditions and subsequently tested according to the methods and parameters specified in the Maserati I.DSPM 020:2018 specification. In this specification, the results are reported for each sampling area and direction — Longitudinal (L) and Transverse (T) to the backbone — following the procedures defined in the respective EN ISO test methods and in the technical

specification itself. This approach ensures that the evaluation fully represents the mechanical and surface performance across the entire hide, providing a reliable assessment of product conformity.

DETERMINATION	TEST METHOD	UNIT	REFERENCE	VALUE
Finishing thickness – Specimen No. 1	EN ISO 17186	µm	≤ 30	18
Finishing thickness – Specimen No. 2				21
Finishing thickness – Specimen No. 3				19
Tensile strength – L (Bend)	EN ISO 3376	MPa	≥ 10	11.2
Tensile strength – T (Bend)				10.4
Tensile strength – L (Shoulder)				11.5
Tensile strength – T (Shoulder)				14.1
Tensile strength – L (Belly)				13.1
Tensile strength – T (Belly)				10.9
Tensile strength – L (Butt)				11.2
Tensile strength – T (Butt)				13.3
Elongation at break – L (Bend)	EN ISO 3376	%	≥ 40 and ≤ 60	57
Elongation at break – T (Bend)				47
Elongation at break – L (Shoulder)				49
Elongation at break – T (Shoulder)				51
Elongation at break – L (Belly)				52
Elongation at break – T (Belly)				41
Elongation at break – L (Butt)				53
Elongation at break – T (Butt)				44
Elongation at 20 newtons – L (Bend)	EN ISO 3376	%	≥ 3 and ≤ 10	7
Elongation at 20 newtons – T (Bend)				8
Elongation at 20 newtons – L (Shoulder)				6
Elongation at 20 newtons – T (Shoulder)				6
Elongation at 20 newtons – L (Belly)				8
Elongation at 20 newtons – T (Belly)				9
Elongation at 20 newtons – L (Butt)				8
Elongation at 20 newtons – T (Butt)				7
Surface tensile strength	EN ISO 3379	mm	≥ 7	10.4
Tear load – L	EN ISO 3377-1	N	≥ 25	34
Tear load – T				30
Stitch tear resistance – L	EN ISO 23910	N	≥ 80	81.6
Stitch tear resistance – T				86.2

Table 12 - Compliance to I.DSPM 020:2018, Mechanical tests

DETERMINATION	TEST METHOD	UNIT	REFERENCE	VALUE
Dry finish adhesion – L11	EN ISO 11644	N/10 mm	≥ 4	16.0
Dry finish adhesion – L12				15.4
Dry finish adhesion – L21				11.1
Dry finish adhesion – L22				10.2
Dry finish adhesion – T11				14.5
Dry finish adhesion – T12				8.9
Dry finish adhesion – T21				9.7
Dry finish adhesion – T22				11.4
Wet finish adhesion – L11	EN ISO 11644	N/10 mm	≥ 2.5	7.9
Wet finish adhesion – L12				7.0
Wet finish adhesion – L21				6.1
Wet finish adhesion – L22				8.2
Wet finish adhesion – T11				7.3
Wet finish adhesion – T12				7.1
Wet finish adhesion – T21				6.4
Wet finish adhesion – T22				6.2

Table 13 - Compliance to I.DSPM 020:2018, Adhesion of finishing results

DETERMINATION	TEST METHOD	UNIT	REFERENCE	VALUE
Flex resistance – 100,000 cycles	EN ISO 5402-1	O.V.	= 100,000 / No damage	No damage
Flex resistance after cold conditioning (-10 °C) – 10,000 cycles			= 10,000 / No damage	No damage
Flex resistance after heat and humidity ageing – 10,000 cycles			= 10,000 / No damage	No damage
Taber abrasion after cyclic ageing – Surface effects after 1,800 cycles (CS10, 1 kg)	EN ISO 17076-1	O.V.	= 1,800 / No damage	No damage
		Index	≥ 4	4.5
Martindale abrasion with metal balls – Number of breaks after 1,000 cycles	EN ISO 17076-2	Number	≤ 13	3.0
Determination of surface soiling (EMPA 128) – 1,000 cycles without cleaning	EN ISO 26082-1	Index	2	2
Determination of surface soiling (EMPA 128) – 1,000 cycles after 24 h at 23 °C with cleaning			3.5	4.5
Determination of surface soiling (EMPA 128) – 1,000 cycles after 24 h at 80 °C with cleaning			3	4

Table 14 - Compliance to I.DSPM 020:2018, Surface resistance tests

DETERMINATION	TEST METHOD	UNIT	REFERENCE	VALUE
Colour fastness to heat and high humidity	EN ISO 17228, 7G	Index	≥ 4.5	5.0
Colour fastness to cyclic ageing	EN ISO 17228, 8B	Index	≥ 4.5	5.0
Colour fastness to phenolic yellowing	EN ISO 105-X18	Index	≥ 4	5
Colour fastness to artificial light (3 cycles)	EN ISO 105-B06	Index	≥ 4	5
Colour degradation by dry rubbing	EN ISO 11640 (1,000 cycles)	Cycles / Index	≥ 4.5	5
Colour transfer by dry rubbing		Cycles / Index	4.5	5
Surface effects by dry rubbing		Cycles / O.V.	No effect	No effect
Colour degradation by wet rubbing	EN ISO 11640 (500 cycles)	Cycles / Index	≥ 4.5	5
Colour transfer by wet rubbing		Cycles / Index	≥ 4	4.5
Surface effects by wet rubbing		Cycles / O.V.	No effect	No effect
Colour degradation by perspiration rubbing	EN ISO 11640 (100 cycles)	Cycles / Index	≥ 4.5	5
Colour transfer by perspiration rubbing		Cycles / Index	≥ 4	5
Surface effects by perspiration rubbing		Cycles / O.V.	No effect	No effect
Colour degradation by ethanol rubbing	EN ISO 11640 (5 cycles)	Cycles / Index	≥ 4	5
Colour transfer by ethanol rubbing		Cycles / Index	≥ 4	5
Surface effects by ethanol rubbing		Cycles / O.V.	No effect	No effect

Table 15 - Compliance to I.DSPM 020:2018, Colour fastness tests

DETERMINATION	TEST METHOD	UNIT	REFERENCE	VALUE
Pipe test with lamination – L (Bend)	VDA 230-205 (Method A)	Index	≥ 2	3.0
Pipe test with lamination – T (Bend)				2.5
Pipe test with lamination – L (Belly)				2.5
Pipe test with lamination – T (Belly)				3.0
Pipe test with lamination – L (Shoulder)				3.5
Pipe test with lamination – T (Shoulder)				3.5
Pipe test with lamination – L (Butt)				4.0
Pipe test with lamination – T (Butt)				3.5

Table 16 - Compliance to I.DSPM 020:2018, Loose grain effects results

DETERMINATION	TEST METHOD	UNIT	REFERENCE	VALUE
Shrinkage tension at high temperature – L (Bend)	I.DSPM.020 §6.2.22	kPa	< 85	65
Shrinkage tension at high temperature – T (Bend)				55
Shrinkage tension at high temperature – L (Shoulder)				71
Shrinkage tension at high temperature – T (Shoulder)				79
Shrinkage tension at high temperature – L (Butt)				48
Shrinkage tension at high temperature – T (Butt)				55

Table 17 - Compliance to I.DSPM 020:2018, Shrinkage tension results

DETERMINATION	TEST METHOD	UNIT	REFERENCE	VALUE
Flame propagation rate – Specimen 1	EN ISO 17074	mm/min	≥ 100	0
Flame propagation rate – Specimen 2				0
Flame propagation rate – Specimen 3				0
Flame resistance	EN 1021-1	O.V.	= No	
Hazardous progressive combustion	[3.1 a)]			No
Test assembly exhausted	[3.1 b)]			No
Slow combustion up to the edge	[3.1 c)]			No
Slow combustion through the entire thickness	[3.1 c)]			No
Slow combustion lasting more than one hour	[3.1 d)]			No
Final examination – presence of active smouldering	[3.1 e)]			No

Table 18 - Compliance to I.DSPM 020:2018, Fire resistance results

DETERMINATION	TEST METHOD	UNIT	REFERENCE	VALUE
Surface shrinkage by heat	EN ISO 17130	%	≤ 5	4.9
Surface shrinkage by heat and humidity				4.0
Surface shrinkage by cyclic ageing				4.7
Average thickness (Bend)	EN ISO 2589	mm	≥ 1 and ≤ 1.4	1.26
Average thickness (Belly)				1.39
Average thickness (Shoulder)				1.17
Average thickness (Butt)				1.24
Gravimetric fogging	EN ISO 17071	mg	< 5	4.1

Table 19 - Compliance to I.DSPM 020:2018, other physical tests

Chapter 2: Recycle Solid Wastes for AM techniques

1. Introduction

In line with circular economy principles, the use of TPU-based the production of composites for Fused Filament Fabrication (FFF) has been selected as a possible solution to recycle glutaraldehyde-tanned leather shavings into new composite materials for additive manufacturing. In the present part of the study, after a brief overview on Additive Manufacturing (AM) with a focus on the Fused Deposition Modeling (FDM) family of technologies and specifically on Fused Filament Fabrication (FFF), in this part of the study the following topics will be described:

- Characterization of leather shavings waste, that is the evaluation of physical and chemical properties to ensure that they do not present harmful substances to be used as by-product for FFF applications.
- Morphological characterization of ground leather particles, with reference to the particle size distribution.
- Preparation and characterization of TPU-composites with varying filler concentrations, and different particle size, with reference to mechanical, thermal, and rheological properties.

- A specific methodology was employed to produce filament and the evaluation of FFF printability, aimed at verifying the suitability of TPU–leather shavings composites for additive manufacturing via FFF.

Each type of analysis was correlated with specific issues of FFF, in order to establish direct relationships with the typical challenges encountered during the printing process. This systematic approach aims to demonstrate the technical feasibility and environmental relevance of converting leather waste into printable, functional materials for advanced manufacturing.

2. Introduction to Additive Manufacturing techniques

Additive Manufacturing (AM), commonly referred to as 3D printing, includes a series of technologies to produce objects by sequentially adding material layer-by-layer based on digital models. This contrasts with traditional subtractive manufacturing methods where material is removed from a solid block to obtain the desired shape and geometry. AM offers significant advantages, including the ability to produce complex geometries, reduce material waste and enable rapid prototyping and customization. These capabilities have led to its adoption across various industrial sectors, including aerospace, automotive, healthcare, and consumer goods (Gibson et al., 2015).

2.1 Fused Filament Fabrication (FFF)

According to the standard ISO/ASTM 52900:2021 “Additive manufacturing — General principles — Fundamentals and vocabulary”, AM processes are categorized into different groups. Among them, Material Extrusion (ME) is one of the most used for its simplicity, scalability and versatility, particularly for the application of thermoplastic polymers. Material Extrusion (ME) refers to additive techniques in which material is selectively dispensed through a nozzle where it solidifies to form an object.

Fused Filament Fabrication (FFF), also known commercially as Fused Deposition Modeling (FDM), is the most widely adopted ME technique. It uses a continuous thermoplastic filament, which is fed into a heated head, melted and deposited layer-by-layer along the defined toolpaths (Ngo et al., 2018). In Figure 19 a schematic representation of FFF is reported (Idà et al., 2022).

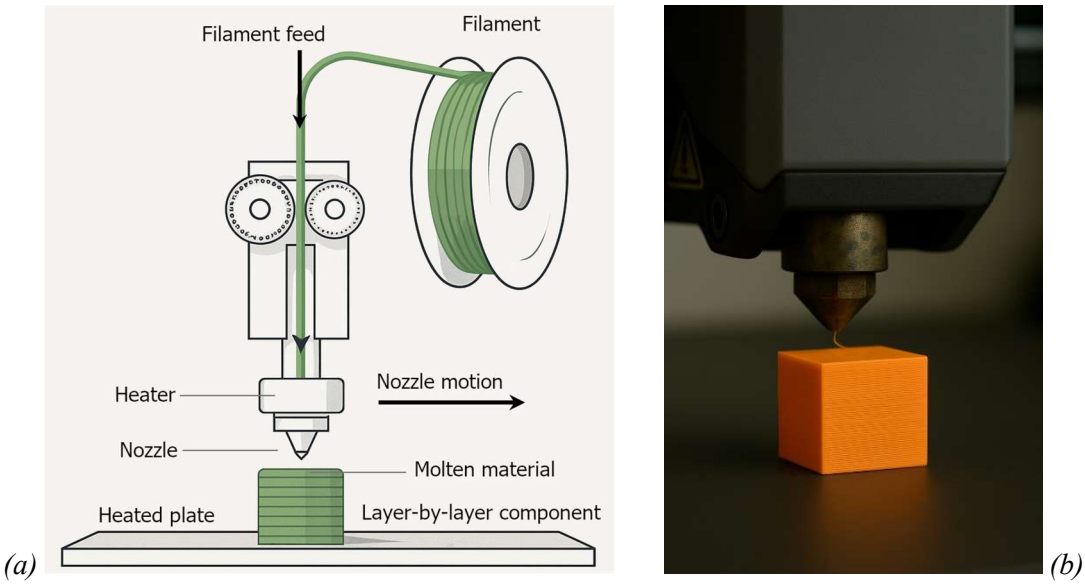

Figure 19 - (a) Scheme of FFF processes and (b) example of layer-by-layer component

During the extrusion process, if the pressure remains constant, the extruded material (the extruded lines are commonly defined as "roads") will flow at a constant rate and will maintain a uniform cross-sectional shape and area. The layer diameter remains constant if the nozzle extrudes the polymer at a constant speed that corresponds to the flow rate. The material that is being extruded must be in a semisolid state when it comes out of the nozzle and must fully solidify while remaining in that shape. Furthermore, the material must bond to the previously deposited one so that a solid layer-by-layer structure can result (Dizon et al., 2018). In this process, the filament thermoplasticity plays a fundamental role because it determines the ability of the filament to bond during the printing process and then solidify at room temperature after printing.

One of the main strengths of FFF technology is its material versatility. In fact, a wide range of thermoplastics and composite filaments are available, having different characteristics suitable for different industrial or commercial applications. The process is simple, cost-effective, and supported by a wide range of materials , from polymers like PLA, TPU and ABS to engineering-grade one like polycarbonate, nylon and TPU (Al-Zaidi and Al-Gawhari, 2023). Furthermore, as with other additive manufacturing (AM) processes based on material extrusion, Fused Filament Fabrication (FFF) also enables multimaterial printing, thereby expanding design flexibility and functional integration.

MATERIAL	PRINT. TEMP (°C)	KEY PROPERTIES	ADVANTAGES	LIMITATIONS
PLA (Polylactic Acid)	180–220	Rigid, biodegradable, low warping	Easy to print, good surface finish, low odor	Brittle, low heat resistance
ABS (Acrylonitrile Butadiene Styrene)	220–250	Tough, impact-resistant	Strong, heat-resistant, widely used	Warps easily, emits fumes, needs enclosure
PETG (Polyethylene Terephthalate Glycol)	220–250	Tough, slightly flexible, moisture-resistant	Strong layer adhesion, chemical resistance	Tends to string, less rigid than PLA
TPU/TPE (Thermoplastic Polyurethane / Elastomer)	210–240	Flexible, abrasion-resistant	Durable, good for gaskets and soft components	Slow print speed, stringing issues
Nylon (PA – Polyamide)	240–270	Strong, durable, flexible	High wear and fatigue resistance	Highly hygroscopic, prone to warping
PC (Polycarbonate)	260–310	High strength and heat resistance	Impact-resistant, transparent	Requires high temp and heated chamber
ASA (Acrylonitrile Styrene Acrylate)	240–260	UV and weather-resistant	Great for outdoor parts, similar to ABS	Still prone to warping without enclosure
PP (Polypropylene)	230–250	Flexible, chemical-resistant, lightweight	Durable, good for living hinges and containers	Poor bed adhesion, high warping
PVA (Polyvinyl Alcohol)	180–200	Water-soluble support material	Excellent for complex multi-material prints	Sensitive to moisture, expensive
Carbon Fiber Composites (e.g., PLA+CF)	200–250	Lightweight, stiff, matte finish	High strength-to-weight ratio	Abrasive to nozzles, may cause delamination

Table 20 - Examples of materials printable with FFF techniques

2.2 Thermoplastic Polyurethane (TPU) in FFF

Thermoplastic Polyurethane (TPU) belongs to the family of thermoplastic elastomers and is characterized by a unique molecular structure consisting of alternating soft and hard domains. Soft domains are characterized by flexible chains, typically polyester- or polyether-based, that provide elasticity and a low glass transition temperature (T_g); at room temperature they remain amorphous and mobile, enabling the material to elastic deformation. Hard domains are formed by diisocyanate-based blocks and extended chains with urethane groups. Due to their strong ability to establish hydrogen bonding, they tend to aggregate, creating semicrystalline or pseudo-crystalline microphases dispersed within the soft matrix. These rigid domains act as reinforcing sites and physical cross-links imparting mechanical stability and abrasion resistance, thereby making TPU highly suitable for demanding applications where resistance to mechanical wear is essential.

Owing to this balance of properties, TPU has become a prominent material in additive manufacturing, particularly in Fused Filament Fabrication (FFF), where it enables the production of functional components requiring resilience and flexibility.

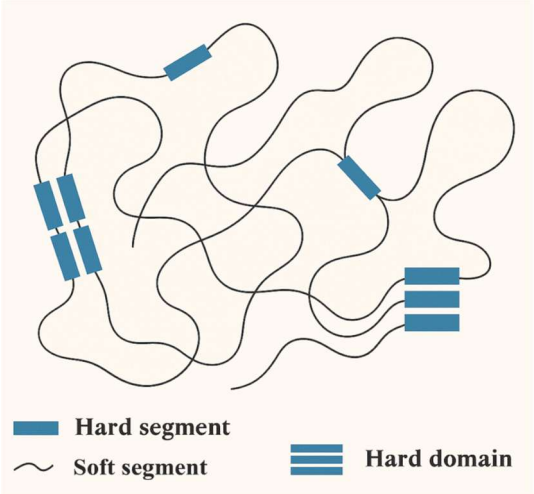

Figure 20 - Schematic representation of TPU structure

Printing with TPUs on FFF machines is a challenging task. The low stiffness of the filaments induces buckling and hinders the extrusion control (Gilmer et al., 2018a), which is intensified the softer the material. Owing to its softness, TPU demands slower print speeds and optimized extrusion systems (preferably direct-drive extruders) to prevent filament buckling and under-extrusion. Moreover, stringing and dimensional inaccuracy are common issues if printing parameters are not properly tuned. The interlayer adhesion is highly dependent on printing orientation, infill strategy, and the use of contour lines; inadequate bonding can lead to delamination and reduced mechanical strength. Despite these limitations, TPU remains attractive for functional components such as seals, gaskets, and flexible hinges, where its elasticity and resilience are essential.

Furthermore, TPU exhibits strong compatibility with a broad range of fillers, including bio-based materials, positioning it as a promising matrix for the valorization of organic residues from industrial and agricultural waste streams. In recent years, several studies explored the incorporation of natural fillers into TPU as new materials for additive manufacturing applications. Examples include cork particles derived from industrial waste, which have been used to produce lightweight and thermally insulating filaments with good printability (Alvarez

Gómez et al., 2023) and wood flour, which, when blended with TPU, improved stiffness and dimensional stability while maintaining adequate processability (Bi et al., 2018). Further developments include TPU blends with thermoplastic starch (TPS) to enhance biodegradability (Lai et al., 2006) and composites reinforced with agricultural residues such as rice husk and microcrystalline cellulose (MCC), which improved thermal and mechanical performance (Mengeloğlu and Çavuş, 2020).

In this paper, the possibility of using TPU–leather waste compounds as feedstock material for Fused Filament Fabrication (FFF) has been investigated, introducing them as a novel circular material within the additive manufacturing framework.

3. Leather waste preparation and characterization

In this section, the analyses carried out on the shavings from glutaraldehyde tanning are reported. Specifically, the investigations focused on two main aspects: on the one hand, the chemical and ecotoxicological characterization, performed in compliance with current legislation (with particular reference to European regulations) as well as sector-specific requirements, in order to classify the waste as by-products suitable for recycling; on the other hand, the morphological and structural features were examined to assess the effects of Additive FFF processing conditions and to identify potential physical and morphological issues of the particulate when used as a filler for TPU in FFF.

3.1 Morphological Characterization of ground leather

When solid leather waste is directly used as a filler for polymeric matrices, mechanical disaggregation processes such as milling or grinding are required to obtain fibrillar, particulate, or powdered forms. The definition of the particle size distribution is crucial, as it strongly influences the interfacial interactions between the filler and the matrix, and consequently the overall properties of the final composite. Since particles with irregular shapes cannot be adequately described by a single dimensional parameter, a more complex parametric analysis is necessary to properly define their geometry and, therefore, their specific surface area. This is particularly relevant in the case of ground leather particles.

This aspect was considered to evaluate whether a high fraction of large particles could lead to imperfections in the printed samples or cause nozzle clogging. In addition, the

definition of a method capable of characterizing particle surface features, rather than relying solely on 2D approximations, was addressed in order to better understand the effects of particle dimensions within the composite filament for FFF.

To verify the efficiency of grinding process and the dimensions of ground particles, a cost-effective image-based test method has been studied for the assessment of the Particle Size Distribution (PSD). The method involves a digital image capture of particulate using an optical microscope and the subsequent image processing using an open-source image editing. In general, the determination of particle size using other image editing software such as Matlab, ImageJ or Photoshop, could be carried out. In the present study, free open-source software for image editing was adopted. The GIMP software was selected since it owns image manipulation features suitable for the scope of the research.

Figure 21 - Grinder (a), glutaraldehyde shavings (b) and ground leather particles (c)

Before grinding, shavings have been dried in oven at 50 °C for 24 hours to eliminate the excess of humidity and volatile substances that could determine problems of agglomeration particles,

the subsequent denaturation of collagen due to the heating of device knives and, so, the impossibility to grind the material. After the conditioning at the temperature above, shavings have been reduced in powder/fibrous state with a grinder model Pulverisette 19 manufactured by Fritsch (Figure 21) using three different sieve dimensions: 0.5 mm, 1.5 mm and 4.0 mm. According to ISO 4044 for the preparation of test samples for chemical tests on leather, grinding has been carried out at 400 r/min, that allows a maximum temperature below 40 °C. Direct characterization of the powder immediately after grinding is not feasible; a pretreatment step involving dispersion in a suitable solvent is required beforehand. The sample powder has been dispersed in ethanol with a ratio of 1:1000 in weight in a Falcon test tube. After agitation of the test tube, the dispersion was transferred into large Petri dishes and left to evaporate at room temperature (Nazir et al., 2025).

When the complete evaporation of ethanol occurs, all the visible particles have been acquired at a magnification of 20x using a Optika microscope model SZP-10 equipped with a high-performance Full HD HDMI camera Optikam HDMI PRO. The image, acquired at a resolution of 1920 × 1080 pixels, was processed using the open-source software GIMP (version 2.10.32). Digital image processing (DIP) was applied to each particle by adjusting brightness and contrast levels, to obtain a white background and a clear definition of particle boundaries. In particular, the following procedure has been followed:

1. Single particles have been isolated from the image,
2. Particle images have been converted to grayscale,
3. The brightness-contrast has been regulated at the first set of values to get a white level of the background of (100, 100, 0) in (R, G, B) units.

After that, the software allows an automatic selection of pixels in the same range of color and so a suitable definition of particle borders. The 2D approximation of the particle surface was determined as the difference between the total pixel count of the image and the selected white area. In some cases, owing to shape inhomogeneity, the overall area of a particle was calculated as the sum of multiple adjacent regions.

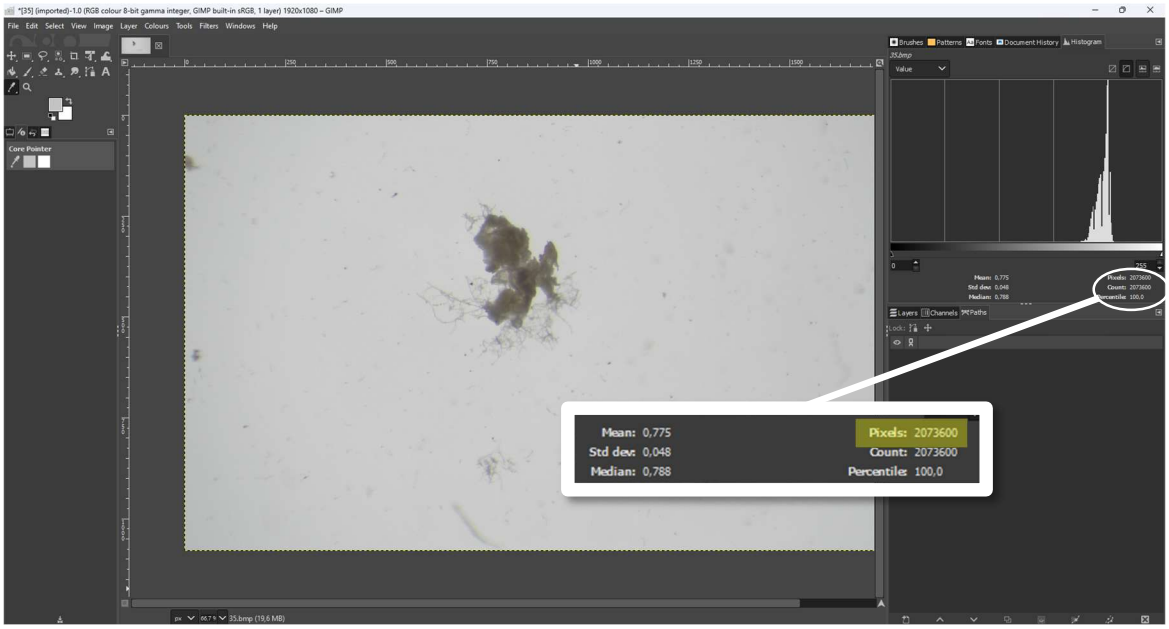

Figure 22 - Gimp v. 2.10.32 image editing software interface

Each particle area was first measured in square pixels and then converted into square microns by applying the pixel-to-length calibration obtained from a reference grid image acquired at the same magnification. For each sieve fraction, more than 500 measurements were collected, and the particle size distribution (PSD) was derived from the corresponding frequency histogram. To define the theoretical particle area, the GIMP software was calibrated using the reference grid image, from which a correction factor was established to convert pixel-based measurements into square microns.

Figure 22 shows the graphical interface of the image editing software, with the 'Histogram' dialogue window activated on the right side. This window provides various information, including the total pixel count within a specified selected area.

Figure 23 shows an example of digital image processing applied to all identifiable particles within the image. For the selected particle, greyscale conversion followed by an increase of 45 contrast points was sufficient to achieve a white background with an RGB value of (100, 100, 0). Particle areas, initially expressed in square pixels, were converted into square microns by applying a correction factor determined from a calibrated grid image acquired at the same magnification. In our case, a correction factor of F = 9.54 was obtained.

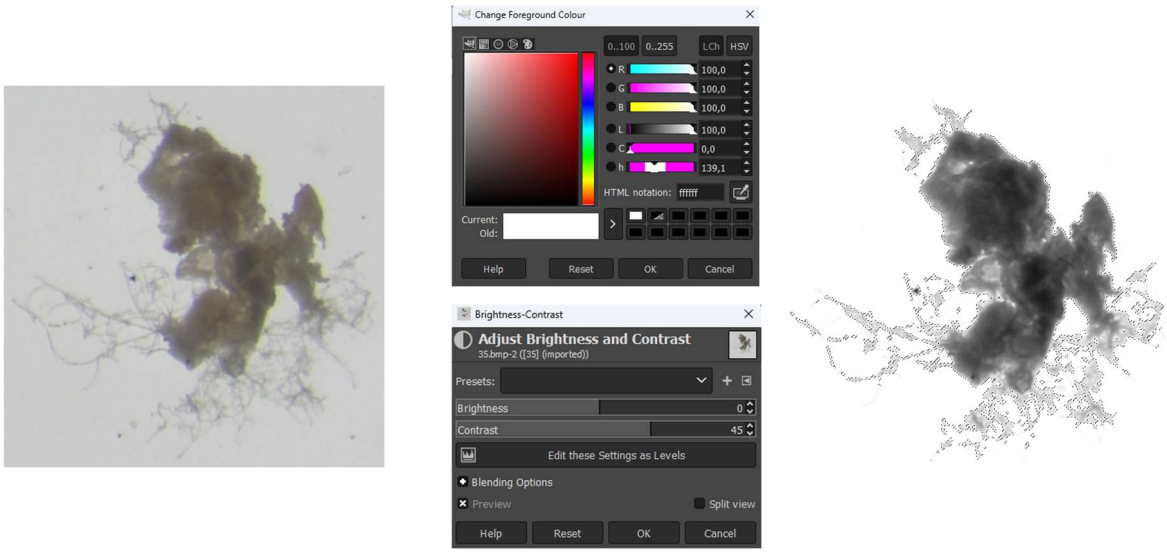

(a) *(b)* *(c)*

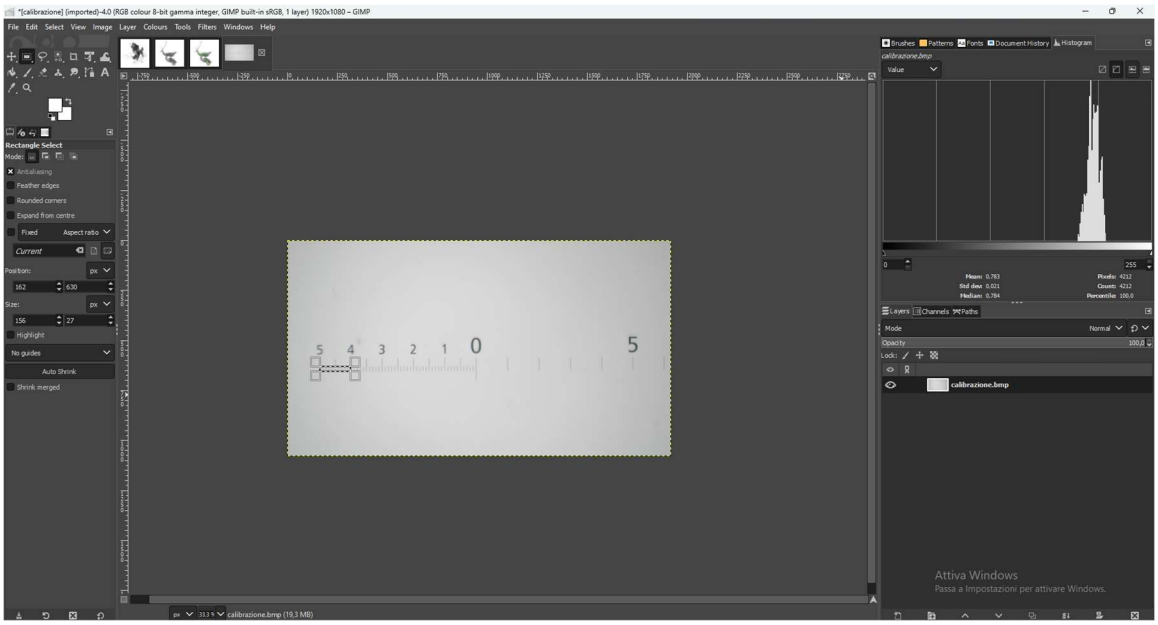

(d)

Figure 23 - (a) Particle, (b) DIP, (c) particle surface after DIP, (d) calibration grid

Particles were characterized not only through a 2D area approximation but also by calculating a specific 'aspect ratio,' defined as the ratio between the particle area and the area of the smallest circumscribing circle. High aspect ratio values indicate agglomerated particles, whereas low values correspond to slender particles such as filaments (Figure 24). This parameter is very important for ground leather particles to be used as fillers in polymeric materials.

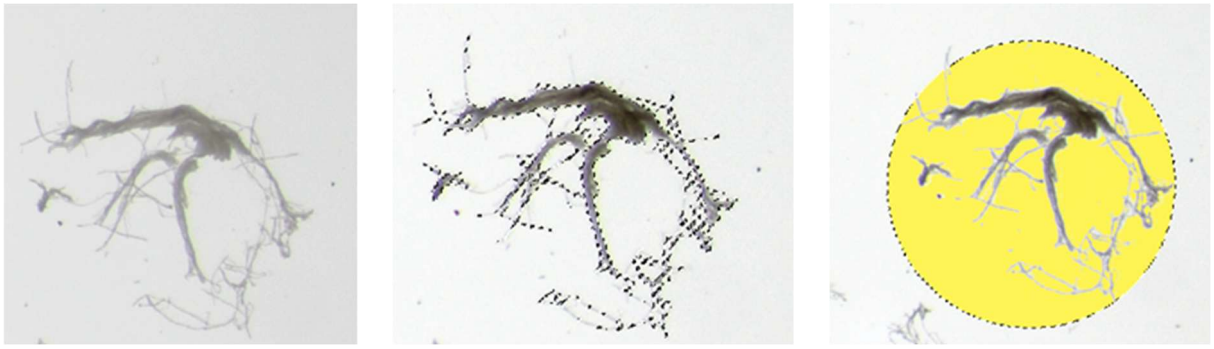

(a) *(b)* *(c)*

Figure 24 - Aspect ratio (a) between (b) surface and (c) smallest circumscribing circle

The particles predominantly appear as agglomerates with complex morphologies resulting from the grinding process. This mechanical treatment generates particulates with heterogeneous shapes, ranging from fibrous structures to irregular agglomerates.

Figure 25, Figure 26 and Figure 27 report the PSDs analysis on samples obtained by grinding and sieving at mesh sizes of 4.0 mm, 1.5 mm, and 0.5 mm, respectively. For each condition, particle size distribution (PSD) analysis was performed to estimate the distribution of particle area and aspect ratio. The three processes yielded average particle areas of approximately 10,000, 7,000, and 7,000 μm^2, respectively.

The results show that the 4.0 mm sieve, as expected, produced larger particles compared to the 1.5 mm and 0.5 mm sieves. The 0.5 mm mesh did not result in a further reduction of shaving size, although it yielded a more homogeneous particle size distribution. From a morphological point of view, figures b show that the 4.0 sieve determines a nonhomogeneous distribution of particles in terms of shape; this means that waste is randomly desegregated in both agglomerated and fibrous states. Instead, grinding using 1.5 mm and 0.5 mm sieves determines a predominance of fibrous state concerning 1.5 mm one. The analysis on the aspect ratio for a sample ground by a 1.5 mm sieve shows as most probable (frequency 30 %), an aspect ratio of 0.1 that is linked to slender objects such as a 1D particulate.

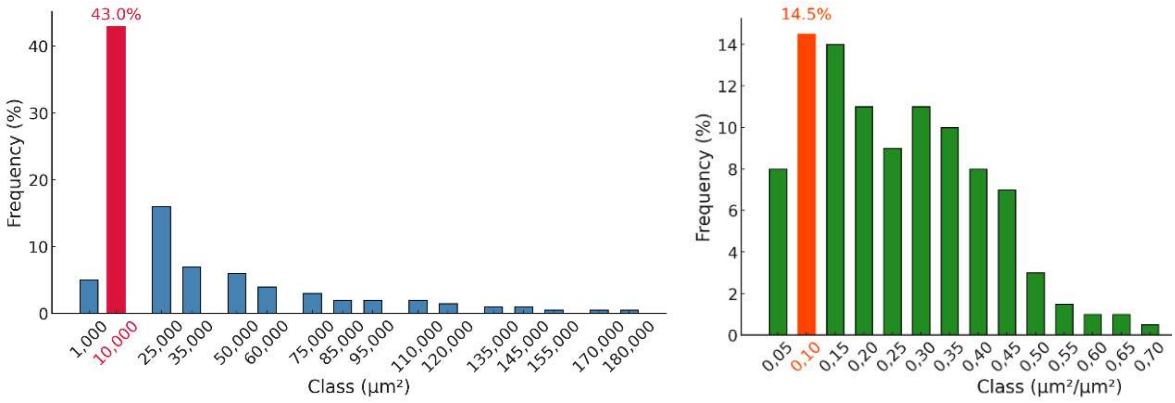

(a) *(b)*

Figure 25 - PSD analysis on wasted ground by 4.0 mm sieve: (a) area, (b) aspect ratio

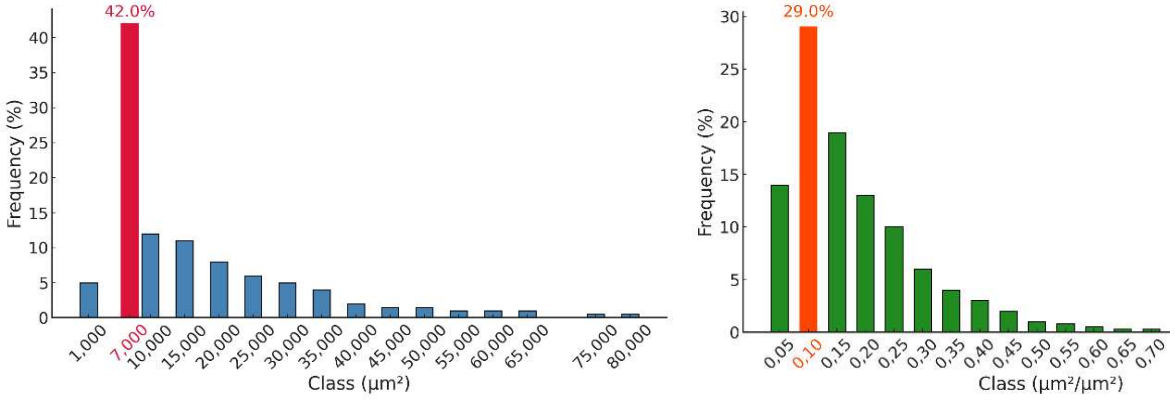

(a) *(b)*

Figure 26 - PSD analysis on wasted ground by 1.5 mm sieve: (a) area, (b) aspect ratio

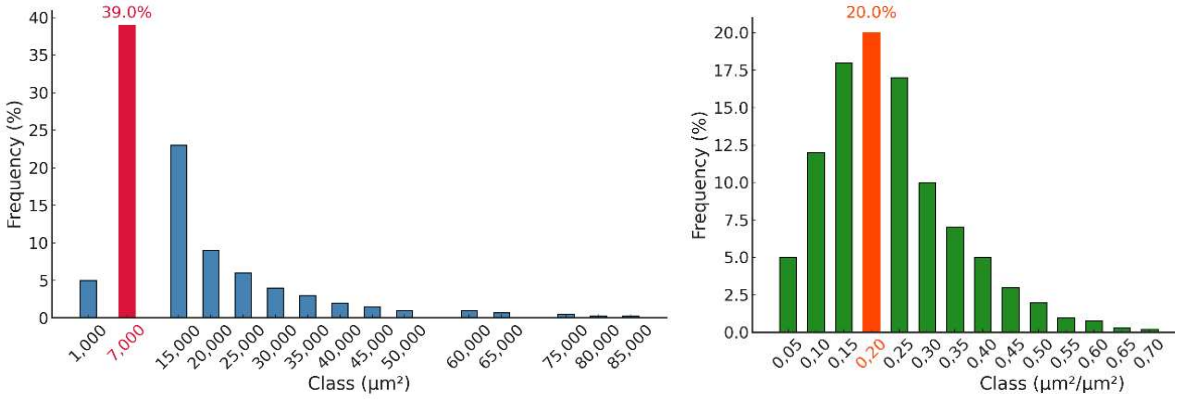

(a) *(b)*

Figure 27 - PSD analysis on wasted ground by 0,5 mm sieve: (a) area, (b) aspect ratio

Concerning the efficiency of the grinding process carried out, comparing the results with a 1.5 mm sieve, the use 0.5 mm sieve does not determine significant benefits in terms of size reduction, also considering the increase in grinding process time.

GRINDING SIEVE	AREA (MAX FREQ.)	ASPECT RATIO (MAX FREQ)	COMMENTS
4.0 mm	10,000 (43%)	0.1 (14%)	Non-uniform distribution
1.5 mm	7,000 (42%)	0.1 (30%)	Uniform distribution, slender shape
0.5 mm	7,000 (39%)	0.2 (20%)	Uniform distribution

Table 21 - PSD Analysis on ground samples

The relatively small size of these particles should have guaranteed a smooth extrusion of the polymer composite in 3D printing, avoiding any clogging of nozzles (Alvarez Gómez et al., 2023). This aspect will be confirmed by the next printability tests.

3.2 Chemical Characterization of ground leather

Chemical and eco-toxicological analyses of the waste were conducted to ensure that the leather waste complies with the requirements established by legislation and other specifications. While these requirements primarily apply to finished leather, in this study they have been considered as a precautionary measure to the leather waste used as filler. Specifically, compliance with Regulation (EC) No. 1907/2006 of the European Parliament and of the Council (Reach, 2006), Regulation (EU) 2022/2400 of the European Parliament and of the Council amending Annexes IV and V to Regulation (EU) 2019/1021 on persistent organic pollutants (POP, 2022) as well as the Oeko-Tex Leather Standard (Oeko-Tex, 2024) have been assessed for specific substances. Additionally, since the material is intended for use at high temperatures in the additive manufacturing process, its compliance with Japan Automobile Manufacturers Association (JAMA) requirements (JAMA, 2023) and Oeko-Tex Leather Standard for VOC emissions was also verified.

As the shavings will be used as a filler for additive manufacturing, it is essential that no hazardous substances are present, and that no volatile compounds are emitted during extrusion or printing processes. The aim of these investigations is to confirm that the waste can be used

as a suitable by-product for compounding with TPU. Given the nature of the tanning agent used, the glutaraldehyde content was also determined in accordance with ISO/CD 25202:2023.

For the quantification of restricted substances, the following instruments were utilized: ICP/MS Thermo Fisher ICAP RQ, HPLC Shimadzu LC 20 AD, Ion Chromatograph Dionex ICS-3000, LC/MS/MS Dionex UltiMate 3000, GC/MS Perkin Elmer Clarus 690, and a pH meter from Mettler Toledo.

Additionally, to complete the characterization of leather wastes, the following tests were carried out: determination of pH following ISO 4045:2018, measurement of substances soluble in dichloromethane according to ISO 4048:2018, determination of sulphated total ash at 800 °C according to ISO 4047:2000, and analysis of humidity and volatile matter at various temperatures according to ISO 4684:2006.

About humidity and volatile substances, the presence of high content could lead to problems during grinding (es. agglomeration), extrusion (voids or defects inside the polymer), or printing processes (clogging of the nozzle). The test temperatures considered are those involved for filament conditioning prior to printing, pre-grinding conditioning, and extrusion process.

Extending as a precaution the leather requirements to the leather waste, Table 22 reports the results of eco-toxicological analysis of glutaraldehyde shavings. As evident, with reference to the listed substances, the leather wastes resulted to be compliant to Annex XVII of Regulation (EC) 1907/2006 (REACh Regulation) (Reach, 2006), Regulation (EU) 2019/1021 on persistent organic pollutants (POP Regulation) (POP, 2022) and Oeko-Tex Leather Standard (Oeko-Tex, 2024) requirements.

The material can, therefore, be considered as a suitable by-product as long as it does not present any critical issues in terms of danger to humans or the environment.

In Table 24, the results of the volatile organic compounds analysis are reported, divided by type into volatiles (VOCs), semi-volatiles (SVOCs) and very volatile organic compounds and carried out on shavings. The results show the compliance with both the JAMA and Oeko-Tex requirements that confirm the absence of eventual hazardous volatile substances at the conditioning, printing and extrusion temperatures. In Table 23 other chemical characteristics of leather waste are reported.

SUBSTANCE	REGULATORY REFERENCE	METHOD	LIMIT	PASS / FAIL
Azodyes	Reg. (EC) 1907/2006 REACh Res. 43	ISO 17234	30 mg/kg	Pass
Hexavalent chromium	Reg. (EC) 1907/2006 REACh Res. 47, Oeko-Tex Leather Standard	ISO 17075-2	3 mg/kg	Pass
Chlorophenol (MCP, DCP, TeCP, TrCP, PCP)	Oeko-Tex Leather Standard	ISO 17070	0.3 – 2 mg/kg	Pass
Dimethyl fumarate (DMFu)	Reg. (EC) 1907/2006 REACh Res. 61, Oeko-Tex Leather Standard	ISO 16186	0.1 mg/kg	Pass
Alkanes, C_{10}-C_{13}, chlorine (SCCP)	Reg. (EU) No 2019/1021,	ISO 18219-1	1500 mg/kg	Pass
Perfluorooctane sulfonate acid PFOA	Reg. (EU) No 2019/1021	LC/MS/MS	0.025 mg/kg	Pass
Perfluorooctane sulfonate acid PFOS			10 mg/kg	Pass
PFOA derivatives			20 mg/kg	Pass
Organostannic compounds	Reg. (EC) 1907/2006 REACh Res. 20	I.M. ISO 17072-2	0.1% tin by weight	Pass
Nonylphenol $C_6H_4(OH)C_9H_{19}$	Reg. (EC) 1907/2006 REACh Res. 46	ISO 18218-2	0.1%	Pass
Nonylphenol ethoxylates $(C_2H_{4O})_nC_{15}H_{24}O$			0.1%	Pass
Nickel	Reg. (EC) 1907/2006 REACh Res. 27	EN 1811	0.5 ug/cm^2/week	Pass
Phtalates (DEHP, DBP, BBP, DIBP)	Reg. (EC) 1907/2006 REACh Res. 51	EN 15777	0.10%	Pass
Phtalates (DINP, DIDP, DNOP)	Reg. (EC) 1907/2006 REACh Res. 52		0.10%	Pass
Formaldehyde	Japan law 112	J.L. 112 Method,	< 16 mg/kg for infants	Pass
	Reg. (EC) 1907/2006 REACh Res. 72	ISO 17226	< 75 mg/kg with contact	Pass
			< 150 mg/kg non-contact	Pass
Glutaraldehyde	Oeko-Tex Leather Standard	ISO/CD 25202	< 1000	Pass
As (Arsenic)	Oeko-Tex Leather Standard	ISO 17072-2	100.0 mg/kg	Pass
Cd (Cadmium)			40.0 mg/kg	Pass
Hg (Mercury)			0.5 mg/kg	Pass
Pb (Lead)			90.0 mg/kg	Pass

Table 22 - Chemical eco-toxicological characterization of leather wastes

TEST ITEM		METHOD	UNIT	VALUE	S.DEV.
Humidity and volatile matter	50 °C	ISO 4684	%	8.3	± 0.8
	65 °C		%	12.4	± 1.1
	80 °C		%	12.6	± 1.3
	102 °C		%	14.7	± 1.9
Substances soluble in dichloromethane		ISO 4048	%	2.2	± 0.4
pH		ISO 4045	U. pH	3.9	± 0.07
Shrinkage temperature		ISO 3380	°C	73.9	± 0.5

Table 23 - Chemical and Physical tests of leather waste

SUBSTANCE	TYPE	OEKO-TEX (mg/kg)	JAMA (mg/m^3)	PASS / FAIL
Bis-(2ethylhexyl) phthalate	SVOC	0.5	0.120	Pass
Di-n-Butyl Phthalate		0.5	0.017	Pass
Paradiclorobenzene		1.0	0.24	Pass
Fenobucarb		-	0.033	Pass
Diazinone		1.0	0.00029	Pass
Cloropirifos		-	0.001	Pass
Tetradecane		0.5	0.330	Pass
Formamide	VOC	0.5	-	Pass
Dimetilformammide		0.5	-	Pass
Amines		0.5	-	Pass
Amides		0.5	-	Pass
Styrene		0.005	0.220	Pass
Xylene		0.3	0.200	Pass
Ethylbenzene		0.3	3.800	Pass
Hexanal		0.5	-	Pass
Toluene		0.1	0.260	Pass
Benzene		0.3	-	Pass
Acetone	VVOC	0.5	-	Pass
Acroelina		0.5	-	Pass
Acetaldehyde		0.5	0.048	Pass
Formaldehyde		0.1	0.100	Pass

Table 24 - VOC results on leather waste

With reference to volatile substances at 102 °C according to ISO 4684, the results show that thermal pretreatment at 50 °C for an effective grinding process leads to a loss of approximately 55 % of the initial humidity content. Additionally, a 6-hours pretreatment of leather powder at a temperature between 65 °C and 80 °C enables the elimination of about 85 % of the initial volatile substances. After assessing the shrinkage temperature of the shavings, a temperature of 70 °C for thermal treatment before extrusion was selected to ensure that leather fibers retain their original state.

3.3 Leather waste FT-IR characterization

To verify whether any changes occur in the morphological structure of collagen within the temperature range under investigation, FT-ATR-IR absorbance spectroscopy was conducted on leather waste samples using a Perkin-Elmer SpectrumOne spectrometer, equipped with Spectrum v5.3.1 software. The spectra of collagen were analyzed after specific thermal conditioning directly on solid samples. Prior to data analysis, the spectra were

baseline-corrected in the 4000–900 cm^{-1} range (64 points) to achieve a flat baseline, minimizing water contributions. The spectra were then smoothed (22 points) to better visualize the peak shapes. Spectral analysis focused on the amide regions: Amide A (3400–3250 cm^{-1}), Amide I (1750–1580 cm^{-1}), Amide II (1570–1480 cm^{-1}), and Amide III (1310–1175 cm^{-1}) (Stani et al., 2020). For each sample, 10 scans with a spectral resolution of 4 cm^{-1} were conducted on 5 different test pieces, and the results were reported as the average wavenumber or intensity.

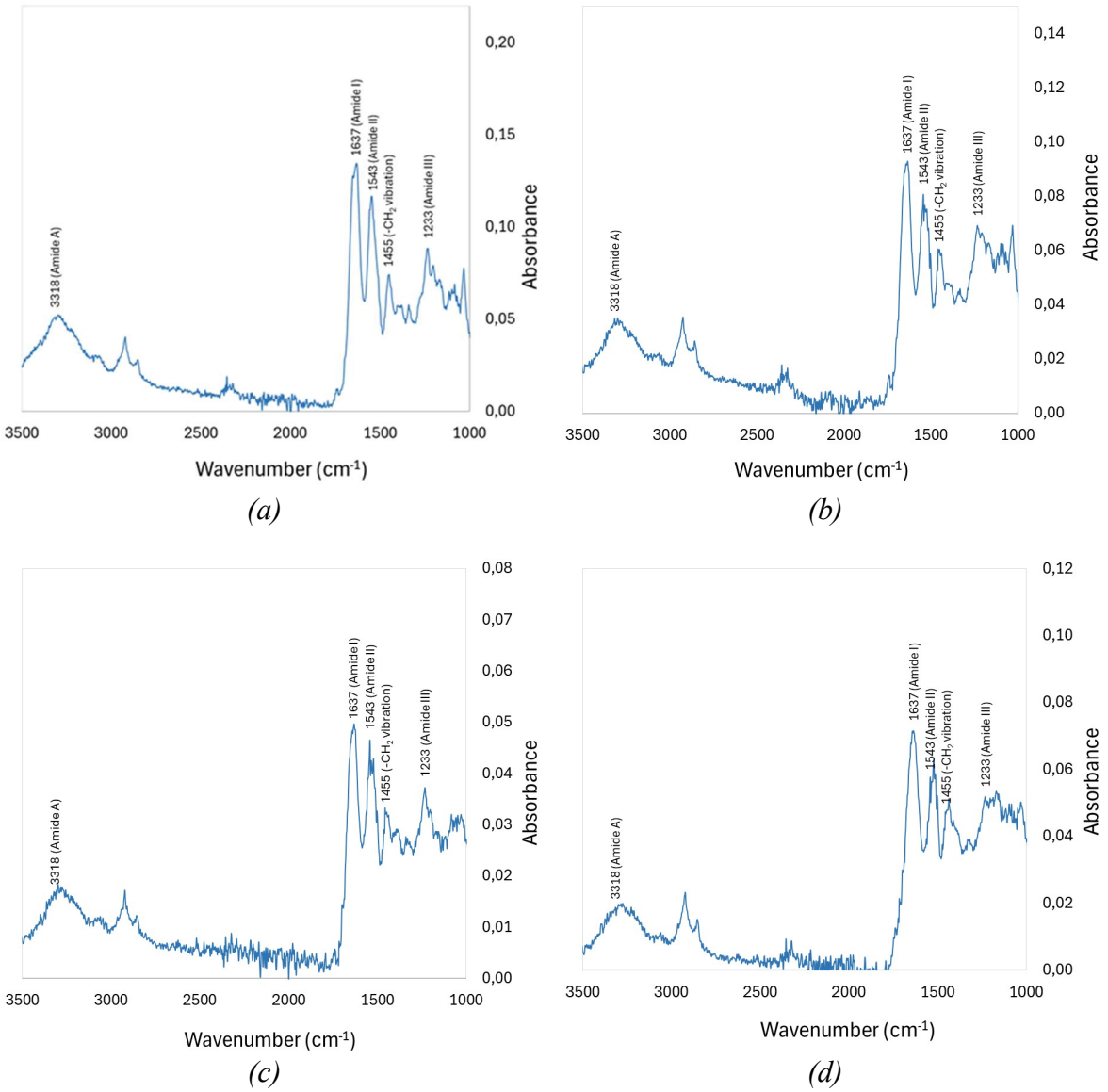

Figure 28 - FT-ATR after conditioning at (a) 23 °C, (b) 50 °C, (c) 65 °C and (d) 185 °C

Samples were conditioned at different temperatures corresponding to specific processes:

- 23 °C for 48 hours, the reference condition for shavings,
- 50 °C for 16 hours, to verify the effects of drying before grinding
- 65 °C for 6 hours, to verify the effects of drying before printing
- 185 °C for 0.25 hours, to verify the effects of high temperatures during extrusion and printing.

In Figure 28, the ATR-IR analysis revealed a substantial preservation of the peaks associated with the collagen structure. Particular attention was devoted to the signal previously described, which confirmed the presence of the triple-helix conformation, a distinctive feature of collagen. However, the ratio between the peaks at 1,240 cm^{-1} and 1,450 cm^{-1}, together with the relative intensity, may suggest the occurrence of partial degradation phenomena affecting the secondary structure of tropocollagen (triple helix) (Gevorkian et al., 2009).

4. TPU-Shavings Composites productions

TPU Hard pellets with an operating temperature between 210 °C and 230 °C purchased from FiloAlpha (Italy) were used as the polymeric matrix. Prior to compounding, TPU pellets and leather shaving powder were dried at 70 °C overnight (Luo et al., 2024). The drying temperature for leather wastes have been chosen after measuring the shrinkage temperature according to ISO 3380:2015 and after determining the volatile substances at different temperatures as described in the next paragraphs.

The compounding of TPU and leather powder was carried out in an Xplore MC 15 HT Micro Compounder (Figure 29) for two minutes at 100 rpm and a temperature of 210 °C. Five compositions were prepared, at weight percentages of 0 wt%, 10 wt%, 20 wt%, 30 wt% and 40 wt% of ground leather in TPU.

For the manufacturing of 1.75 mm filaments for 3D printing, composites were pelletized and extruded again using the same Xplore MC 15 HT Micro Compounder with a continuous feeding at 15 rpm. A Felfil Filament Extruder connected to the Xplore micro compounder was used as a stretching line to control the diameter of the final filament within the range of 1.75 ± 0.02 mm.

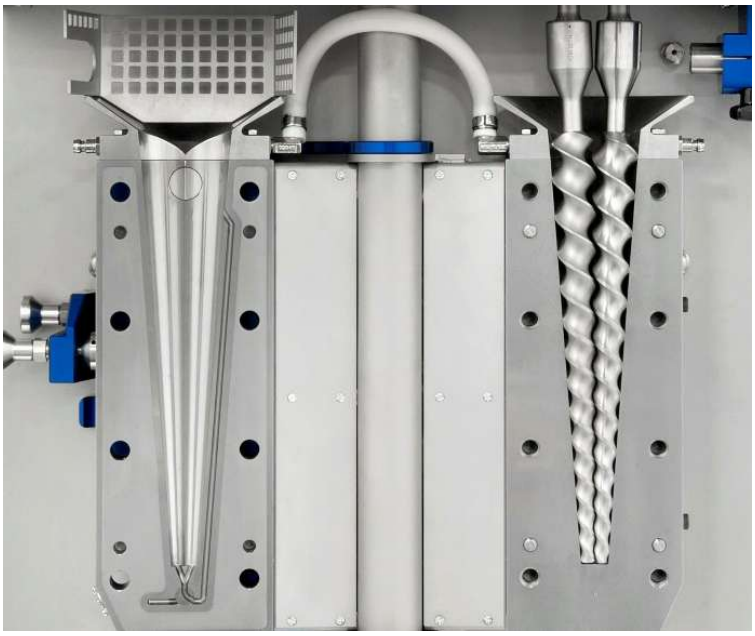

Figure 29 - A detail of the Microcompounder X-Plore MC-15 HT for producing composites

Figure 30 shows a schematic representation of the production process, including a detail of the filament and its surface

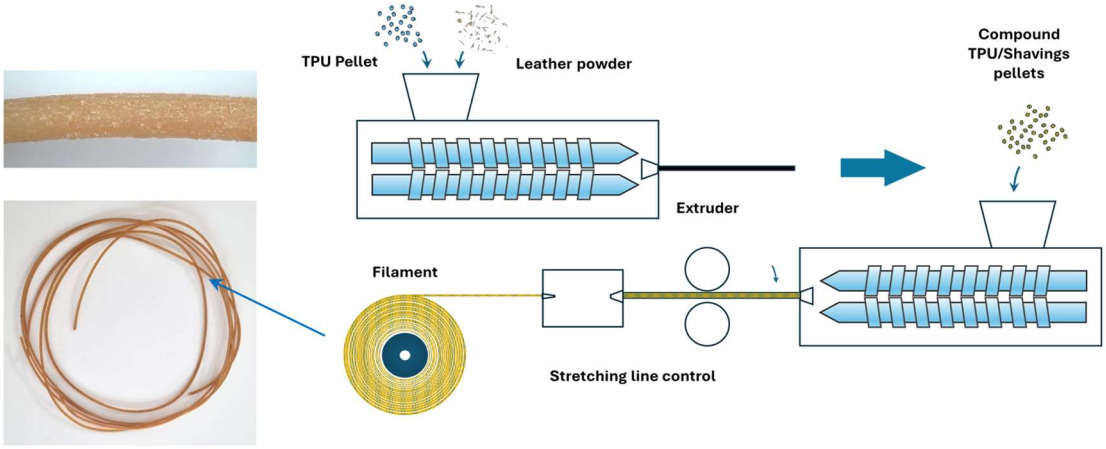

Figure 30: Schematic diagram of TPU/leather shaving filament production

During the extrusion process, it was noted that a filler concentration of 40 wt % determined such embrittlement of the composite that the filament could not be collected and rolled up in the spools for FFF applications without preventing breakage of the filament. This might occur because an excess of leather waste tends to aggregate, disrupting the continuous phase of the

original TPU and restricting the movement of the molecular chains (Wilkinson et al., 2016). For this reason, a content of 30 wt % of leather waste has been identified as the technological limit to produce materials in filament state for FFF Additive Manufacturing techniques.

5. TPU-Shavings Composites Characterization

5.1 Optical and Scanning Electron Microscopy characterization

The surface of filaments produced as well as their cross-sectional areas were analyzed using SEM-EDS Microscope Zeiss model EVO MA 10 to verify the quality of leather power dispersion in the TPU. In particular, the analyses were carried out to assess the wettability of the TPU matrix and to evaluate its surface quality, as these factors can significantly affect the overall quality and surface finish of the printed parts.

Before SEM analysis, the specimens were coated with a 10 nm gold layer using an automatic Sputter coater by Agar Scientific. Microscopic analysis was conducted to visualize the fiber distribution resulting from the composite fabrication via extrusion and to observe the wetting behavior of the fibers by the polymer matrix. This morphological inspection helps to identify possible fiber agglomeration, dispersion uniformity, and the quality of the fiber–matrix interface, which are key factors influencing the mechanical and functional properties of the material (Nazir et al., 2025) and so of the printed objects.

The SEM micrographs of the filament external surface and cross-sectional areas are reported in Figure 31. Image (a) is the surface of neat TPU, images (b) and (c) show the 20 wt % and 30 wt % composites external surface (i) and cross section (j). The morphological analysis of the images shows a good dispersion and adhesion of the leather fibers into the TPU matrix, after the extrusion process.

The increase of the filler concentration seems to determine some agglomeration of leather fiber waste, much more evident in composites containing the 30 wt % of fibers, with a possible negative influence on the mechanical characteristics of the material being points of inhomogeneity. Furthermore, at 30 % filler content, some voids are visible too (Figure 31 b_{i2}), probably related to the local detachments of TPU from the residual high surface fraction of particles after grinding process.

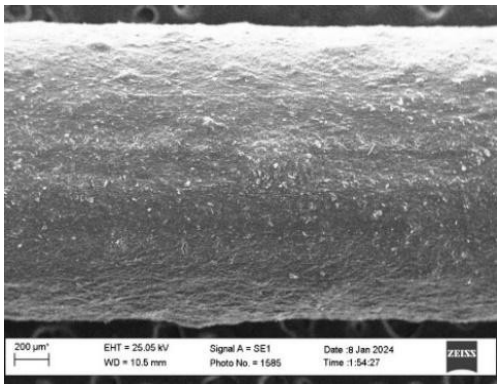

(a)

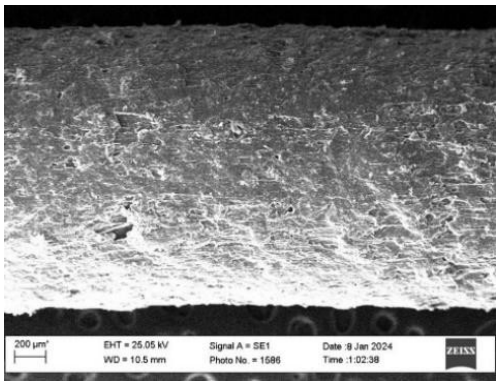

(b_{i1})

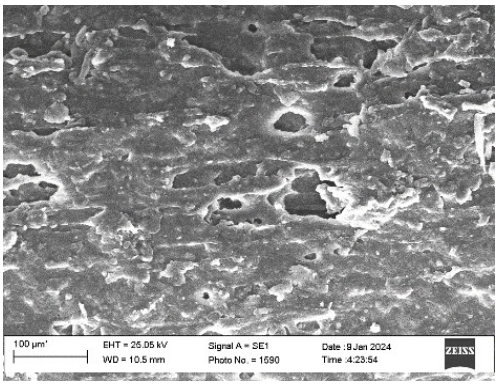

(b_{i2})

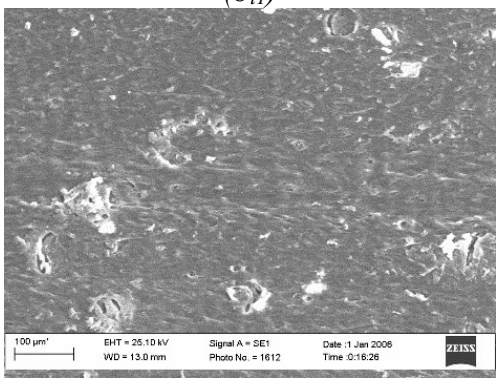

(b_j)

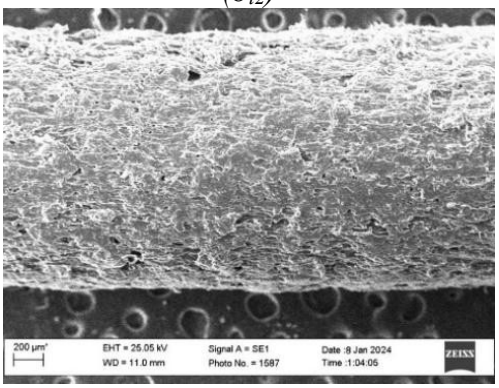

(c_{i1})

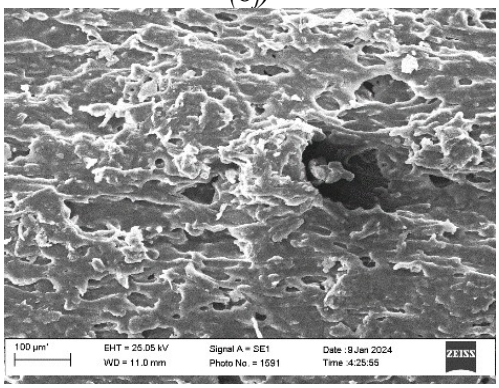

(c_{i2})

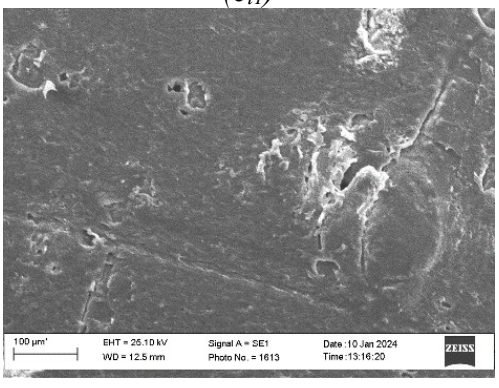

(c_j)

Figure 31 - SEM micrographs of the filaments external surface (i) and cross-sectional areas (j) of TPU (a), 20 wt % (b) and 30 wt % (c) composites.

Finally, as the concentration of the filler increases, the surface roughness of the filament increases due to the presence of particulate, with predictable effects on the surface finish of objects printed via FFF.

5.2 DSC and TGA Thermal Analysis

Thermal Gravimetric Analysis (TGA) and Differential Scanning Calorimetry (DSC) were carried out to identify the decomposition temperatures and thermal phase transitions of TPU, leather waste and their composites. TGA was carried out under nitrogen atmosphere using a TA Instrument TGA 5500 from room temperature to 800 °C at a rate of 10 °C per minute. DSC was carried out with a TA Instruments DSC 25, with heating/cooling cycles between -50 °C and 250 °C, at a rate of 10 °C per minute, under nitrogen atmosphere (Naderizadeh et al., 2025).

The DSC analysis focused on changes in the glass transition temperature, melting temperature, and degree of crystallinity of the polymer matrix. These parameters are particularly relevant for assessing how the presence of collagen-based filler influences the molecular mobility and crystallization behavior of thermoplastic polyurethane. A shift in glass transition or melting temperature may indicate interactions at the filler–matrix interface with consequent changes into polymer chain movement. Moreover, understanding the crystallization behavior is essential for FFF applications, as it can affect the nozzle temperature, the solidification rate and dimensional stability during printing (Rodzeń et al., 2023).

TGA was carried out to evaluate thermal stability by the determination of the onset degradation temperature and maximum degradation rate temperature, that are essential for ensuring the thermal stability of the material within the temperature range typical of FFF processing (i.e., 200 – 240 °C).

The DSC of neat TPU (Figure 32) showed three main features: two glass transitions temperatures, at 0 °C and 118 °C, related to soft and hard segments of the TPU, respectively (Aurilia et al., 2011; Xu et al., 2021) and a small exothermic peak at 183 °C and 204 °C, attributed to a slight degree of crystallinity, most probably within the hard segment region of TPU (Nofar et al., 2019).

The DSC analysis highlighted how the addition of the leather filler determines some variations in the properties of the material, with reference to the crystallization and melting temperatures. Adding leather into the TPU determines significant variations of both temperatures (Figure 32.b). Increasing the leather powder concentration determines a shift in the melting temperature of pure TPU towards higher values from 205 °C to 221 °C which can be ascribed to a reduction in the mobility of the polymeric macromolecules due to the presence of the filler. Similarly, the TPU crystallization temperature showed a noticeable temperature shift from 106 °C to 162 °C that can be related to a nucleating effect of the filler particles (Figure 32.c) (Khalifa et al., 2020).

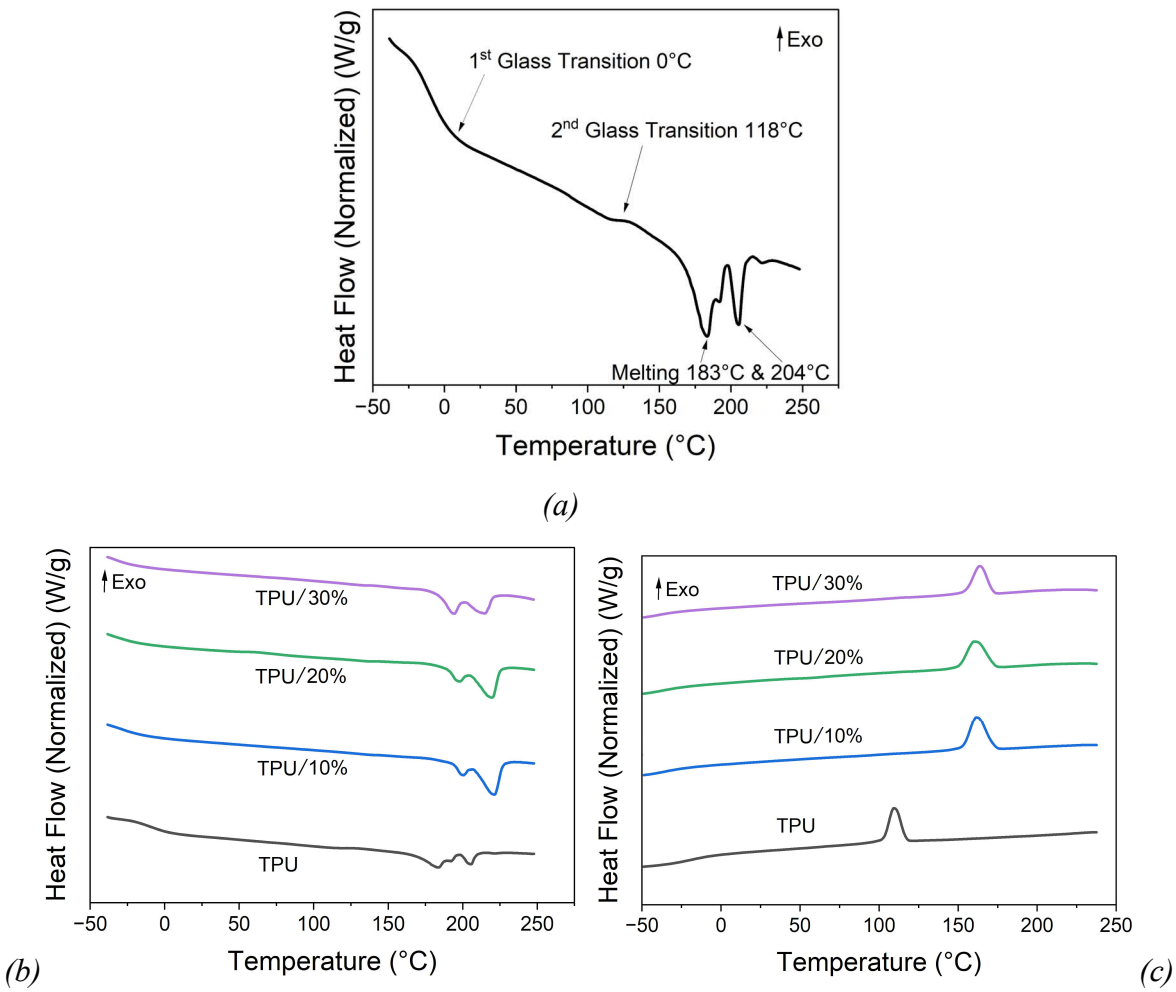

Figure 32 – DSC curves: a) DSC second heating curve of TPU; b) melting temperatures of TPU/leather powder composites; c) crystallization temperatures of TPU/leather powder

However, the comparison of the exothermic peaks between TPU and composites with different concentrations does not highlight evident variations in the amplitude of the peaks for the composites, i.e. the degree of crystallization remains constant as the filler concentration varies.

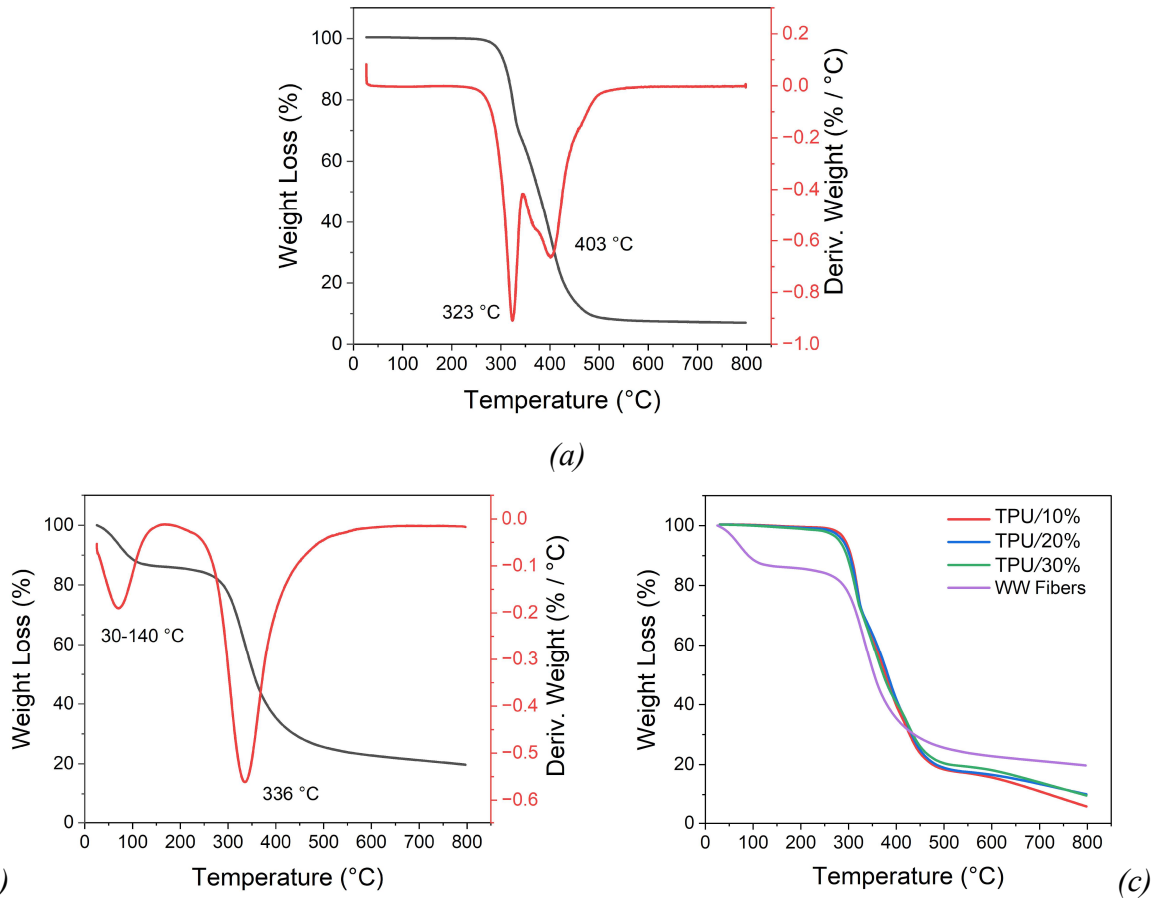

Figure 33 - TGA curves: d) TGA analysis of TPU; e) TGA analysis of wet-white shavings leather fibers; f) TGA curves of TPU composites, compared with wet-white (WW)

The TGA analysis in nitrogen (Kannan et al., 2013) of glutaraldehyde shavings powder, TPU and their composites are reported in Figure 33.a, b and c. For TPU the decomposition begins at 323 °C, that corresponds to the dissociation of urethane groups and the subsequent formation of diols, di-isocyanates and CO_2 (Tabuani et al., 2012). A second degradation peak occurs at 403 °C (Figure 33.a), that corresponds to the decomposition of the soft segment of the TPU, leading to the formation of a complex mixture of molecular species derived from the fractioning of polyol segments. After 600 ° C, a solid residue of approximately 6 - 7 % can be

detected. Results with increasing filler content do not markedly delay the initial degradation process, while the decomposition profiles showed notable differences. TPU composites with higher filler loadings exhibited broader degradation ranges and a more gradual weight loss slope, suggesting a more complex degradation mechanism likely due to interactions between the polymer matrix and the proteinaceous nature of the fibers (Figure 33.c) (Naderizadeh et al., 2025).

TGA analysis in nitrogen of glutaraldehyde wet-white waste showed two distinct degradation steps (Figure 33.b): the first, between 30 °C and 140 °C, is related to the loss of humidity and volatile substances (as described above), while the second, between 270 °C and 500 °C with a peak at 336 °C, is related to the decomposition of its collagenic structure. A third degradation step can also be observed at temperatures between 500 °C and 800 °C and it is related with the carbonization of the material with a solid residue of about 15 - 25 %.

In relation to the printing trials, the increase in the melting temperature with higher filler concentrations revealed in DSC analyses is a factor that must be considered in the subsequent setting of printability tests. Moreover, TGA results indicated that no material degradations are expected at the extrusion and printing temperatures.

5.3 Rheological Testing

The rheological behavior of TPU and its composites was assessed by measuring the complex viscosity in a frequency sweep test. Discovery Hybrid Rheometer (Rheo-DHR3) by TA Instrument was used to conduct this analysis with a parallel plate geometry of 20 mm diameter. Samples were cylinders of 0.5 mm thickness and a gap distance of 750 μm. The frequency sweeps were performed at a temperature of 200 °C, across a frequency range from 0.1 to 100 Hz, at 1 % strain rate.

These tests are complementary to 3D printability tests, providing insight into the material's behavior during extrusion at different filler concentrations, because materials with too low viscosity may spread excessively, while highly viscous formulations may clog the nozzle or produce inhomogeneous layers. Furthermore, the assessment of G′ and G″ in the rheological tests provides information about the stability of the flow at the printing shear rate (Candal et al., 2020; Das et al., 2021; O'Mahony et al., 2020).

The viscoelastic properties of the filament composites and their rheological behaviour are critical factors in FFF-based additive manufacturing, as they govern the extrusion of the

molten polymer through the nozzle and the interlayer welding during deposition. The complex viscosity, storage and loss modulus G′ and G″ of TPU and TPU composites at 200 °C are presented in Figure 34 and Figure 35.

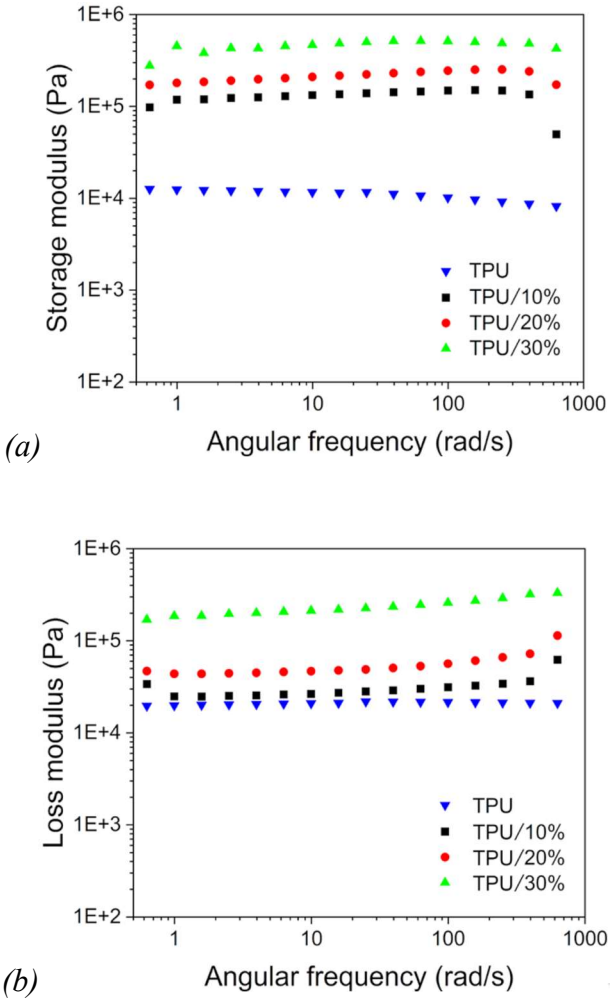

Figure 34 - (a) Storage Modulus, (b) Loss Modulus of TPU and TPU composites containing wet-white leather.

Results showed a distinctive non-Newtonian within the selected frequency range with the complex viscosity decreases rapidly by about two to three orders of magnitude with increasing angular frequency. To ensure stable extrusion and avoid filament buckling during feeding and nozzle clogging, the melt viscosity must remain below a practical upper limit.
Although no universal limit exists, it is generally accepted that, under processing conditions, viscosity should not exceed approximately 10^{-5} Pa.s in the shear rate range relevant to printing operations (Candal et al., 2020).

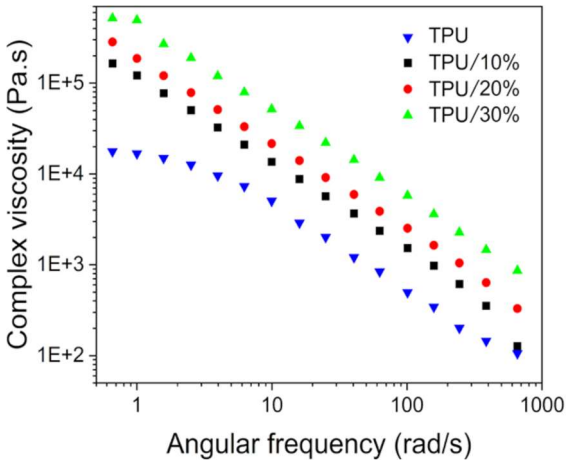

Figure 35 - Complex Viscosity of TPU and TPU composites containing wet-white leather.

Beyond this value, extrusion becomes unstable, and the risk of nozzle clogging increases significantly. In FFF, shear rates inside the nozzle can be estimated as:

$$\dot{\gamma} \approx \frac{4\nu}{D} \qquad \text{(Eq. 1)}$$

where ν is the extrusion velocity and D is the nominal nozzle diameter (0.4 mm). For printing speeds of 50 mm/s and 100 mm/s it is about 500 s^{-1} and 1000 s^{-1}. These shear rates define the processing window within which the melt viscosity should be evaluated. The correlation between steady shear viscosity (η(γ̇)) and complex viscosity from oscillatory tests (|η*|) is often approximated using the Cox–Merz rule:

$$\eta(\dot{\gamma}) \approx |\eta^*(\omega)| \qquad \text{(Eq. 2)}$$

This empirical rule allows predicting shear viscosity from frequency sweep data, assuming that the material structure responds similarly under oscillatory and steady shear flows. However, it must be applied cautiously. The use of this correlation, even in cases where it does not precisely define a correspondence between the two types of viscosity, can still allow for the identification of an order of magnitude capable of characterizing the extrudability of the polymer melt (Cox and Merz, 1958). In this study, the frequency sweep performed at 200 °C covered a range from 0.1 to 100 Hz (0.63–628 rad/s). According to Cox–Merz, this corresponds approximately to shear rates up to ~628 rad/s, which closely matches the

condition for a printing speed of 50 mm/s (500 rad/s) but does not fully capture high-speed conditions (100 mm/s → ~1000 rad/s). Consequently, for high-speed printing scenarios, extrapolation of rheological data or direct steady shear measurements at higher shear rates would be necessary. However, at angular frequencies approximating the shear rates experienced during FFF at the aforementioned speeds (500 – 1000 rad/s), the complex viscosity of the tested materials remains sufficiently low to guarantee proper flowability and process stability, while avoiding excessively low viscosity values that may lead to dripping or uncontrolled spreading of the melt after extrusion (Candal et al., 2020; Das et al., 2021; O'Mahony et al., 2020).

The storage and loss modulus with the increase of frequency, G′ and G″ do not suffer noticeable variations. Furthermore, in all the range of shear rates of the tests, composites G′ and G″ were larger than pure TPU and values increase with the increasing of filler content. This suggests that higher concentrations of leather fibers have an inhibitory effect on the motion of macromolecular chains because the filler reduces the free volume and the macromolecules thus prohibiting the movement of polymer chains (Zhong et al., 2019; Zhou et al., 2022) For the neat TPU, G″ remains consistently higher than G′ across the entire frequency range at the testing temperature, indicating a dominant viscous behavior. In contrast, the composite exhibits G′ > G″ throughout, reflecting a more elastic nature. However, at high frequencies, which best approximate the shear conditions encountered during extrusion, G′ becomes comparable to G″, indicating a transition from predominantly elastic to increasingly viscous behavior. This viscoelastic balance reduces the risk of nozzle clogging, as the material flows more readily under stress (Calafel et al., 2020).

5.4 Tensile properties

Tensile properties of neat TPU, and the TPU/leather composites was determined respectively in accordance with ASTM D638-14 and ISO 3376:2020 using a 35 kN dynamometer Acquati model AG/9E equipped with a 100 daN load cell with a deformation rate of 20 mm/min.

Composites test pieces have been prepared using Hot Press 3100 (Collins, Germany) at a temperature of 180 °C and pressure 100 ± 10 bar for 2 minutes after which the samples were allowed to cool down under same pressure, using circulation of cold water. Tensile tests were carried out on dog-bone-shaped specimens, in accordance with type V of the ASTM

D638-14. For reference, tests were conducted also on the original wet-white leather (before grinding), sampling in two directions, parallel and perpendicular to the backbone, from a whole leather in accordance with ISO 2418:2023 (Figure 36). Leather samples and composite test pieces have been conditioned before testing for 40 hours at 23 °C and 50 % R.H. in accordance with ISO 2419:2024 and ASTM D618-21. For all composite composition and leather direction, tensile strength, elongation at break and Young Modulus have been assessed as the average of six test pieces. Young's modulus has been determined in the linear region of the curves in the strain range from 0.01 to 0.025.

Tensile characterization of the composite filaments is crucial for understanding the mechanical behavior of the final printed object, as it represents the inherent ability of the material to sustain mechanical loads. Furthermore, in FFF techniques it is important to verify the stiffness of the material because the elastic modulus significantly influences the interaction between the extruded layer and the previously deposited one. A higher modulus reduces local deformations under the pressure of the nozzle, thereby improving dimensional accuracy and ensuring better structural stability of the printed part (Elmrabet and Siegkas, 2020; Lanzotti et al., 2015; Tymrak et al., 2014).

Tensile curves of neat TPU, leather and leather waste composite and presented in Figure 37 and Figure 38.

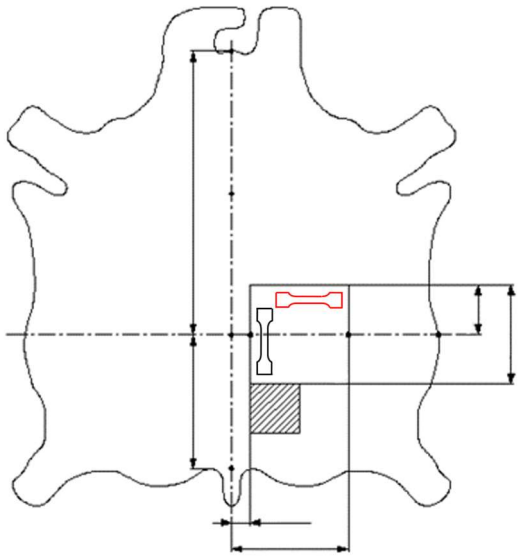

Figure 36 - Sampling area for leather tests in accordance with ISO 2418 standard

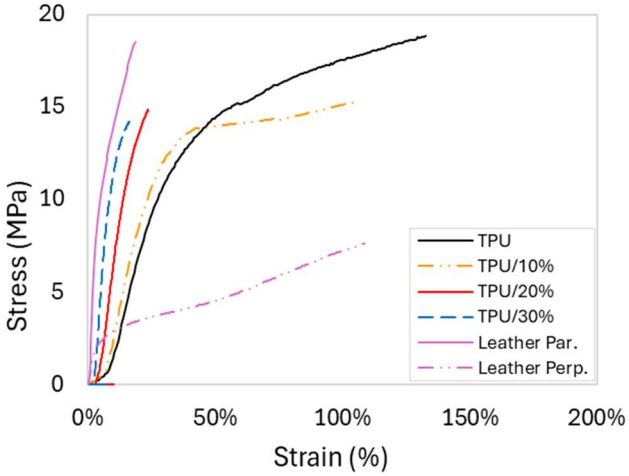

(b)

Figure 37 - Stress-Strain curves

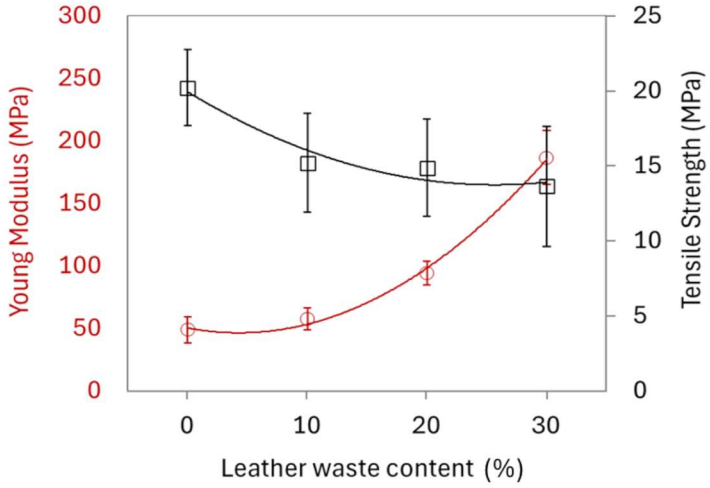

(a)

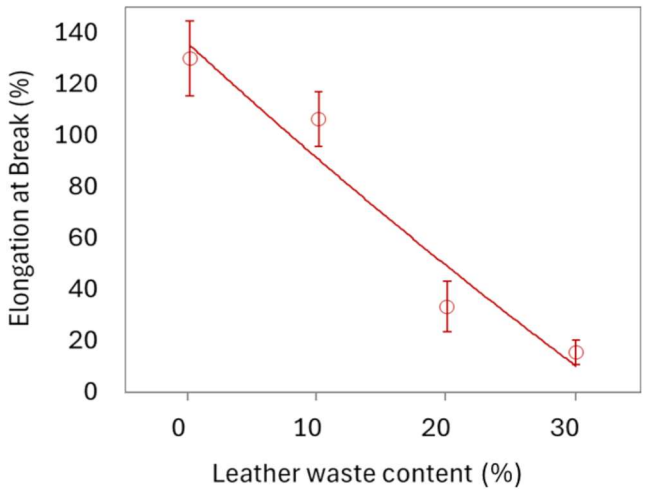

(b)

Figure 38 - (a) Tensile strength and Young's modulus and (b) Elongation at break values at different concentrations

Leather was also tested for comparison purposes in accordance with ISO 3376. Leather properties are anisotropic, meaning they depend on the area and direction of sampling. The fiber orientation is mostly radial, starting from the center of the skin, with the preferential alignment along the backbone and secondary from the center to the paw area (Manzo G., n.d.). This is the reason why, for the evaluation of leather mechanical properties, sampling is always carried out by cutting test pieces in two different directions with reference to the backbone line in specific leather area as specified in ISO 2418 (Figure 36).

As expected, the results show an evident anisotropy, with higher values of strength and Young's modulus in the direction parallel to the backbone. The comparison between TPU, leather and composites at the different concentrations shows an evident decreasing trend of elongation at break with increasing filler content. The shape of the stress-strain curve shows a change at 20 wt % of filler content. At this concentration, composites lose most of the initial ductility of TPU becoming more brittle, with results similar to the original leather tested along the direction parallel to the backbone.

Tensile results (Figure 38) are crucial, since variations in properties due to different filler concentrations will likely affect the behavior of the printed parts. From the perspective of filler concentration effects on FFF extrusion, the increase in elastic modulus (Figure 38.a) with increasing filler content is not expected to negatively affect the dimensional stability of the printed part. In fact, a higher modulus helps limit local deformations caused by nozzle pressure during deposition, thereby enhancing dimensional accuracy and contributing to the overall structural integrity of the printed object (Elmrabet and Siegkas, 2020; Lanzotti et al., 2015; Tymrak et al., 2014).

5.5 Abrasion tests

Abrasion resistance of the composites was evaluated using a Rotating Cylindrical Drum Abrader (Figure 39) model IG/ABR by Giuliani Tecnologie (Italy) in accordance with ISO 4649:2017, on circular specimens with 16 mm diameter and 5 mm thickness. For each composition, at least three specimens were tested and the average values reported. The test pieces were prepared following the same procedure used for the tensile tests, employing a Hot Press 3100 (Collins, Germany) at 180 °C under a pressure of 100 ± 10 bar for 2 minutes.

Figure 39 - Abrader device in accordance with ISO 4649

The results are summarized in Figure 40. Increasing the filler content led to a higher abraded volume, resulting in a slight reduction of abrasion resistance.

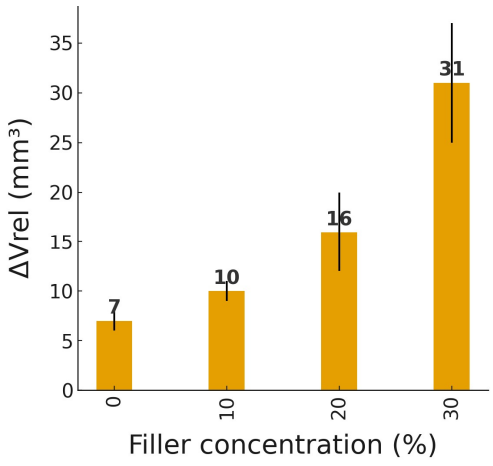

Figure 40 - Abrasion resistance according to ISO 4649 for composites at different filler concentrations

This reduction is closely related to the collagenous component of the leather fibers, which intrinsically exhibits lower mechanical resistance. However, the decrease remains moderate and does not compromise the overall performance of the 3D-printed products.

6. Printability tests

For the modeling of the objects to be printed, Autodesk Fusion 360 and Bambu Studio slicing software were used. The materials considered included neat TPU and TPU compounds containing 20 wt % and 30 wt % leather shavings, as these have the highest leather waste concentration. All samples were produced using a Bambu Lab X1C 3D printer. In Figure 41 a picture of the device used, and a detail of its heating system are reported.

(a) *(b)*

Figure 41 - (a) Bambu XC1 and a detail of the hotend (b)

Before printing, all filaments were thermally pre-treated at 65 °C for at least 6 hours to remove excess moisture and minimize material degradation. After setting key printing parameters such as nozzle diameter and plate temperature, printability tests were conducted to evaluate the influence of extrusion temperature and speed. Printing trials were performed at 215 °C, 220 °C, 225 °C, and 230 °C, with nozzle speeds of 50 mm/s and 100 mm/s. The parameters selected for layer deposition, particularly nozzle temperature and layer height, are consistent with those previously reported in the literature for TPU-based materials and by producers. Several studies have demonstrated that a layer height of 0.20 mm combined with nozzle

temperatures in the range of 215 – 230 °C provides a reliable balance between print quality, mechanical performance, and process stability during FFF of thermoplastic polyurethanes (Kechagias et al., 2023).

SETTING	UNIT	VALUE	SETTING	UNIT	VALUE
Filament diameter	mm	1.75	First layer width	mm	0.50
Nozzle temperatures	°C	215 / 220 / 225 / 230	External wall	mm	0.42
Speed	mm/sec	50 / 100	Internal wall	mm	0.45
Nozzle diameter	mm	0.40	Upper surface	mm	0.42
Plate temperatures	°C	45	Filling	mm	0.45
Layers height	mm	0.20	Internal solid filling	mm	0.42
Default width	mm	0.42			

Table 25 - Settings of FFF device for printability tests.

To assess material printability, two different tests were performed: a 1D test and a 3D test. In 1D tests, single filaments (100 mm in length) were extruded to analyze adhesion, filament integrity, precision, and homogeneity as a function of material, temperature, and speed. Adhesion and filament integrity were assessed visually, while precision was evaluated by comparing the average filament width to the nominal value of 0.42 mm (Table 1). A maximum deviation of ± 20 % was set as an acceptable threshold, considering a measurement uncertainty guard band (g = 1.645, corresponding to 95 % confidence level). Filament width was measured using an Optika SZP-10 microscope (80 X magnification) with an Optikam HDMI PRO camera and Optika Vision Lite 2.1 software. For each material-temperature-speed combination, three filaments were produced, and five equally spaced width measurements (approximately every 20 mm) were taken per filament. Before calculations, statistical tests were conducted at a 0.05 significance level, including the Shapiro-Wilk normality test and one-way Grubbs tests to detect outliers.

Homogeneity was evaluated by analyzing the standard deviation of the filament width measurements. An initial test series focused solely on TPU to eliminate unsuitable temperature-speed combinations. Subsequent 1D tests were then performed on 20 wt % and 30 wt % leather shaving filaments. At the end of these tests, the optimal temperature and speed settings were determined.

For the 3D test, 25 mm side cubes (without top covers) were printed. The deposition strategy included two base layers with alternating 45° orientations and four perimeter layers. For each optimal extrusion condition identified in the 1D tests, a visual inspection analysis was executed to evaluate print quality, and the tensile tests were performed to evaluate interlayer cohesion. Small rectangular specimens (15 mm × 5 mm) were cut perpendicular to the layer direction and tested using a TA Instruments Discovery DMA850 at a rate of 20 mm/min. Samples were conditioned at 23 °C and 50 % relative humidity for 40 hours before testing. Interlayer cohesion was evaluated in terms of elongation at break and welding strength. Welding strength was calculated as the ratio of maximum load to specimen width (N/mm). Finally, welding strength and elongation-at-break data were statistically analyzed using the Analysis of Variance (ANOVA) test to determine the impact of printing conditions.

1D tests were firstly performed solely on TPU in all the conditions reported in Table 25. In Figure 42, as an example, detailed images of the printed paths acquired by optical microscopy are reported.

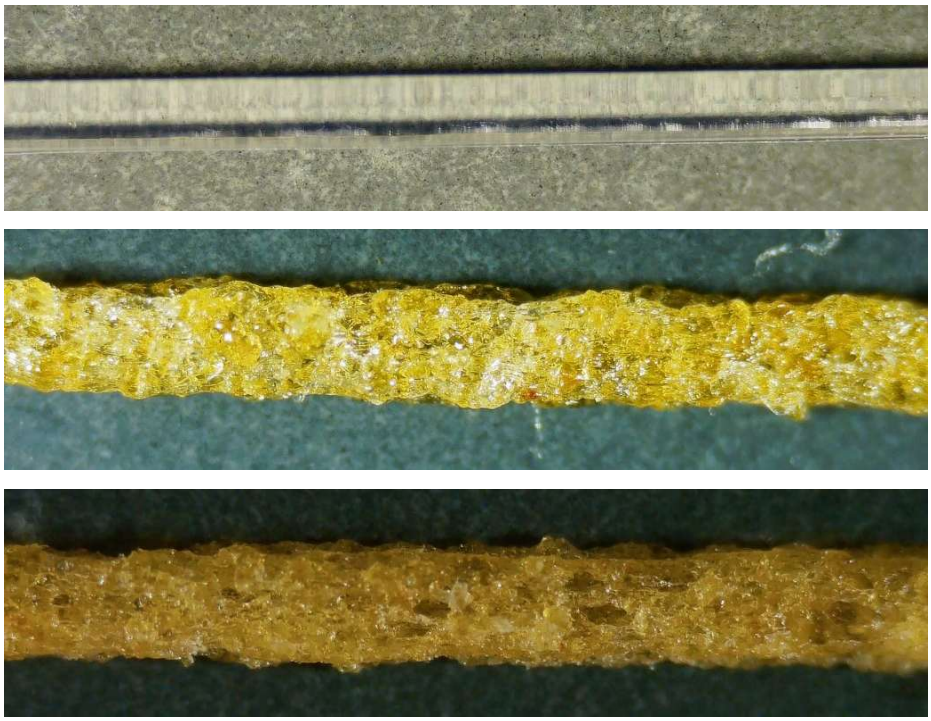

(a)

(b)

(c)

Figure 42 - Details of paths printed at 50 mm/s for (a) TPU at 220 °C, (b) 20 wt % and (c) 30 wt % at 225 °C

In all cases, no interruption of the filament run line was detected, that means that filament integrity was preserved. Regarding adhesion, in one case of filament printed at 215 °C a partial detachment of the layer from the printing plate was observed so that the authors excluded this level of temperature from subsequent analysis.

After the verification of filament integrity and adhesion, TPU filaments width have been analyzed to determine the process precision; for this scope, before the application of the guard band criteria, Shapiro-Wilks normality test and one-side and two sides Grubbs tests have been carried out.

T (°C)	**215**		**220**		**225**		**230**	
r (mm/s)	**50**	**100**	**50**	**100**	**50**	**100**	**50**	**100**
SHAPIRO-WILKS NORMALITY TEST								
P-value	0.91	0.16	0.14	0.26	0.95	0.36	0.57	0.05
W	0.98	0.93	0.93	0.94	0.98	0.95	0.96	0.91
H_0	Accepted	Accepted	Accepted	Accepted	Accepted	Accepted	Accepted	Questionable
ONE-SIDED GRUBBS' TEST								
$G_{1,n}$ (Largest)	2.02	1.31	1.97	2.31	2.45	2.11	1.46	2.33
$G_{1,1}$ (Smallest)	1.76	2.02	1.32	2.33	1.86	1.56	1.91	1.36
$S_{k,Lk}$ (0.05)	2.71	2.71	2.71	2.71	2.71	2.71	2.71	2.71
$S_{k,Lk}$ (0.01)	3.00	3.00	3.00	3.00	3.00	3.00	3.00	3.00
Outliers	No	No	No	No	No	No	No	Questionable
TWO-SIDED GRUBBS' TEST								
$G_{2;n-1,n}$ (Largest)	0.62	0.82	0.65	0.65	0.55	0.54	0.75	0.42
$G_{2;1,2}$ (Smallest)	0.67	0.60	0.82	0.56	0.68	0.74	0.62	0.82
$S_{k,Lk}$ (0.05)	0.44	0.44	0.44	0.44	0.44	0.44	0.44	0.44
$S_{k,Lk}$ (0.01)	0.36	0.36	0.36	0.36	0.36	0.36	0.36	0.36
Outliers (Largest)	No	No	No	No	No	No	No	Questionable
Outliers (Smallest)	No	No	No	No	No	No	No	No

Table 26 - Shapiro Wilks normality test, Grubbs' outliers test results on TPU

Results of *Table 26* show the impossibility to reject the null hypothesis H_0 for the approximation to a normal distribution with a confidence interval corresponding to 95%. Furthermore, no outliers with a significance level of 0.05 were detected. So, the average width

values and the guard band on TPU 1D layers compared to the 20 % tolerances of the nominal value are reported in Figure 43.

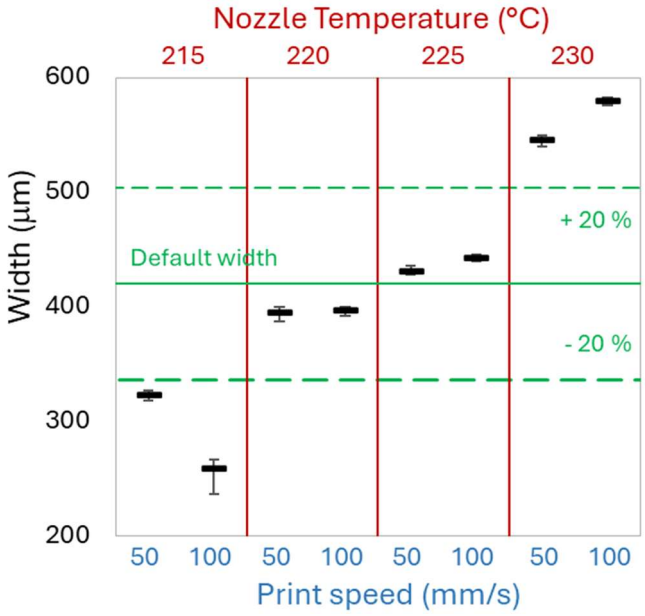

Figure 43 – 1D printability tests results for neat TPU

The analysis of the graph shows that extrusion at 230 °C, regardless of the printing speed (50 mm/s or 100 mm/s), results in a filament width that significantly exceeds the upper tolerance limit (+ 20 % compared to the nominal reference width). This indicates excessive material expansion during deposition, compromising the dimensional accuracy of the printing process. Therefore, the 230°C temperature level is excluded from the optimal conditions, as it does not ensure compliance with the required dimensional specifications.

On the contrary, the results for 220 °C and 225 °C demonstrate good dimensional accuracy, as the filament width remains within the defined tolerance range (± 20 % of the nominal width) for both printing speeds (50 mm/s and 100 mm/s). This indicates controlled material deposition, ensuring consistency and stability in the printing process. These temperatures are considered optimal as they allow for precise extrusion while maintaining filament integrity, making them suitable conditions for achieving high-quality prints.

The results of the statistical analysis for test 1D at 220 °C and 225 °C for leather waste composites at 20 wt % and 30 wt % are reported in Table 27. Also in this case, the results showed the impossibility to reject the null hypothesis H_0 for the approximation to a normal

distribution with a confidence interval corresponding to 95 %. Furthermore, no outliers with a significance level of 0.05 were detected.

	COMPOSITE TPU / 20 wt %				COMPOSITE TPU / 30 wt %			
T (°C)	**220**		**225**		**220**		**225**	
r (mm/s)	**50**	**100**	**50**	**100**	**50**	**100**	**50**	**100**
SHAPIRO-WILKS NORMALITY TEST								
P-value	0.57	0.62	0.31	0.24	0.06	0.52	0.23	0.14
W	0.96	0.96	0.95	0.93	0.91	0.96	0.94	0.93
H_0	Accepted	Accepted	Accepted	Accepted	Accepted	Accepted	Accepted	Accepted
ONE-SIDED GRUBBS' TEST								
$G_{1,n}$ (Largest)	2.21	1.77	2.39	1.77	2.06	1.96	1.44	1.30
$G_{1,1}$ (Smallest)	1.60	1.78	1.37	1.49	1.28	1.92	2.56	2.63
$S_{k,Lk}$ (0.05)	2.71	2.71	2.71	2.71	2.71	2.71	2.71	2.71
$S_{k,Lk}$ (0.01)	3.00	3.00	3.00	3.00	3.00	3.00	3.00	3.00
Outliers	No	No	No	No	No	No	No	No
TWO-SIDED GRUBBS' TEST								
$G_{2;n-1,n}$ (Largest)	0.61	0.67	0.54	0.71	0.63	0.71	0.76	0.82
$G_{2;1,2}$ (Smallest)	0.77	0.68	0.78	0.77	0.82	0.60	0.48	0.52
$S_{k,Lk}$ (0.05)	0.44	0.44	0.44	0.44	0.44	0.44	0.44	0.44
$S_{k,Lk}$ (0.01)	0.36	0.36	0.36	0.36	0.36	0.36	0.36	0.36
Outliers (Largest)	No	No	No	No	No	No	No	No
Outliers (Smallest)	No	No	No	No	No	No	No	No

Table 27 - Shapiro Wilks normality test, Grubbs' outliers test results on 20 wt % and 30 wt % composites

Figure 44 reports the average width values and the guard band on 20 % wt and 30 % wt composites 1D layers compared with the 20 % tolerances of the nominal value.

Comparing these results with the previous analysis on neat TPU (Figure 43), it is evident that the presence of leather waste affects the filament width. In both 20 wt% and 30 wt% waste compositions, the average filament width is generally larger than that observed for neat TPU under the same printing conditions. This suggests that the inclusion of leather particles

influences the material's flow behavior during extrusion, likely due to changes in viscosity and filler distribution.

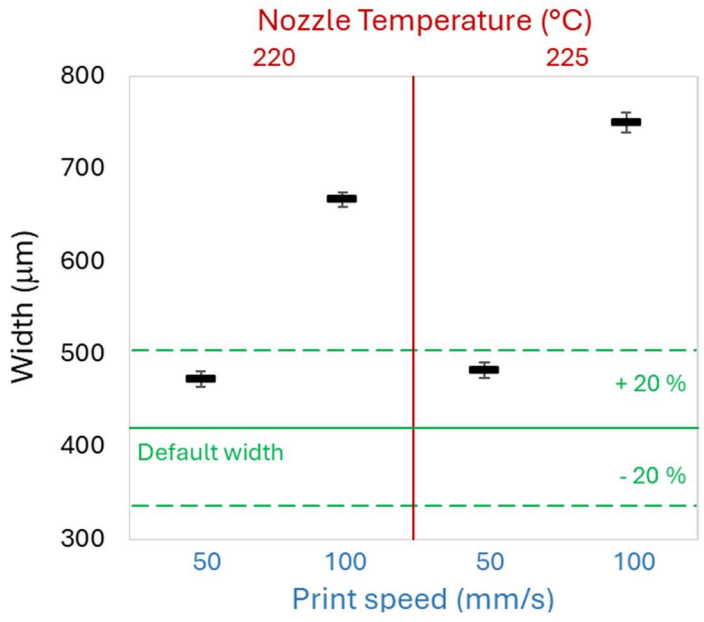

(a)

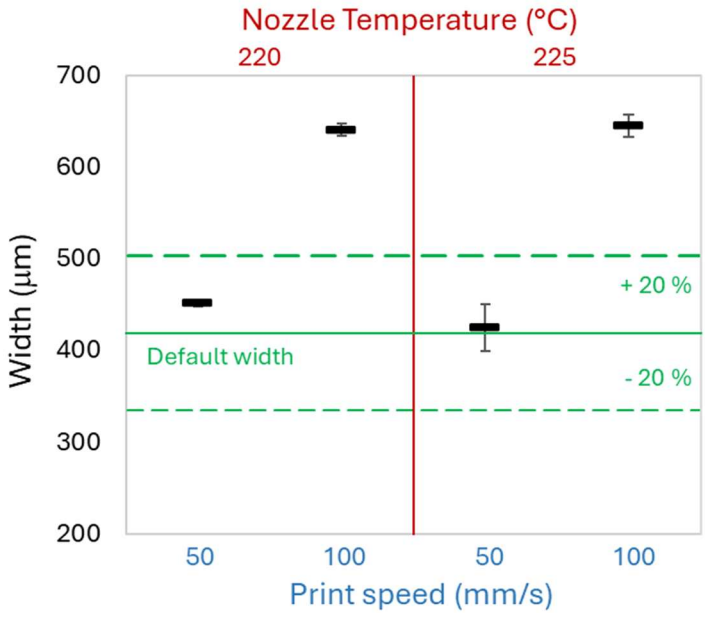

(b)

Figure 44 – 1D printability tests results for (a) 20 wt % and (b) 30 wt % TPU/Leather waste composites

Moreover, the effect becomes more pronounced as the waste concentration increases in the 30 wt % waste composition, the filament width is generally higher than in the 20 wt % waste composition, indicating a stronger impact on material expansion and extrusion stability.

Despite these variations, at 50 mm/s, both waste-containing compositions still maintain filament widths within the acceptable tolerance range, confirming that proper printing parameters (220 °C –225 °C, 50 mm/s) allow for controlled deposition even with the presence of waste. However, at 100 mm/s, the excessive deviation from the nominal width becomes even more evident compared to neat TPU, reinforcing the need to discard this higher speed setting.

Ultimately, the 1D test has identified 220 °C and 225 °C at 50 mm/s as the optimal parameters for ensuring accurate and consistent filament deposition, even when incorporating leather waste into the TPU matrix.

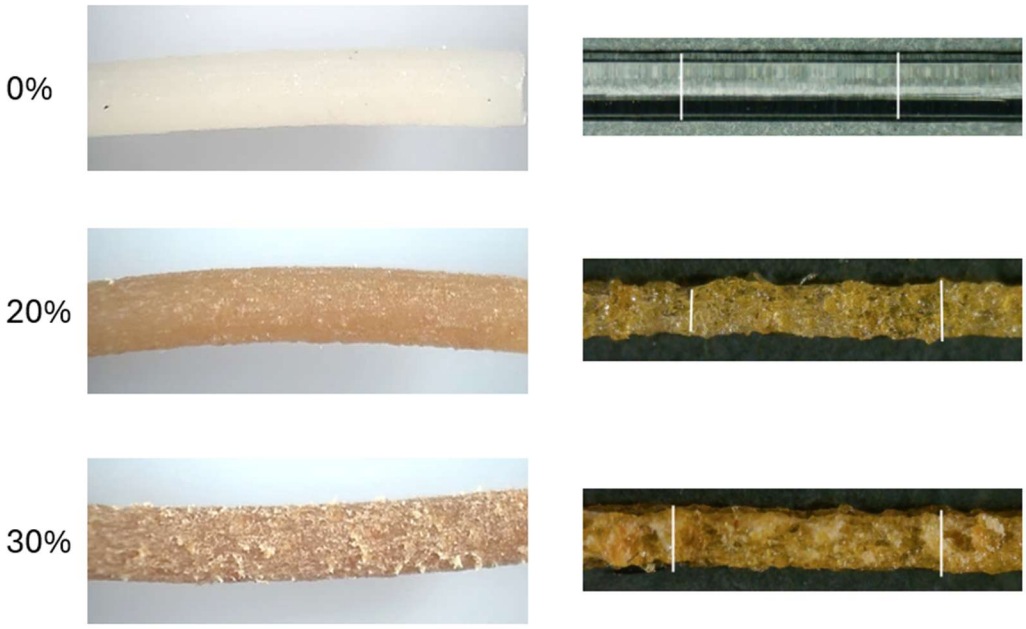

(a) *(b)*

Figure 45 - Filament used (a), single 1D layers (b)

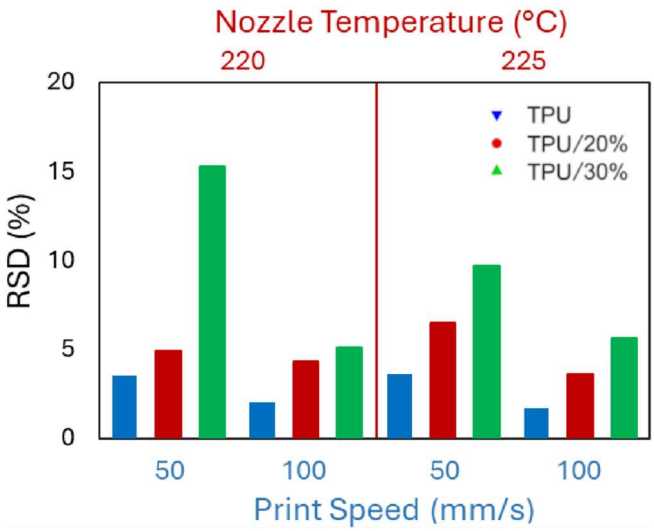

Figure 46 - Homogeneity values in RDS %

In Figure 45 and Figure 46, filaments produced at 0 wt %, 10 wt % and 20 wt % (a), 1D layers width measurements (b) and homogeneity values expressed in terms of relative standard deviation (Figure 46) are reported. As evident, the increase in filler content determines the reduction of the homogeneity in the width for all the speed and temperature conditions of printing.

After the evaluation of printability of single layers, 3D tests were printed at 50 mm/s speed and at 220 °C and 225 °C. In Figure 47 a detail of positioning on the printing plate and printing of process of test cubes are shown.

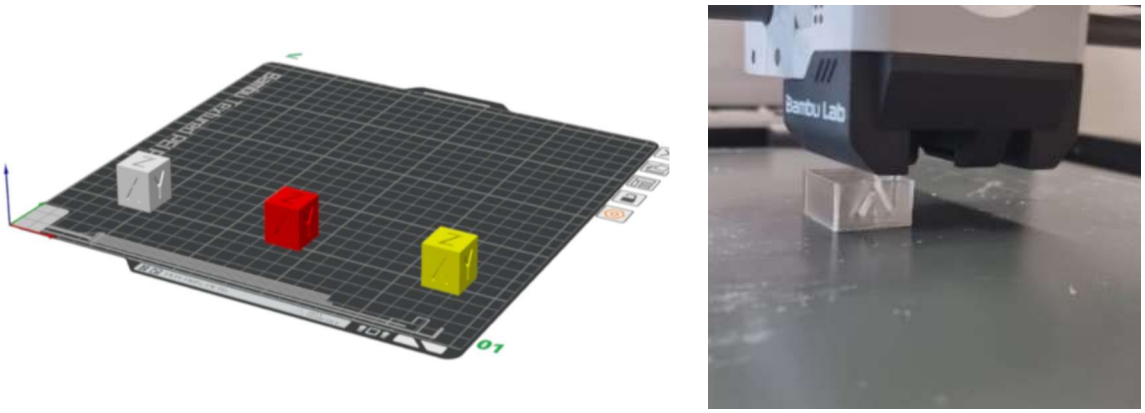

(a) *(b)*

Figure 47 - (a) Position on the printing plate, (b) 3D Printing process

In Figure 48, as an example, pictures of 3D test cubes printed in TPU and TPU-30 wt % composite is shown.

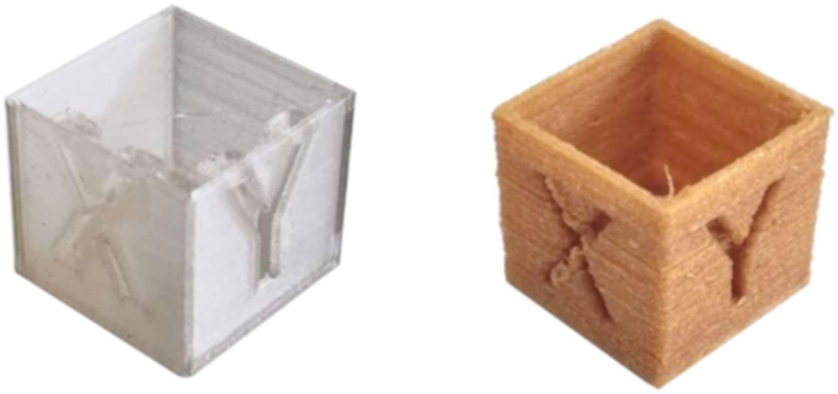

(a) *(b)*

Figure 48 - Test cubes printed using (a) TPU and (b) 30 wt % composite

For all the above conditions, the FFF equipment was able to print the object. Major findings of inspection analysis are illustrated in Figure 49. Analyzing the figure, it is evident that the addition of leather waste significantly alters the surface texture of the printed samples. In (a) neat TPU, the surface appears smooth, with well-defined and uniform layer lines, indicating a consistent material deposition. In (b) 20 wt % waste TPU and (c) 30 wt % waste TPU, the surface becomes progressively more irregular and rougher, with a noticeable loss of layer definition. The texture appears rougher, likely due to the presence of leather particles disrupting the uniformity of the deposited layers. This confirms that higher waste content leads to increased surface unevenness and a more irregular appearance, which may affect mechanical properties and adhesion between layers.

Observing each individual test cubes, a reduction in the number of print interruptions of the equipment was noticed when the composites have been used compared to the neat TPU. As known, printing TPU using FFF techniques is complex due to the filament's low stiffness, which could cause buckling and make extrusion control difficult (Gilmer et al., 2018b), which is intensified the softer the material is. The improvement in extrusion can be attributed to the increase in stiffness of the composite materials, which enhances the printer's feeding towards the nozzle resulting in less interruptions of print jobs (Herzberger et al., 2019).

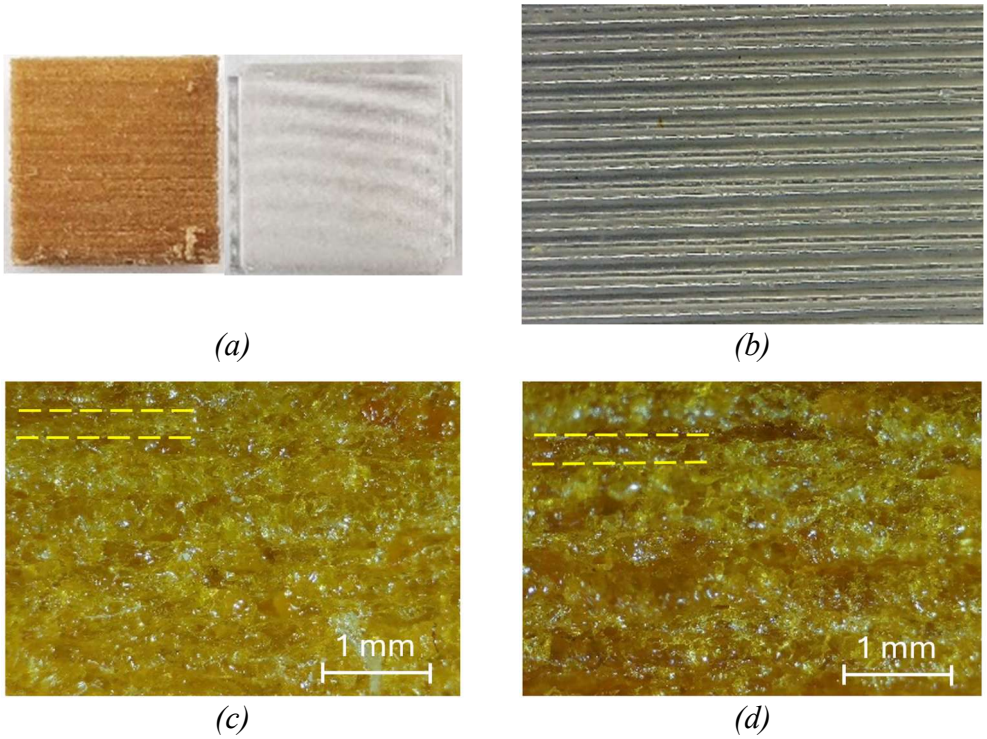

Figure 49 - Details of lateral surface of test cubes for (a) TPU, (b) 20 wt %. and (c) 30 wt %. composites

The main results of the interlayer cohesion analysis are summarized in Table 28 and Table 29 which illustrate the ANOVA results for welding strength and elongation at break parameters.

SOURCE	DF	Adj SS	Adj MS	F-Value	P-Value
wt%	1	10.5675	10.5675	149.81	0.000
T (°C)	1	1.8602	1.8602	26.37	0.001
wt%*T (°C)	1	0.0080	0.0080	0.11	0.745
Error	8	0.5643	0.0705		
Total	11	13.0000			

Table 28 - Anova table for welding

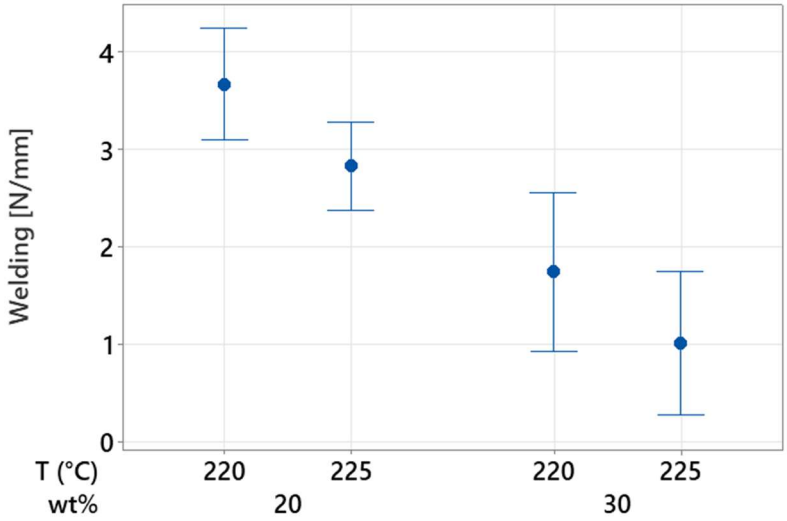

Figure 50 - Interval plot of welding

SOURCE	DF	Adj SS	Adj MS	F-Value	P-Value
wt%	1	358.479	358.479	110.52	0.000
T (°C)	1	0.258	0.258	0.08	0.785
wt%*T (°C)	1	26.931	26.931	8.30	0.020
Error	8	25.948	3.244		
Total	11	411.616			

Table 29 - Anova table for elongation at break

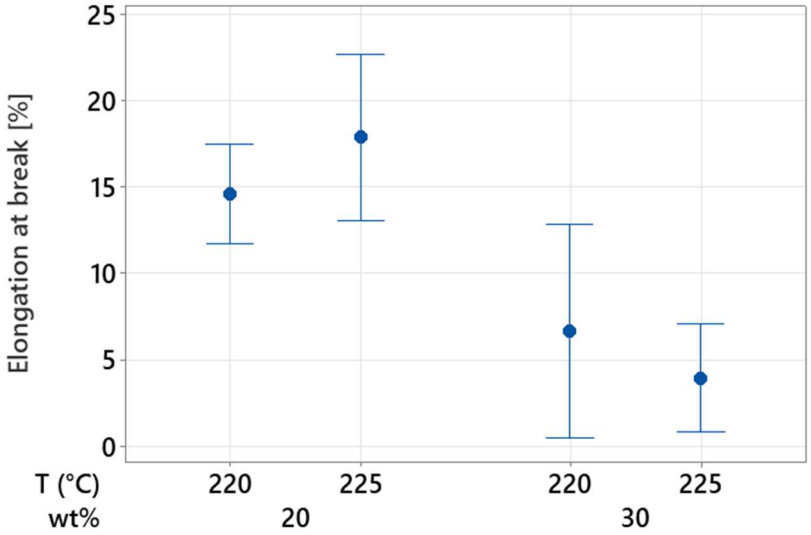

Figure 51 - Interval plot of elongation at break

By examining the results presented in Figure 50 and Figure 51, the same observations can be made for both measured parameters:

- The ANOVA analysis (Table 28 and Table 29) revealed that the collagen percentage (wt %) is the only significant factor influencing the measured parameters, with a p-value lower than 0.05.
- On average, an increase in collagen content leads to a decrease in welding and elongation at break values but improves the standard deviation. Specifically, as the collagen percentage increases from 20 wt% to 30 wt%, the welding value decreases from an average of 2.52 N/mm to 1.12 N/mm, marking a 52 % reduction, while the elongation at break decreases by 75 %, from an average of 18 % to 4.5 %.

The results demonstrate that, despite the limitations in mechanical properties, the composites developed with up to 30 wt % leather waste are still printable via FFF, albeit within a narrow range of process parameters to ensure adequate final part quality.
Based on the results shown in Figure 50 and Figure 51, this material could be suitable for applications where high flexibility is not required, such as semi-rigid components subjected to low mechanical stress. Its good printability via FFF makes it a promising option for fashion accessories, decorative elements for bags and footwear, and sustainable packaging solutions. Additionally, its use in automotive interiors, such as inserts for door panels or aesthetic trims, could contribute to reducing environmental impact. The material's balance between sustainability and processability also makes it a viable choice for custom furniture elements, handles, and other design products.

Chapter 3: Conclusions

1. Conclusions

This PhD research focused on the application of sustainability and circular economy principles within the leather tanning industry, a sector traditionally associated with high resource consumption and complex waste management. To fulfil the intended purposes, the tanning process was schematized into its individual stages, and the corresponding solid and liquid waste streams were identified to qualify their environmental impacts. To demonstrate that each phase of the tanning process can be addressed through the paradigms of sustainability and circularity, two specific stages of leather production were selected for specific investigation. In particular, the first stage involved the application of sustainability principles to the tanning process for the production of glutaraldehyde "wet-white" leathers. The scope was to optimize the use of processing chemicals in order to minimize the environmental impact of wastewater, mainly through a more rational use of glutaraldehyde-based tanning agents. The second stage addressed the concept of circularity, focusing on the valorization of leather shaving residues by recycling them as fillers for the development of TPU-based composite materials suitable for additive manufacturing via Fused Filament Fabrication (FFF). Through this integrated approach, the research demonstrates that the leather tanning process can be effectively redesigned according to sustainable and circular models, contributing to the mitigation of its environmental footprint while creating opportunities for material recovery and upcycling into high-value applications.

In the first part, to assess the environmental impact of traditional automotive leather tanning and to quantify the potential benefits achievable through process optimization, the first step was the development of a dedicated tool (SSIP's "Faibenelapelle"). This tool defines

a calculation model for the environmental footprint of leather products in accordance with the Product Environmental Footprint Category Rules (PEFCR) (Leather, 2018). The metamodel implemented enabled a detailed analysis of the entire tanning process, with the possibility to quantify the specific environmental impacts considering also the contributions of individual subprocesses. By quantifying impacts, tanneries can enhance their awareness of process-related environmental effects, optimize resource use, and improve the overall eco-efficiency of production. In particular, the computational model was studied and validated for the quantification of the environmental impacts providing a level of detail exceeding the requirements set by the PEFCR. The approach was based on the direct analysis from processes of a "model tannery," which enabled the acquisition of high-resolution primary data and the structured representation of the process into macro-groups and individual operational stages. The integration of three different bovine leather processing routes allowed the formulation of a flexible meta-model capable of representing the entire leather production that was described through detailed flow diagrams, identifying the key variables required for model parameterization and ensuring adaptability to different industrial configurations. Internal validation was carried out by assessing the environmental performance of three benchmark leather articles produced by the model tannery, confirming the methodological robustness and internal consistency of the meta-model. In the initial absence of specific data from an automotive tannery, the model was constructed based on chrome tanning and subsequently extended to include glutaraldehyde tanning, thereby ensuring broader representativeness across the leather sector. Overall, the meta-model developed in this study constitutes a reliable and versatile operational tool for the environmental assessment of tanning processes or subprocesses, suitable for supporting LCA and PEF applications for a whole production or a specific mechanical or chemical stage.

After defining the environmental impact assessment method, laboratory-scale tanning trials were conducted to reduce wastewater load by decreasing the glutaraldehyde concentration in the tanning formulation. Reductions of 25% and 50% from the standard formulation were tested, and tanning efficiency was evaluated through shrinkage temperature measurements. For each tanning trial, shrinkage temperature was calculated by means of a novel instrumental approach based on Dynamic Mechanical Analysis (DMA) able to detect slight changes in temperature and defined for more accurate assessment of crosslinking efficiency. The results showed that the reduction of tanning agent determines a slight decrease in shrinkage

temperature and so it is possible to reduce the chemical concentration. The optimized process significantly reduced also the residual aldehyde content in the residual bath, improving wastewater treatment performance and decreasing the overall pollutant load, as also confirmed by the PEF tool, through which we measured the reduction of specific environmental impacts. When scaled to an industrial production, in fact, the optimized formulation resulted in a 25–65% reduction of glutaraldehyde in wastewater, corresponding to a saving of 0.5–1.0 kg of chemical product per drum load. This outcome provides tangible environmental advantages during wastewater treatment due to the lower residual aldehyde load entering the depuration system. In the end, to verify that non changes occur on the final product, the optimized tanning process was validated through the production of five finished leathers, on which compliance with the requirements for automotive interior leathers defined by Maserati standard I.DSPM 020:2018 was verified. The results confirmed full conformity with the specified quality and performance criteria.

In the second part of this work, focused on the recycling of solid leather shaving wastes, thermoplastic polyurethane (TPU) composites incorporating wet-white leather shavings as filler materials were successfully developed for the production of filaments suitable for Fused Filament Fabrication (FFF). A complete characterization on the material was carried out to investigate specific issues related to the specific AM technique.

The chemical characterization of the glutaraldehyde-tanned wet-white leather shavings confirmed their full compliance with the main international regulatory frameworks governing the safety of leather materials, that have been considered as a precautionary approach. The analyses demonstrated conformity with the applicable requirements of the REACh Regulation, the POP Regulation, and the Oeko-Tex Leather Standard, ensuring the absence of restricted or hazardous substances commonly associated with tanning processes. Considering the material's intended application at elevated temperatures during extrusion and additive manufacturing, additional investigation against JAMA standards and Oeko-Tex limits for volatile organic compounds confirmed the compliance to the requirements and the absence of harmful emissions after thermal processing. In fact, no critical concentrations of heavy metals, chlorinated compounds, or residual aldehydes were detected, and the emissions of VOCs and

SVOCs were found to be negligible. These results indicate the possibility to classify this material as a safe by-product.

A morphological study was conducted on wet-white leather waste after pulverization using a grinder and subsequently sieved through three different mesh sizes (4.0 mm, 1.5 mm, and 0.5 mm) to evaluate the influence of grinding conditions on particle geometry and homogeneity and subsequently on the TPU composites. For each sieve, the particle size distribution (PSD) was determined by introducing a new microscopy-based method employing Digital Image Processing through an open-source image editing software (GIMP), which allowed the quantitative analysis of 2D particle dimension and aspect ratio. The results demonstrated that the grinding process using a 1.5 mm sieve produced particles with a predominantly fibrous morphology and uniform dimensions, whereas larger particles obtained with the 4.0 mm sieve showed irregular and heterogeneous shapes, often agglomerated or lamellar in structure. The 0.5 mm sieve did not lead to a significant reduction in particle size compared to the 1.5 mm one, although it provided a slightly narrower size distribution. The measured aspect ratios confirmed the predominance of elongated, one-dimensional fragments typical of fibrous materials, which favor better interfacial adhesion with the polymer matrix. From a processing standpoint, the 1.5 mm grinding condition represented the optimal compromise between dimensional uniformity, fibrous morphology, and process efficiency, avoiding excessive grinding time and energy consumption. The resulting fine, homogeneous particles ensured smooth extrusion during filament production, reducing the of nozzle clogging during the printing and consistent material flow.

Ground leather waste was compounded with a thermoplastic polyurethane (TPU) matrix for the production of filament intended for fused filament fabrication (FFF). A loading of 40 wt% leather waste was identified as the technological limit, as the resulting filament became excessively brittle and tended to break during the spool installation phase within the printer's feeding system. Neat TPU and composite materials containing different filler concentrations (from 0 wt% to 30 wt%) were therefore physically and mechanically characterized in order to identify the material properties related with specific issues of additive manufacturing by FFF.

SEM analysis of composites materials demonstrated a good dispersion of the leather fibers within TPU. Thermal analyses provided valuable insights into the influence of leather waste incorporation on the thermal behaviour of TPU-based composites. The addition of shavings

induced noticeable variations in both the crystallization and melting behaviour of the polymer. In particular, increasing the filler concentration resulted in a shift of the TPU melting temperature from 205 °C to 221 °C, suggesting a reduction in polymer chain mobility due to the presence of the filler. Similarly, the crystallization temperature increased from 106 °C to 162 °C, which can be attributed to a nucleating effect of leather particles. These modifications in the thermal transitions are particularly relevant for the definition of suitable printing parameters, as the higher melting temperatures observed in DSC analyses must be taken into account when setting up extrusion and FFF processing conditions. Furthermore, TGA results confirmed the thermal stability of both TPU and leather-filled composites within the extrusion and printing temperature ranges, indicating that no significant degradation is expected during processing.

The rheological analysis of TPU and its leather waste composites provided essential insights into their suitability for FFF processing. The frequency sweep tests revealed a typical non-Newtonian shear-thinning behavior, with the complex viscosity decreasing by two to three orders of magnitude as the angular frequency increased. This behavior is consistent with polymer melts suitable for extrusion-based additive manufacturing. The results confirmed that melt viscosity plays a crucial role in printability, since excessively low values may lead to uncontrolled spreading of the extruded material, while high viscosities can cause nozzle clogging or filament buckling during feeding. At angular frequencies corresponding to shear rates experienced during printing (approximately 500–1000 rad/s), all tested materials exhibited complex viscosities within the optimal range for steady flow and process stability, ensuring adequate layer deposition without dripping or flow interruptions. Overall, these results confirm that the developed TPU/leather composites maintain rheological characteristics compatible with reliable FFF processing.

Mechanical characterization revealed an evident influence of the filler content on the tensile behavior of TPU-based composites. The comparison between neat TPU, leather waste, and the corresponding composites at different filler concentrations highlighted a progressive decrease in elongation at break with increasing filler content. A distinct transition was observed at 20 wt%, where the composites exhibited a marked loss of ductility, becoming significantly more brittle and displaying mechanical behavior comparable to that of the original leather tested along the backbone direction. These findings are particularly relevant

for additive manufacturing applications, as the mechanical properties of the filament strongly influence the behavior of the printed components. As verified in the printability tests, the increase in elastic modulus with higher filler concentrations did not adversely affect the dimensional stability of printed parts.

Printing trials conducted using a Bambu Lab X1C printer allowed the identification of optimal processing parameters for TPU/leather waste composite filaments. Extrusion tests were performed at 215 °C, 220 °C, 225 °C, and 230 °C, with nozzle speeds of 50 mm/s and 100 mm/s, through both 1D and 3D printing evaluations. The 1D tests, focused on assessing dimensional accuracy by comparing the measured filament width to the nominal value (0.42 mm, with an acceptable deviation of ± 20 %), revealed significant differences among the tested conditions. Extrusion at 215 °C resulted in poor adhesion to the print plate and an excessive reduction of the deposited path cross-section, indicating insufficient melt flow and incomplete fusion. Conversely, extrusion at 230 °C caused excessive material expansion during deposition, compromising dimensional accuracy. Both temperatures were therefore excluded from the optimal processing window. Printing at 220 °C and 225 °C ensured stable and accurate filament deposition, maintaining dimensional consistency and filament integrity. Statistical analysis confirmed that the incorporation of 20 wt% and 30 wt% leather waste affects filament width, generally producing slightly larger dimensions than neat TPU under the same conditions. This can be attributed to modifications in viscosity and filler distribution, which influence melt flow behavior during extrusion. Nevertheless, the selected parameters (220 °C–225 °C, 50 mm/s) enabled controlled and reproducible deposition, even at higher filler loadings. In contrast, printing at 100 mm/s led to excessive deviations from the nominal width, particularly for filled composites, and was therefore deemed unsuitable for precision printing. Overall, the 1D printing tests identified 220 °C and 225 °C at 50 mm/s as the optimal process parameters for TPU/leather waste composites, ensuring proper adhesion, dimensional reliability, and high-quality extrusion performance within the FFF process.

Finally, 3D-printed test cubes validated the experimental results and actual feasibility of using these materials in additive manufacturing, while interlayer adhesion tests quantified their mechanical performance. The 3D printing trials, performed at 50 mm/s and extrusion temperatures of 220 °C and 225 °C, provided further insight into the processability and surface quality of TPU/leather waste composites. Visual inspection of the printed test cubes revealed

a clear correlation between filler concentration and surface morphology. As the leather waste content increased, the surface became progressively rougher and less uniform, with a noticeable loss of layer definition. This effect is attributed to the presence of leather particles, which disrupt the regularity of the extruded paths and contribute to the formation of uneven textures. Consequently, higher filler contents lead to increased surface irregularity, potentially affecting interlayer adhesion and mechanical performance of the printed parts. The ANOVA results for welding strength and elongation at break confirmed that the collagen content (wt%) is the only statistically significant factor influencing these mechanical parameters ($p < 0.05$). From a mechanical point of view, increasing collagen content resulted in a progressive reduction of both welding strength and elongation at break, while slightly improving the standard deviation. Specifically, when the filler concentration increased from 20 wt% to 30 wt%, the welding strength decreased by about 52 % (from 2.52 N/mm to 1.12 N/mm) and the elongation at break decreased by approximately 75 % (from 18 % to 4.5 %).

Despite these limitations, the results demonstrate that the developed TPU/leather waste composites remain printable via FFF up to 30 wt% filler content, although within a narrow process window to ensure adequate final quality.

Their reliable printability and distinctive appearance make them promising candidates for fashion accessories, decorative elements for bags and footwear, and sustainable packaging. Moreover, potential applications extend to automotive interiors such as door panel inserts or aesthetic trims and custom furniture components (e.g., handles or decorative fittings), where the material’s balance between processability, aesthetic value, and environmental benefit can be fully exploited.

References

Akter, N., Chakma, S., Fatama, K., Alam, M.N., Azad, M.A.K., 2024. Impact of polyvinyl alcohol for bio-adhesives preparation from tannery solid waste and its application in leather products industry. Bangladesh J. Sci. Ind. Res. 59, 7–16. https://doi.org/10.3329/bjsir.v59i1.70040

Alptekin, E., Canakci, M., Sanli, H., 2012. Evaluation of leather industry wastes as a feedstock for biodiesel production. Fuel 95, 214–220. https://doi.org/10.1016/j.fuel.2011.08.055

Alvarez Gómez, M., Moreno Nieto, D., Moreno Sánchez, D., Sanz De León, A., Molina Rubio, S., 2023a. Additive Manufacturing of Thermoplastic Polyurethane-Cork Composites for Material Extrusion Technologies. Polymers 15, 3291. https://doi.org/10.3390/polym15153291

Al-Zaidi, A.A.M.A., Al-Gawhari, F.J.J., 2023. Types of Polymers Using in 3D Printing and Their Applications: A Brief Review. ejtas 1, 978–985. https://doi.org/10.59324/ejtas.2023.1(6).94

Ambone, T., Joseph, S., Deenadayalan, E., Mishra, S., Jaisankar, S., Saravanan, P., 2017. Polylactic Acid (PLA) Biocomposites Filled with Waste Leather Buff (WLB). J Polym Environ 25, 1099–1109. https://doi.org/10.1007/s10924-016-0891-3

Aurilia, M., Piscitelli, F., Sorrentino, L., Lavorgna, M., Iannace, S., 2011. Detailed analysis of dynamic mechanical properties of TPU nanocomposite: The role of the interfaces. European Polymer Journal 47, 925–936. https://doi.org/10.1016/j.eurpolymj.2011.01.005

Bi, H., Ren, Z., Guo, R., Xu, M., Song, Y., 2018. Fabrication of flexible wood flour/thermoplastic polyurethane elastomer composites using fused deposition molding. Industrial Crops and Products 122, 76–84. https://doi.org/10.1016/j.indcrop.2018.05.059

Calafel, I., Aguirresarobe, R.H., Peñas, M.I., Santamaria, A., Tierno, M., Conde, J.I., Pascual, B., 2020. Searching for Rheological Conditions for FFF 3D Printing with PVC Based Flexible Compounds. Materials 13, 178. https://doi.org/10.3390/ma13010178

Candal, M.V., Calafel, I., Aranburu, N., Fernández, M., Gerrica-Echevarria, G., Santamaría, A., Müller, A.J., 2020. Thermo-rheological effects on successful 3D printing of biodegradable polyesters. Additive Manufacturing 36, 101408. https://doi.org/10.1016/j.addma.2020.101408

Cavalcante, D.G.S.M., Gomes, A.S., Santos, R.J., Kerche-Silva, L.E., Danna, C.S., Yoshihara, E., Job, A.E., 2018. Composites Produced from Natural Rubber and Chrome-Tanned Leather Wastes: Evaluation of their In Vitro Toxicological Effects for Application in Footwear and Textile Industries. J Polym Environ 26, 980–988. https://doi.org/10.1007/s10924-017-1002-9

China, C.R., Maguta, M.M., Nyandoro, S.S., Hilonga, A., Kanth, S.V., Njau, K.N., 2020. Alternative tanning technologies and their suitability in curbing environmental pollution from the leather industry: A comprehensive review. Chemosphere 254, 126804. https://doi.org/10.1016/j.chemosphere.2020.126804

Cohen, N.S., Odlyha, M., Foster, G.M., 2000. Measurement of shrinkage behaviour in leather and parchment by dynamic mechanical thermal analysis. Thermochimica Acta 365, 111–117. https://doi.org/10.1016/S0040-6031(00)00618-3

Cox, W.P., Merz, E.H., 1958. Correlation of dynamic and steady flow viscosities. J. Polym. Sci. 28, 619–622. https://doi.org/10.1002/pol.1958.1202811812

Das, A., Gilmer, E.L., Biria, S., Bortner, M.J., 2021. Importance of Polymer Rheology on Material Extrusion Additive Manufacturing: Correlating Process Physics to Print Properties. ACS Appl. Polym. Mater. 3, 1218–1249. https://doi.org/10.1021/acsapm.0c01228

Dettmer, A., Nunes, K.G.P., Gutterres, M., Marcílio, N.R., 2010. Production of basic chromium sulfate by using recovered chromium from ashes of thermally treated leather. Journal of Hazardous Materials 176, 710–714. https://doi.org/10.1016/j.jhazmat.2009.11.090

Ding C, Zhang M, Dai L, Qi Y, Shi R, Yang J, 2017. Fabrication and characterization of regenerated leather using chrome shavings as raw materials. JALCA 112(5):145–52.

Dizon, J.R.C., Espera, A.H., Chen, Q., Advincula, R.C., 2018. Mechanical characterization of 3D-printed polymers. Additive Manufacturing 20, 44–67. https://doi.org/10.1016/j.addma.2017.12.002

Elmrabet, N., Siegkas, P., 2020. Dimensional considerations on the mechanical properties of 3D printed polymer parts. Polymer Testing 90, 106656. https://doi.org/10.1016/j.polymertesting.2020.106656

EN 15987, 2015. Key definition for leather trade, EN.

Esteban, B., Baquero, G., Cuadros, R., Morera, J.M., 2021. Proposal and application of a new method to determine leather shrinkage temperature. Thermochimica Acta 698, 178880. https://doi.org/10.1016/j.tca.2021.178880

EU, 2018. Product Environmental Footprint Category Rules Guidance.

Gevorkian, S.G., Allahverdyan, A.E., Gevorgyan, D.S., Simonian, A.L., 2009. Thermal (In)Stability of Type I Collagen Fibrils. Phys. Rev. Lett. 102, 048101. https://doi.org/10.1103/PhysRevLett.102.048101

Gibson, I., Rosen, D., Stucker, B., 2015. Additive Manufacturing Technologies: 3D Printing, Rapid Prototyping, and Direct Digital Manufacturing. Springer New York, New York, NY. https://doi.org/10.1007/978-1-4939-2113-3

Gilmer, E.L., Miller, D., Chatham, C.A., Zawaski, C., Fallon, J.J., Pekkanen, A., Long, T.E., Williams, C.B., Bortner, M.J., 2018a. Model analysis of feedstock behavior in fused filament fabrication: Enabling rapid materials screening. Polymer 152, 51–61. https://doi.org/10.1016/j.polymer.2017.11.068

Gilmer, E.L., Miller, D., Chatham, C.A., Zawaski, C., Fallon, J.J., Pekkanen, A., Long, T.E., Williams, C.B., Bortner, M.J., 2018b. Model analysis of feedstock behavior in fused filament fabrication: Enabling rapid materials screening. Polymer 152, 51–61. https://doi.org/10.1016/j.polymer.2017.11.068

Handbook of Thermoplastic Elastomers, 2014. . Elsevier. https://doi.org/10.1016/C2013-0-00140-5

Hassan, M.M., Harris, J., Busfield, J.J.C., Bilotti, E., 2023. A review of the green chemistry approaches to leather tanning in imparting sustainable leather manufacturing. Green Chem. 25, 7441–7469. https://doi.org/10.1039/D3GC02948D

Herzberger, J., Sirrine, J.M., Williams, C.B., Long, T.E., 2019. Polymer Design for 3D Printing Elastomers: Recent Advances in Structure, Properties, and Printing. Progress in Polymer Science 97, 101144. https://doi.org/10.1016/j.progpolymsci.2019.101144

Idà, E., Nanetti, F., Mottola, G., 2022. An Alternative Parallel Mechanism for Horizontal Positioning of a Nozzle in an FDM 3D Printer. Machines 10, 542. https://doi.org/10.3390/machines10070542

Irwanto, D., 2021. Purification of Gelatin from Leather Waste into Pharmaceutical Grade Gelatin. SSRN Journal. https://doi.org/10.2139/ssrn.3796718

ISO 15115, 2019. Leather Vocabulary, ISO.

JAMA, 2023. The Motor Japan Industry 2023.

Kale, R.D., Jadhav, N.C., 2019. Utilization of waste leather for the fabrication of composites and to study its mechanical and thermal properties. SN Appl. Sci. 1, 1231. https://doi.org/10.1007/s42452-019-1230-9

Kannan, M., Bhagawan, S.S., Thomas, S., Joseph, K., 2013. Thermogravimetric analysis and differential scanning calorimetric studies on nanoclay-filled TPU/PP blends. J Therm Anal Calorim 112, 1231–1244. https://doi.org/10.1007/s10973-012-2693-8

Kechagias, J.D., Vidakis, N., Petousis, M., 2023. Parameter effects and process modeling of FFF-TPU mechanical response. Materials and Manufacturing Processes 38, 341–351. https://doi.org/10.1080/10426914.2021.2001523

Khalifa, M., Anandhan, S., Wuzella, G., Lammer, H., Mahendran, A.R., 2020. Thermoplastic polyurethane composites reinforced with renewable and sustainable fillers – a review. Polymer-Plastics Technology and Materials 59, 1751–1769. https://doi.org/10.1080/25740881.2020.1768544

Kiliç, E., Tarrés, Q., Delgado-Aguilar, M., Espinach, X., Fullana-i-Palmer, P., Puig, R., 2020. Leather Waste to Enhance Mechanical Performance of High-Density Polyethylene. Polymers 12, 2016. https://doi.org/10.3390/polym12092016

Lai, S. -M., Don, T. -M., Huang, Y. -C., 2006. Preparation and properties of biodegradable thermoplastic starch/poly(hydroxy butyrate) blends. J of Applied Polymer Sci 100, 2371–2379. https://doi.org/10.1002/app.23085

Lanzotti, A., Grasso, M., Staiano, G., Martorelli, M., 2015. The impact of process parameters on mechanical properties of parts fabricated in PLA with an open-source 3-D printer. Rapid Prototyping Journal 21, 604–617. https://doi.org/10.1108/RPJ-09-2014-0135

Li, C., Li, R., Lyu, P., Wang, Y., Zhang, C., Dai, F., Liu, X., 2021. The fabrication of thermoplastic polyurethane/leather powder composite film with excellent mechanical property. Composites Communications 25, 100694. https://doi.org/10.1016/j.coco.2021.100694

Ligon, S.C., Liska, R., Stampfl, J., Gurr, M., Mülhaupt, R., 2017. Polymers for 3D Printing and Customized Additive Manufacturing. Chem. Rev. 117, 10212–10290. https://doi.org/10.1021/acs.chemrev.7b00074

Liu, Y., Wang, Q., Li, L., 2016. Reuse of leather shavings as a reinforcing filler for poly (vinyl alcohol). Journal of Thermoplastic Composite Materials 29, 327–343. https://doi.org/10.1177/0892705713518794

Luo, M., Yang, T., Wang, T., Yan, Z., Zhang, J., 2024. The effect of filler size on the properties of TPU / BN flexible thermal conductive composites prepared by Fused Filament Fabrication. Polymer 296, 126810. https://doi.org/10.1016/j.polymer.2024.126810

Maistrenko, L., Iungin, O., Pikus, P., Pokholenko, I., Gorbatiuk, O., Moshynets, O., Okhmat, O., Kolesnyk, T., Potters, G., Mokrousova, O., 2022. Collagen Obtained from Leather Production Waste Provides Suitable Gels for Biomedical Applications. Polymers 14, 4749. https://doi.org/10.3390/polym14214749

Manzo G., n.d. Leather Chemistry and Technology. Media Service Edizioni.

Mengeloğlu, F., Çavuş, V., 2020. Preparation of thermoplastic polyurethane-based biocomposites through injection molding: Effect of the filler type and content. BioRes 15, 5749–5763. https://doi.org/10.15376/biores.15.3.5749-5763

Morelli C., 2022. Next Generation Leather: pathways to sustainability (KERING Group). Presented at the III IULTCS EuroCongress, Vicenza.

Muralidharan, V., Palanivel, S., Balaraman, M., 2022. Turning problem into possibility: A comprehensive review on leather solid waste intra-valorization attempts for leather processing. Journal of Cleaner Production 367, 133021. https://doi.org/10.1016/j.jclepro.2022.133021

Naderizadeh, S., Faggionato, A., Nazir, M.U., Mascolo, R., Hassan, M.M., Bilotti, E., Busfield, J.J.C., 2025. The Thermal and Mechanical Performance of Leather Waste-Filled Bio-Based Thermoplastic Polyurethane Composites. Polymers 17, 1202. https://doi.org/10.3390/polym17091202

Nazir, M.U., Mascolo, R., Bouic, P., Hassan, M.M., Harris, J., Naderizadeh, S., Busfield, J.J.C., Zhang, H., Papageorgiou, D., Bilotti, E., 2025. Upcycling leather waste: The effect of leather type and aspect ratio on the performance of thermoplastic polyurethane composites. Sustainable Materials and Technologies 43, e01221. https://doi.org/10.1016/j.susmat.2024.e01221

Ngo, T.D., Kashani, A., Imbalzano, G., Nguyen, K.T.Q., Hui, D., 2018. Additive manufacturing (3D printing): A review of materials, methods, applications and challenges. Composites Part B: Engineering 143, 172–196. https://doi.org/10.1016/j.compositesb.2018.02.012

Nofar, M., Büşra Küçük, E., Batı, B., al, 2019. Effect of hard segment content on the microcellular foaming behavior of TPU using supercritical CO2. The Journal of Supercritical Fluids 153, 104590. https://doi.org/10.1016/j.supflu.2019.104590

Oeko-Tex, 2024. Oeko-Tex Leather Standard.

O'Mahony, C., Gkartzou, E., Haq, E.U., Koutsoumpis, S., Silien, C., Charitidis, C.A., Tofail, S.A.M., 2020. Determination of thermal and thermomechanical properties of biodegradable PLA blends: for additive manufacturing process. J Therm Anal Calorim 142, 715–722. https://doi.org/10.1007/s10973-020-09859-6

Pati, A., Chaudhary, R., Subramani, S., 2014. A review on management of chrome-tanned leather shavings: a holistic paradigm to combat the environmental issues. Environ Sci Pollut Res 21, 11266–11282. https://doi.org/10.1007/s11356-014-3055-9

POP, 2022. REGULATION (EU) 2022/2400 OF THE EUROPEAN PARLIAMENT AND OF THE COUNCIL of 23 November 2022 amending Annexes IV and V to Regulation (EU) 2019/1021 on persistent organic pollutants, POP.

Reach, 2006. Regulation of the European Parliament and of the Council (Reach) concerning the Registration, Evaluation, Authorisation and Restriction of Chemicals (REACH), establishing a European Chemicals Agency, amending Directive 1999/45/EC and repealing Council Regulation (EEC) No 793/93 and Commission Regulation (EC) No 1488/94 as well as Council Directive 76/769/EEC and Commission Directives 91/155/EEC, 93/67/EEC, 93/105/EC and 2000/21/EC, REACH.

Rodzeń, K., McIlhagger, A., Strachota, B., Strachota, A., Meenan, B.J., Boyd, A., 2023. Controlling Crystallization: A Key Factor during 3D Printing with the Advanced Semicrystalline Polymeric Materials PEEK, PEKK 6002, and PEKK 7002. Macro Materials & Eng 308, 2200668. https://doi.org/10.1002/mame.202200668

Sammarco U., 2011. Tecnologia Conciaria, 2nd ed. EDITMA.

Schröpfer M., Meyer M., 2011. Dimensional and structural stability of leather under alternating climate conditions, in: XXXI IULTCS Congress. Presented at the XXXI IULTCS Congress, Valencia (Spain).

Stani, C., Vaccari, L., Mitri, E., Birarda, G., 2020. FTIR investigation of the secondary structure of type I collagen: New insight into the amide III band. Spectrochimica Acta Part A: Molecular and Biomolecular Spectroscopy 229, 118006. https://doi.org/10.1016/j.saa.2019.118006

Stefan, D.S., Bosomoiu, M., Dancila, A.M., Stefan, M., 2022. Review of Soil Quality Improvement Using Biopolymers from Leather Waste. Polymers 14, 1928. https://doi.org/10.3390/polym14091928

Tabuani, D., Bellucci, F., Terenzi, A., Camino, G., 2012. Flame retarded Thermoplastic Polyurethane (TPU) for cable jacketing application. Polymer Degradation and Stability 97, 2594–2601. https://doi.org/10.1016/j.polymdegradstab.2012.07.011

Toxicological Profile for Glutaraldehyde, 2017. , Agency for Toxic Substances and Disease Registry (ATSDR) Toxicological Profiles. Agency for Toxic Substances and Disease Registry (US), Atlanta (GA).

Tymrak, B.M., Kreiger, M., Pearce, J.M., 2014. Mechanical properties of components fabricated with open-source 3-D printers under realistic environmental conditions. Materials & Design 58, 242–246. https://doi.org/10.1016/j.matdes.2014.02.038

UN, 2015. UN Resolution adopted by the General Assembly on 25 September 2015, 70/1, Transforming our world.

UNIC, 2023. Report di Sostenibilità.

Verheijen, Wiersema D W, Hulshoff, 1996. Management of Waste from Animal Product Processing. FAO.

Wilkinson, A.N., Kinloch, I.A., Othman, R.N., 2016. Low viscosity processing using hybrid CNT-coated silica particles to form electrically conductive epoxy resin composites. Polymer 98, 32–38. https://doi.org/10.1016/j.polymer.2016.06.009

Xu, D.-H., Liu, F., Pan, G., Zhao, Z.-G., Yang, X., Shi, H.-C., Luan, S.-F., 2021. Softening and hardening of thermal plastic polyurethane blends by water absorbed. Polymer 218, 123498. https://doi.org/10.1016/j.polymer.2021.123498

Yorgancioglu, A., Başaran, B., Sancakli, A., 2020. Value Addition to Leather Industry Wastes and By-Products: Hydrolyzed Collagen and Collagen Peptides, in: Körlü, A. (Ed.), Waste in Textile and Leather Sectors. IntechOpen. https://doi.org/10.5772/intechopen.92699

Zhong, B., Zou, J., An, L., Ji, C., Huang, X., Liu, W., Yu, Y., Wang, H., Wen, G., Zhao, K., Lin, X., 2019. The effects of the hexagonal boron nitride nanoflake properties on the thermal conductivity of hexagonal boron nitride nanoflake/silicone rubber composites. Composites Part A: Applied Science and Manufacturing 127, 105629. https://doi.org/10.1016/j.compositesa.2019.105629

Zhou, X., Ren, Z., Sun, H., Bi, H., Gu, T., Xu, M., 2022. 3D printing with high content of lignin enabled by introducing polyurethane. International Journal of Biological Macromolecules 221, 1209–1217. https://doi.org/10.1016/j.ijbiomac.2022.09.076

List of Congress and Publications

Mascolo R., De Piano F., Nogarole M., Bilotti E. - Surface shrinkage: Determination of stress at high temperatures on leathers of different origins using DMA - III IULTCS EuroCongress 2022 (Vicenza, Italy), Poster

Mascolo R., De Piano F.,Giorleo L., Fiorentino A., Battini D. - Surface deformation comparison of leather with different EN ISO 5402-1 flexometer clamps using DIC technologies - III IULTCS EuroCongress 2022 (Vicenza, Italy), Poster

Mascolo R., Calvanese G., Scaglia E. - Legal metrology in tanning industry: statistical analysis and critical issues using pin-wheel machines - III IULTCS EuroCongress 2022 (Vicenza, Italy), Poster

Bresolin B., Mascolo R., Nogarole M., Zamagni A. - Product Environmental Footprint of tanning industry: a case of Study - XXXVII IULTCS Congress 2023 (Cehgdu, China), Poster

Mascolo R., Calvanese G., M. Bruno, Scaglia E. - Study of the variability of the surface measurement of leathers in different conditioning atmospheres - XXXVII IULTCS Congress 2023 (Cehgdu, China), Poster

Mascolo R., Vietri F. Martone A., Florio C. - Insights on the estimation of particle size distribution (PSD) of grinded leather particulate using a Digital Image Processing Method (DIP) - XXXVII IULTCS Congress 2023 (Cehgdu, China), Poster

Mascolo R., De Piano F., Bilotti E., Calvanese G. - Innovative method for the determination of hydrothermal stability of leathers using DMA techniques - XXXVII IULTCS Congress 2023 ((Cehgdu, China), Poster

Mascolo R., Giorleo L., Bilotti E., Nazir M. U. - Novel PLA and TPU bio-composites from leather wastes for Fused Filament Fabrication Additive Manufacturing technologies - XXXVII IULTCS Congress 2023 (Cehgdu, China), Oral presentation

Claudia F., Rosario M., Cirillo C., Maffei G., Loi A., Sarno M. - Zero chemical treatment of leather waste for highly performing, circular and sustainable finishings - XXXVII IULTCS Congress 2023 (Cehgdu, China), Oral presentation

B.M. Bresolin, M. Nogarole, R. Mascolo, A. Sarnataro, C. Florio . Application of the circular economy model to leather tannery waste - 7-10 novembre 2023, ECOMONDO, Rimini, Poster

Romani A., Riccardi G., Guida L., Florio C., Mascolo R., Levi M. - Valorizing scraps from the leather industry through additive manufacturing: Direct Ink Writing and nonplanar slicing for personalized products in the watch sector - XIV Convegno INSTM, 9-12 giugno 2024, Cagliari, Oral presentation

Venturelli G., Guida L., Fasani M.G.T., Mantero S., Petrini P., Florio C., Mascolo R., Levi M. - 3D-printable composite materials as alternatives to leather for the upcycling of leather waste - XIV Convegno INSTM, 9-12 giugno 2024, Cagliari, Oral presentation

Guida L., Florio C., Mascolo R., Levi M. - 3D-Printable leather scrap-polymer composite materials in a circular economy perspective - XIV Convegno INSTM, 9-12 giugno 2024, Cagliari, Oral presentation

Ravelli, M.; Giorleo, L.; Papa, I.; Silvestri, A.; Mascolo, R.; Squillace, A. - Effect of Tightening Torque on Bearing Performance of Kevlar Fiber Composite Bolted Joints Produced by Additive Manufacturing - Lecture Notes in Mechanical Engineering, Oral presentation. doi: 10.1007/978-3-031-77697-7_7

Mascolo R., Calvanese G., Giorleo L., Scaglia E. - Statistical Analysis and Critical Aspects of Surface Measurement using Mechanical Pin-Wheel Machines - JALCA, VOL. 119, 2024. doi.org/10.34314/0gfn4326

E. Bilotti, M.U. Nazir, R. Mascolo, P. Bouic, M.M. Hassan, J. Harris, S. Naderizadeh, J. Busfield, H. Zhang, D. Papageorgiou. Upcycling Leather Waste: The Effect of Leather Type and Aspect Ratio on the Performance of Thermoplastic Polyurethane Composites - Sustainable Materials and Technologies 43 (2025). doi: e0122110.1016/j.susmat.2024.e01221

J. Busfield, S. Naderizadeh, A. Faggionato, M.U. Nazir, R. Mascolo, M.M. Hassan, E. Bilotti. The Thermal and Mechanical Properties of Leather Waste-Filled Bio-Based Thermoplastic Polyurethane Composites - Polymers 2025, 17(9), 1202. doi.org/10.3390/polym17091202

Mascolo R., Vietri F., Giorleo L., Martone A. - Estimation of Particle Dimension and Particle Size Distribution (PSD) of Ground Leather using a Digital Image Processing Method (DIP) - JALCA, VOL. 120 No. 9 (2025). doi.org/10.34314/q3wq0y12

Mascolo R., Esposito L., Bertazzo M., Pierro G., Calvanese G. - Degradability by micro-organisms of tanned leather: a case study of different kinds of tannings for the sustainability of the processes - XXXVIII IULTCS Congress 2025 (Lione, Francia), Poster

R. Mascolo, C. Siviello, F. Bertocchi, C. Azzaretto, F. Cilento, B. Palmieri, A. Martone. Sustainable Leather Finishing: Optimizing Thermal Properties with Graphene Nanoplatelet-Polyurethane Nanocomposites - XXXVIII IULTCS Congress 2025 (Lione, Francia), Oral Presentation

R. Mascolo, Giorleo L., Cacciatori T., Piccirillo F. - Direct Pellet Material Extrusion of PLA-Collagen Composites: A Circular Approach to Leather Waste Valorization - XXXVIII IULTCS Congress 2025 (Lione, Francia), Oral presentation

C. Brondi, A. Zangiacomi, M. Cornaro, J. Maciel, A. Boffelli, B. Colombo, F. Visintin, G. Revol, M. Nogarole, R. Mascolo. Transitioning Towards Circularity in the Italian Leather Industry: Insights from a Qualitative Comparative Analysis - XXXVIII IULTCS Congress 2025 (Lione, Francia), Poster

Mascolo R., Nazir M.U., Giorleo L., Bilotti E. - Thermoplastic Polyurethane Composites Reinforced with Leather Waste: Influence of Particle Size on Performance for Footwear Applications - XXXVIII IULTCS Congress 2025 (Lione, Francia), Poster

Sanfelice M., Farroni F., Mascolo R. - Viscoelastic characterization of leathers properties: a novel nondestructive method using micro-indentation technique - XXXVIII IULTCS Congress 2025 2025 (Lione, Francia), Oral presentation

Mascolo R., Calvanese G., Nazir M.U., Bilotti E., Giorleo L. - Approaching the threshold of leather waste percentage within the TPU matrix for the manufacture of filament used in Fused Filament Fabrication applications - Collagen and Leather